SYNTHESIS AND EVALUATION OF NEW BISPHOSPHONATE-FUNCTIONALIZED (METH)ACRYLATES FOR BIOMEDICAL APPLICATIONS

by

Melek Naz Güven

B.S., Chemistry, Boğaziçi University, 2014

Submitted to the Institute for Graduate Studies in

Science and Engineering in partial fulfillment of

the requirements for the degree of

Master of Science

Graduate Program in Chemistry

Boğaziçi University

2016

To my family…

ACKNOWLEDGEMENTS

First of all, I would like to express my deepest gratitude to my thesis supervisor Prof. Duygu Avcı Semiz for her valuable guidance, advice and encouragement throughout my research. I gained plenty of experience thanks to her endless support and attention since my junior year.

I would like to express my thanks to my committee members Prof. İlknur Doğan and Prof. Funda Yağcı Acar for generously giving their valuable time for reviewing the final manuscript and for their constructive comments and suggestions.

I would like to thank dear members of Avcı lab. Ece, Sesil, Tuğçe, Betül, Miraç, Seçkin and Türkan for their help and supportive friendship. I also thank to Fatma for her great contribution.

I wish to thank my dear friends especially Işıl, Esra, Büşra, Erhan, Can, Buğra, Eren, Furkan, Pelin, Şeyma, Selen and Emre for their supportive and fun-filled company since the day I met them.

I would also like to thank all members of Chemistry Department who were always very helpful.

Finally, my greatest gratitude is extended to my mother, father and my sisters for their endless love, support and understanding through my whole life.

This research has been financially supported by The Scientific and Technological Research Council of Turkey (TÜBİTAK) [114Z926].

ABSTRACT

In the first part of this work, new urea dimethacrylates functionalized with bisphosphonate (1a, 1b) and bisphosphonic acid (2a, 2b) groups were synthesized and evaluated for dental applications. Monomers 1a and 1b were synthesized from 2-isocyanatoethyl methacrylate (IEM) and two bisphosphonated amines (BPA1 and BPA2, prepared by the reaction of 1,4-butanediamine and 1,6-hexanediamine with ethylidene bisphosphonate, respectively). Selective cleavage of the bisphosphonate ester groups of 1a and 1b was achieved using trimethylsilyl bromide (TMSBr) to give monomers 2a and 2b. These acid monomers were found to be hydrolytically stable and have pH values (1.73 and 1.81) in the range expected for mild self-etching dental adhesives. Monomers were copolymerized with 2-hydroxyethyl methacrylate (HEMA), triethylene glycol dimethacrylate (TEGDMA) and bisphenol A-glycolate methacrylate (Bis-GMA) using real time FT-IR with 2,2'-dimethoxy-2-phenyl acetophenone (DMPA) as photoinitiator. Conversions obtained for the bisphosphonic acid monomer formulations were about the same as the bisphosphosphonate formulations, but the polymerization rates were faster due to hydrogen bonding. XRD spectrum of HAP treated with 2a/EtOH/H_2O solutions proved formation of hydrolytically stable monomer Ca salts and $CaHPO_4.2H_2O$ (DCPD) induced by demineralization. Also these monomers were found show no significant toxicity. All these properties indicated that the synthesized monomers are suitable candidates for dental materials.

In the second part of this work, four novel bisphosphonate-functionalized poly(β-amino ester) (PBAE) macromers were synthesized through aza-Michael addition of 1,6-hexane diol diacrylate (HDDA) or poly(ethylene glycol) diacrylate (PEGDA, M_n=575), and BPA1 or BPA2. The macromers were homo- and co polymerized with HEMA in the presence of DMPA as photoinitiator to give biodegradable gels and their properties were studied (degradation). The mass loss of the homopolymers were found to be similar and around 53-69% at 37 °C in 1 day. It was shown that PBAE macromers can be used as crosslinkers for the synthesis of HEMA hydrogels. These hydrogels showed higher and mass loss than those made with PEGDA crosslinkers. These materials have potential in tissue engineering applications.

ÖZET

Bu çalışmanın ilk bölümünde, bisfosfonat (1a, 1b) ve bisfosfonik asit (2a, 2b) grupları ile fonksiyonlandırılmış yeni üre-dimetakrilatlar sentezlenmiştir. Monomer 1a ve 1b 2-isosiyanatoetil metakrilat (IEM)'ın iki bisfosfonat içeren amin (bunlardan BPA1, 1,4-bütandiaminin BPA2 ise 1,6-hekzandiaminin etiliden bisfosfonat ile reaksiyonundan hazırlanmış olmak üzere) ile reaksiyonundan sentezlenmiştir. 1a ve 1b'nin bisfosfonat gruplarının trimetilsilil bromür (TMSBr) ile seçici kırılması 2a ve 2b monomerlerini vermiştir. Bu asit monomerlerinin hidrolize dayanıklı olduğu ve yumuşak "self-etching" diş yapıştırıcılarından beklenen pH değerlerine (1.73 ve 1.81) sahip oldukları bulunmuştur. Monomerler foto diferansiyel taramalı kalorimetrede 2,2'-dimetoksi-2-fenil asetofenon (DMPA) fotobaşlatıcısı kullanılarak 2-hidroksietil metakrilat (HEMA), trietilen gikol dimetakrilat (TEGDMA) ve bisfenol A-glikolat metakrilat (Bis-GMA) ile kopolimerize edildi. Bisfosfonik asit monomer formülasyonlarının polimerleşme verimleri bisfosfonatlılarınki ile benzer, fakat polimerizasyon hızları hidrojen bağı yetenekleri dolayısıyla daha yüksektir. 2a/EtOH/H_2O çözeltileri ile muamele edilmiş HAP'ın XRD spektrumu monomerin hidrolize dayanıklı Ca tuzları ve demineralizasyon sonucu $CaHPO_4.2H_2O$ (DCPD) oluşumunu kanıtlamıştır. Ayrıca bu monomerlerin önemli bir toksisiteye sahip olmadıkları bulunmuştur. Bütün bu özellikler, sentezlenen monomerlerin diş malzemeleri için uygun adaylar olduğunu göstermektedir.

Çalışmanın ikinci bölümünde, bisfosfonat grubu içeren dört yeni poli(β-amino ester) (PBAE) makromerleri 1,6-hekzan diol diakrilat (HDDA) veya poli(etilen glikol) diakrilat (PEGDA, M_n=575) ve BPA1 veya BPA2'nin Michael katılma reaksiyonu ile sentezlendi. Makromerler DMPA fotobaşlatıcı ile homo ve HEMA ile kopolimerleştirilerek biyobozunur jeller elde edilerek özellikleri (bozunurluk) incelendi. Homopolimerlerin kütle kayıpları 37 °C de iki günde benzer ve 53-69% olarak bulundu. PBAE makromerlerin HEMA hidrojellerinin sentezinde çapraz bağlayıcı olarak kullanılabileceği gösterildi. Bu hidrojeller PEGDA çapraz bağlayıcıları kullanılarak hazırlanmış hidrojellerden daha yüksek ve ayarlanabilir kütle kaybı göstermiştir. Bu malzemeler doku mühendisliği uygulamalarında kullanılma potansiyeline sahiptirler.

TABLE OF CONTENTS

LIST OF FIGURES

LIST OF TABLES

LIST OF SYMBOLS

Abs	Absorption
$A_{control}$	Absorption of control cell
A_{sample}	Absorption of treated cell
Mp	Melting point
Ppm	Parts per million
pH	Power of Hydrogen
β	Beta
θ	Theta

LIST OF ACRONYMS/ABBREVIATIONS

AMP	Adenosine monophosphate
ATP	Adenosine triphosphate
Bis-GMA	Bisphenol A-glycolate methacrylate
BP	Bisphosphonate
CAN	Ceric ammonium nitrate
DBC	Double bond conversion
DBU	1,8-Diazabicyclo[5.4.0]undec-7-ene
DMPA	2,2'-Dimethoxy-2-phenyl acetophenone
FT-IR	Fourier transform infrared spectroscopy
GPC	Gel permeation chromatography
HAP	Hydroxyapatite
HEMA	2-Hydroxyethyl methacrylate
HDDA	1,6- Hexane diol diacrylate
IEM	2-isocyanatoethyl methacrylate
MDP	10-Methacryloyloxydecyl dihydrogen phosphate
MTT	Thiazolyl blue tetrazolium bromide
NMR	Nuclear magnetic resonance spectroscopy
NVP	N-vinylpyrrolidone
PBAE	Poly β-amino ester
PBS	Phosphate buffered saline
PEGDA	Poly(ethylene glycol) diacrylate
PLA	Polylactic acid
p-TsOH	Para-toluene sulfonic acid
SEM	Scanning electron microscope
TEGDMA	Triethylene glycol dimethacrylate
TGA	Thermogravimetric analysis
TMSBr	Trimethylsilyl bromide
UV	Ultraviolet
XRD	X-ray diffraction

1. INTRODUCTION

1.1. Bisphosphonates

Bisphosphonates (BPs) are a class of therapeutic agents commonly used in the treatment of bone diseases. Bisphosphonates were discovered in 1894 by the pharmacist Theodor Salzer [1], but they have been used as therapeutic agents since 1960s when it was found that inorganic pyrophosphate could prevent bone diseases by binding to hydroxyapatite (HAP) and inhibits its dissolution [2].

Pyrophosphates are present in living organisms, they are byproducts of some biological process such as hydrolysis of ATP to AMP. Despite strong binding ability to HAP crystals due to their two phosphonate groups, pyrophosphates fail to inhibit HAP dissolution because of their easy hydrolysis. BPs are stable analogs of pyrophosphates (P–O–P backbone, Figure 1.1) and are suited to be adsorbed onto hydroxyapatite crystals, thus prohibiting its dissolution. The replacement of the central oxygen atom in the bisphosphonate structure with a carbon unit (P–C–P backbone) provides the bisphosphonates resistance against hydrolysis compared to pyrophosphates [3, 4].

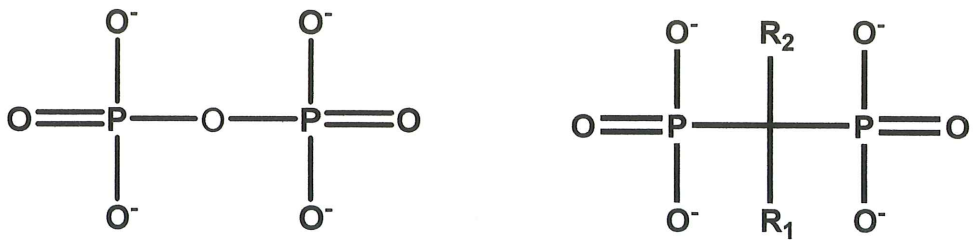

Figure 1.1. Structures of pyrophosphate and bisphosphonate.

Bisphosphonates have two geminal substituents, R_1 and R_2, attached to central carbon atom, which provide variety for the activities for BPs. A hydroxyl group (-OH) or an amino group ($-NH_2$) (compared to H) in the R1 chain increases binding to calcium minerals. The presence of a nitrogen or amino group in the R2 chain enhances the anti-resorptive potency and also affects binding to hydroxyapatite (HAP).

To date, eight bisphosphonates (Figure 1.2) with various side groups and binding constants to hydroxyapatite are in clinical use. Bisphosphonates containing a basic primary nitrogen atom in an alkyl chain as R_2 substituent (e.g., pamidronate and alendronate) are more potent antiresorptive agents than those with other small substituents, e.g. etidronate or clodronate. Also, the most potent antiresorptive bisphosphonates have a nitrogen atom within a heterocyclic ring (e.g., risedronate and zoledronate). These variations in antiresorptive potency occur due to the differences in the R_2 substituents, and influence the biochemical activities of these drugs [2,5,6].

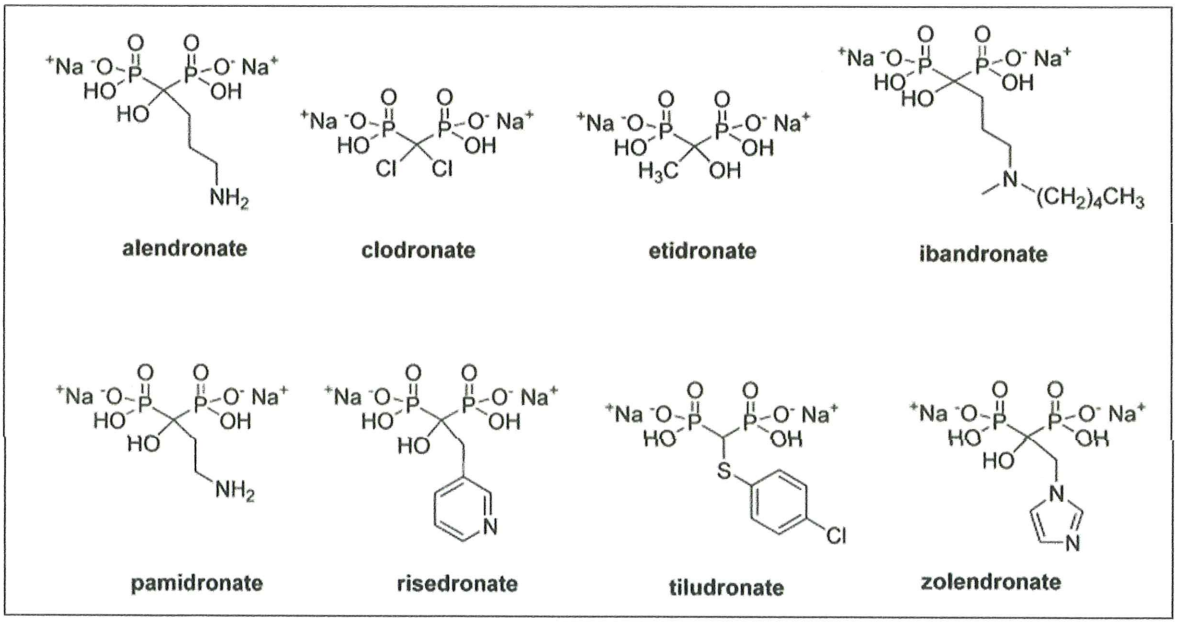

Figure 1.2. Eight clinically used BPs [6].

1.1.1. Biomedical Applications of BPs

The distance between the two deprotonated hydroxyls of the two phosphonates in BPs (2.9-3.1 Å) is similar to the distance between the two calcium-chelating oxygen atoms in HAP [7]. Because of this, BPs are in an ideal situation for binding to the Ca^{2+} in HAP and hence showing a strong interaction to HAP-based tissues such as dentin, enamel and bone.

The application areas of BPs vary from dental materials to bone targeting systems for the delivery of therapeutic agents such as drugs and proteins or imaging agents (Figure 1.3). Due to BPs inhibition of HAP dissolution and bone resorption, they are used in the treatment of many bone diseases such as osteoporosis, Paget's disease and bone metastasis [8,9,10].

Enamel and dentin, the two types of dental tissues, have similar structure to bone. Good adhesion between them and dental restorative materials is one of the main considerations in dentistry [11]. BPs are used to achieve high affinity between tooth surface and restorative materials.

BPs are also used in bone targeting for delivery of drugs. There are a number of drug, protein, imaging agent ect. delivery strategies such as polymer scaffolds, liposomes, dendrimers, micelles, hydrogels, peptides, and antibodies. However, bone targeting delivery requires molecules that have high affinity to bone. Because of this conjugates of BPs to small molecule drugs [12-15], imaging agents [16,17], proteins [18] and polymers [19,20] are used for bone targeting [21]. Also BP coated surfaces improve bone formation around implants and stabilize nanoparticles [22-25].

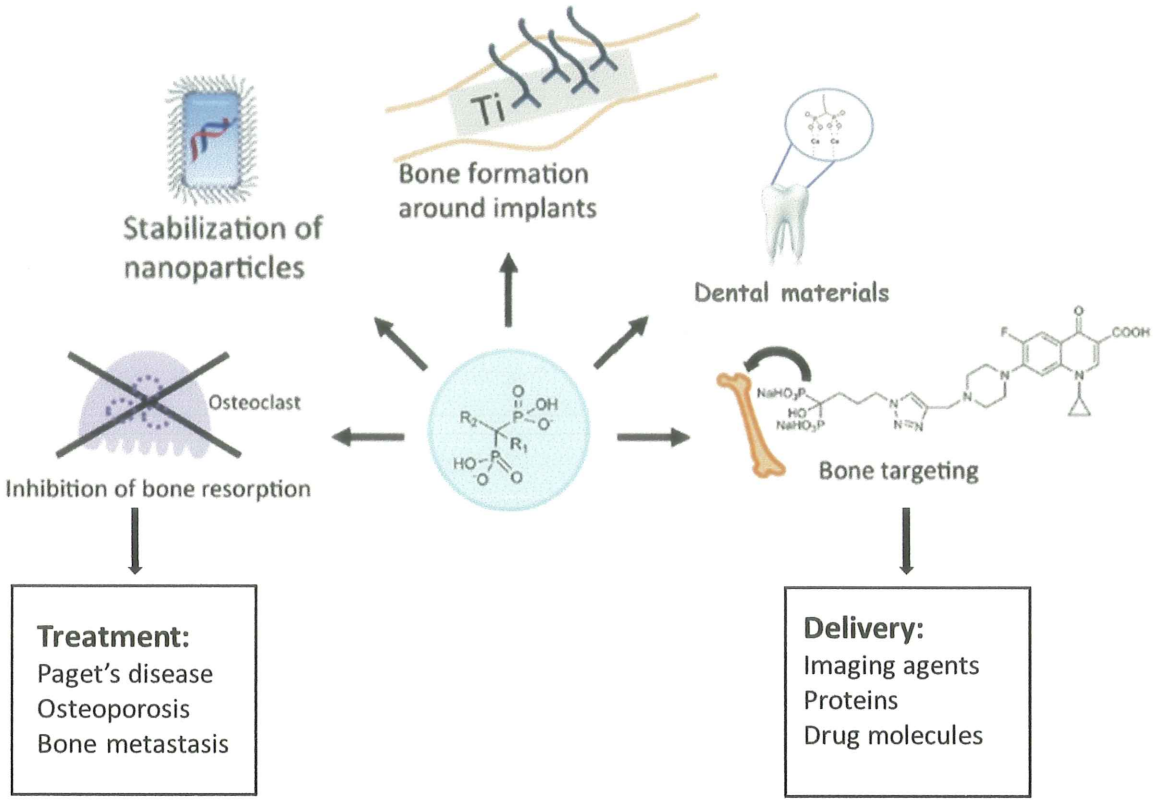

Figure 1.3. Biomedical application areas of BPs [26].

1.1.2. Bisphosphonate Containing Molecules for Use in Dental Applications

Dental restorative composites are biomaterials which are composed of a mixture of about 60–88 wt% of inorganic fillers and 12–40 wt% of a polymerizable resin which in turn consists of a mixture of crosslinking monomers, a photoinitiator system, and additives. The main problems of dental restoratives are their polymerization shrinkage, wear due to mechanical stresses, instability due to hydrolysis in the aqueous mouth environment and lack of adhesion to tooth tissue [27,28]. To obviate the adhesion problem, efforts have been made to include binding groups in filling composites but the main approach involves the use of dental adhesives to achieve a strong, durable bond between a filling composite and tooth tissue [29-32]. Self-etching adhesives are introduced as the best solution of this problem [33].

1.1.2.1. Self-etching Dental Adhesives. Self-etching adhesives systems are used to achieve a strong and stable bond between the dental tissues and dental filling materials [34]. These systems are composed of three main groups: self-etching adhesive monomers, crosslinking monomers and monofunctional co-monomers; in addition to these, some additives such as photoinitiators, solvents and fillers can be used (Figure 1.4).

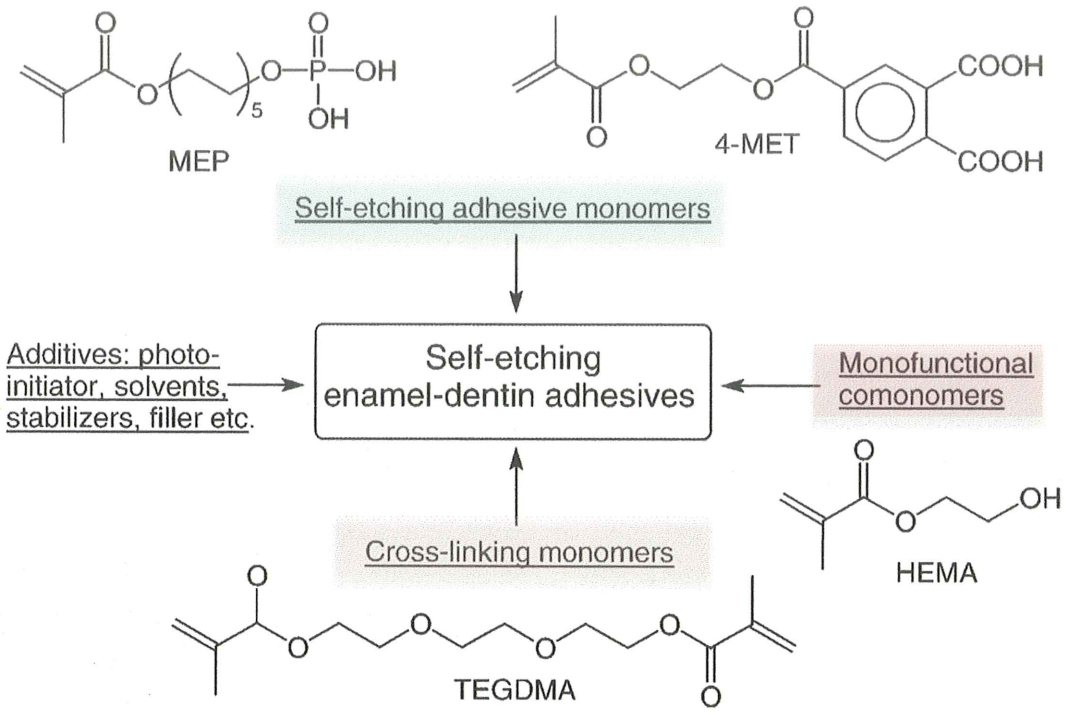

Figure 1.4. Components of self-etching enamel-dentin adhesives [31].

The most important components of adhesive systems are the self-etching adhesive monomers. These adhesive monomers are bifunctional molecules, they should have the capability to etch the enamel and dentin and the capability to form bonds with the tooth material. Also they should satisfy some requirements such as high rate of homo and copolymerization; high mechanical properties; low volume shrinkage; low oral and cytotoxicity and solubility in ethanol, water and the adhesive composition. Self-etching adhesive monomers contain a polymerizable group, for example, a methacrylate group, which can react both with the other monomers of the adhesive and the restorative material by copolymerization, an adhesive group, such as a strong acidic group, to etch the dental hard tissues and interact with the tooth substance, and a spacer group designed to influence

the solubility, flexibility and the wetting properties of the adhesive monomer (Figure 1.5) [31,36].

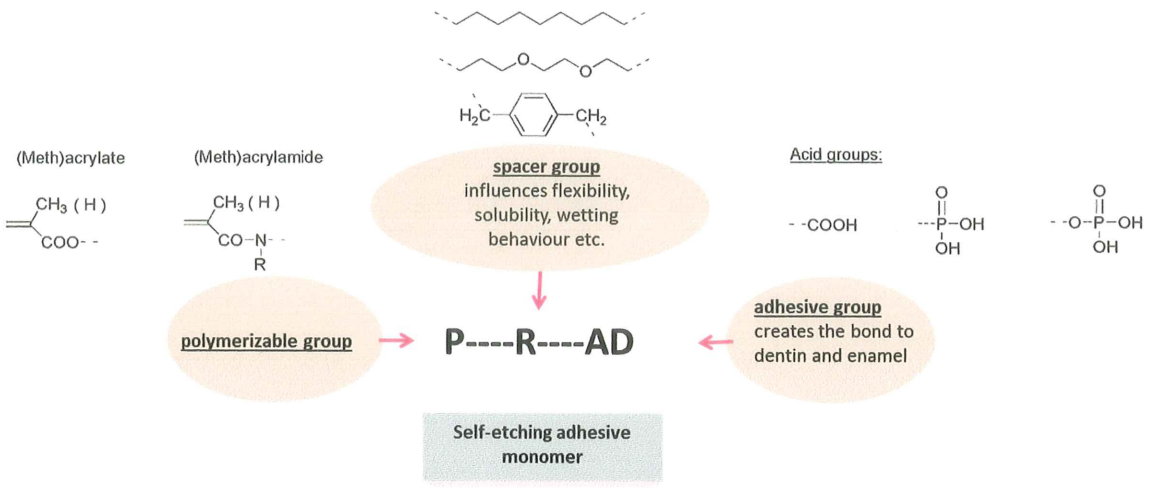

Figure 1.5. Components of self-etching enamel-dentin adhesive monomers [31].

Both the restorative composites and self-etching adhesive materials have been intensively worked on to improve their performances by developing novel monomers. Functional monomers with the ability to achieve a strong interaction with HAP have been prepared. Recently, monomers with bisphosphonic acid functional groups were investigated for self-etching dental adhesive applications due to the strong affinity of these groups for HAP [37-42]. Some examples of self-etching dental adhesive monomers containing bisphosphonates are shown in Figure 1.6. [43,44]. Moreover, it was also reported that bisphosphonates can inhibit enzymes (metalloproteinases) which degrade the collagen network [45].

It is also reported that dental monomers with high rate of homo- and copolymerization with other monomers in the formulation can constitute further improvement in dental materials. Among the hydrogen bonding monomers investigated by Jansen and Berchtold, monomers containing urea were found to be the most reactive [46,47]. The high reactivities were explained by a hydrogen bonding-induced pre-organization that brings double bonds close to each other, enhancing propagation. Also, a reduction in termination rate may also be involved in the observed reactivity.

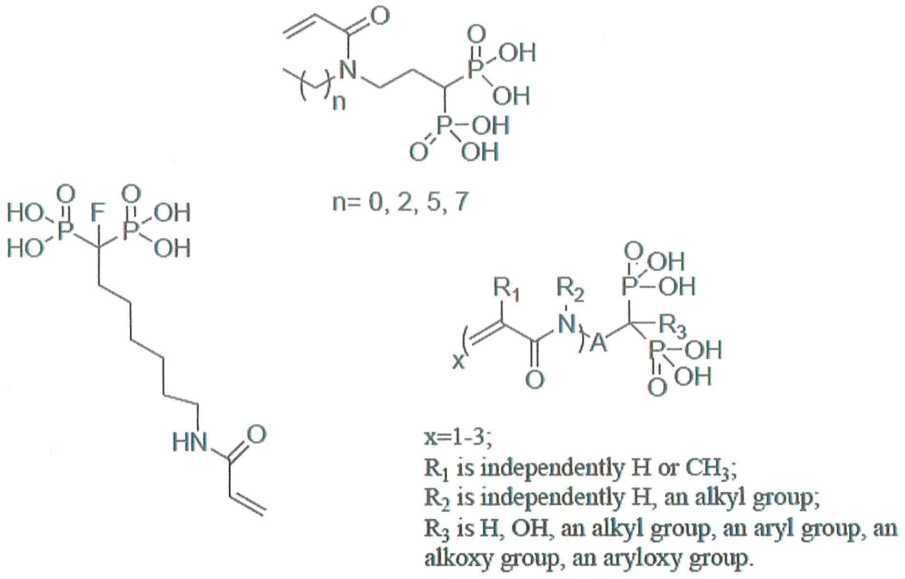

Figure 1.6. Self-etching dental adhesive monomers containing bisphosphonates.

Recently, two monofunctional phosphonated urea methacrylates to be used as reactive diluents for dental formulations were synthesized by our group (Figure 1.7) [35]. They were found to be more reactive than TEGDMA due to a combination of hydrogen abstraction/chain transfer reactions stemming from the labile hydrogens and hydrogen bonding caused by the urea linkage. Moszner et al. described synthesis of polymerizable phosphonic acids bearing urea groups and showed that the presence of the urea group leads to a significant increase in both rate of polymerization and shear bond strength to dental tissues (Figure 1.8) [48].

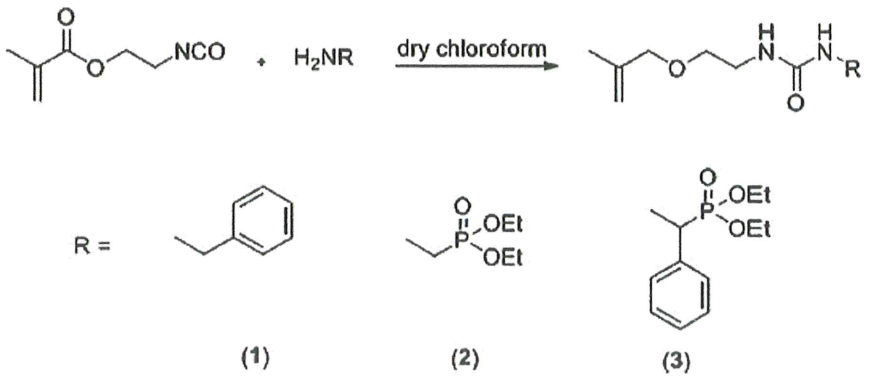

Figure 1.7. The structures of monofunctional phosphonated urea methacrylates previously synthesized by our group.

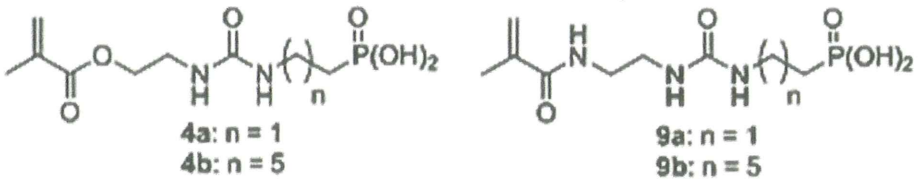

Figure 1.8. The structures of polymerizable phosphonic acids monomers bearing urea groups synthesized by Moszner.

1.1.3. Bisphosphonate Containing Molecules and Hydrogels for Use in Drug and Gene Delivery and Tissue Engineering

In recent years, injectible, photopolymerizable and degradable biomaterials have gained in importance for many different applications such as drug and gene delivery and tissue engineering [49-55]. Among these biomaterials, hydrogels have been more attractive candidates since they are biocompatible, and also since they are capable of swelling to several times their original size.

Hydrogels are generally composed of a crosslinked polymer system. Commonly, synthetic monomers and polymers are used to synthesize hydrogels such as poly-(ethylene glycol) (PEG), N-substituted acrylamides, 2-hydroxy ethyl methacrylate (HEMA), N-vinylpyrrolidone (NVP) and poly-(lactic acid) (PLA) [56,57,58].

On the other hand, new biomaterials produced by attaching phosphorus-containing building blocks to polymers have been investigated since this attachment can improve their performance, adding desired properties such as biodegradability, hemocompatibility and strong affinity for hydroxyapatite (HAP)-based tissues i.e. dentin, enamel, and bone.

Therefore, polymer-drug conjugates with bisphosphonic acid groups are expected to both improve efficiency of drugs by increasing half-life of drugs in circulation and solubility of drugs, and to decrease their toxicity. Bone-targeting drug conjugates based on poly(ethylene glycol) and poly[N-(2-hydroxypropyl)methacrylamide] containing alendronate as the bone targeting group were tested [59], a hydrogel prepared from a

copolymer of N-acrylpamidronate and N-isopropylacrylamide was used as scaffold for mineralization of HAP [19] and bisphosphonate derivatives of cationic polymers such as poly(l-lysine) and poly(ethylenimine) were tested for affinity to HAP [20] (Figure 1.9). Also a hyaluronic acid hydrogel was synthesized with BPs covalently attached to the matrix and its potential to be used in bone tissue engineering was observed (Figure 1.10) [60]. Surface functionalization of a BP containing PEG polymer was investigated for biomedical imaging and the method was extended to other inorganic nanomaterials of interest in biomedical imaging and engineering to which recently synthesized BPs bind very strongly [61].

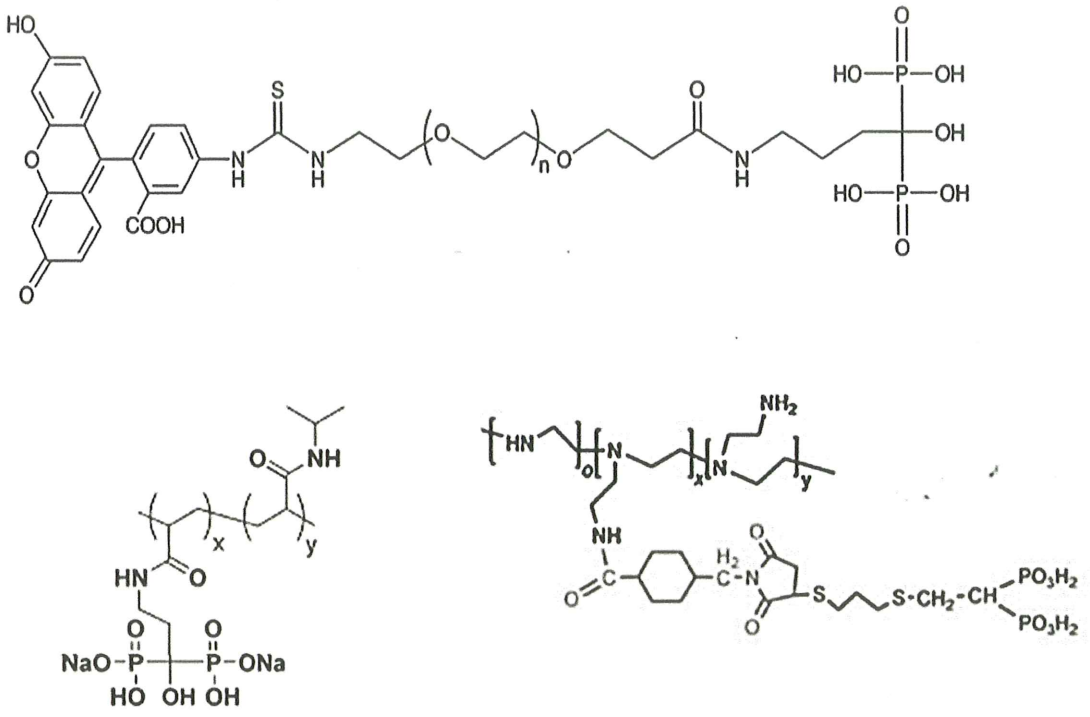

Figure 1.9. Structures of some bisphosphonic acid containing bone targeting polymers [19,20].

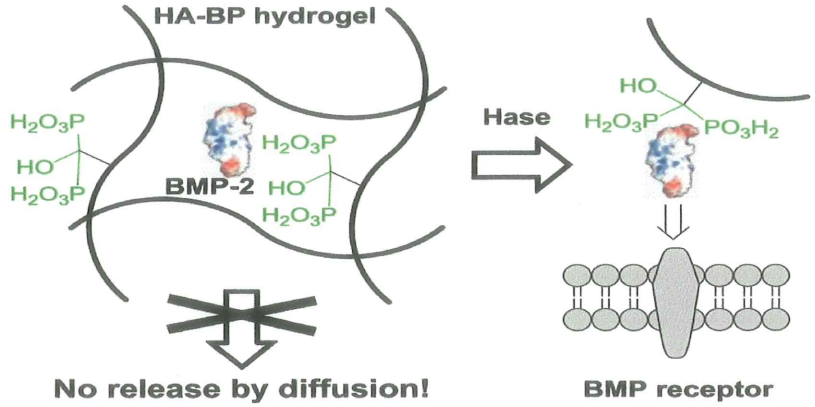

Figure 1.10. Hyaluronic acid hydrogel with BPs covalently attached to the matrix for using in bone tissue engineering [60].

1.2. Poly (β-Amino Ester)s

Poly(β-amino ester)s (PBAEs) have been developed in recent years as potentially very good biodegradable materials for use in gene [62] and drug [63-66] delivery and tissue engineering [67-70] due to their pH sensitivity, biodegradability and high biocompatibilities. It has been found by Langer et al. that in the synthesis of PBAEs made from the Michael addition of diamines and diacrylates, a step-growth polymerization process, if the diacrylate is used in slight molar excess, that will result in PBAEs with acrylate end groups (Figure 1.11) [56,62,71,72].

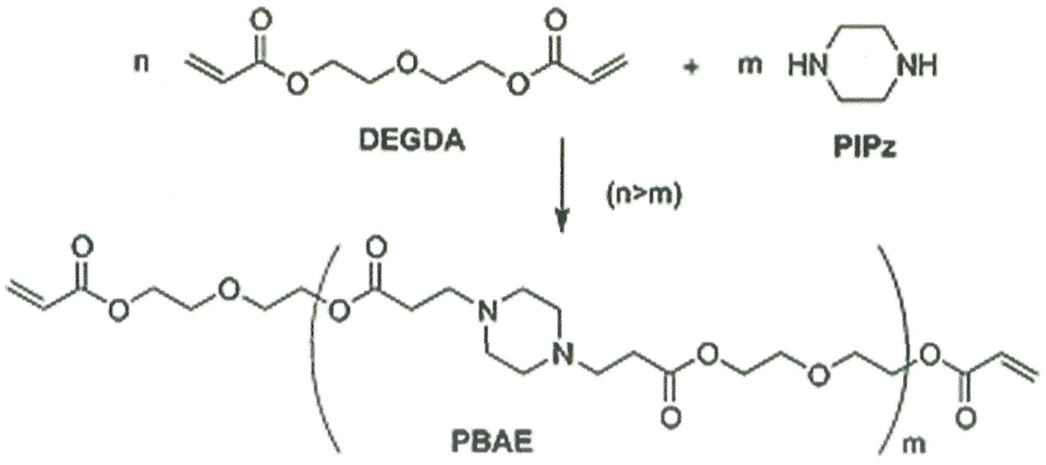

Figure 1.11. Synthesis of PBAE crosslinkers [56].

Polymerization of the macromers gives crosslinked and degradable networks which can be used as scaffolds for tissue engineering. A library of 120 such diacrylate terminated PBAE macromers were synthesized from reactions of various primary and secondary amines with diacrylates by Anderson *et al.* (Figure 1.12)[73].

The large chemical diversity in PBAE structures provide materials with different gelation or degradation profiles and elastic moduli as well as cell interactions [70]. PBAEs show different degradation properties according to their hydrophilicity/hydrophobicity. For example, the degradation profile of some PBAEs (from the library of 120 photopolymerizable macromers) proved that PBAEs containing hydrophilic ethylene glycol units degraded faster than the other ones (Figure 1.13). Also, PBAEs from different amines that polymerized with one specific diacrylate showed different degradation behavior according to hydrophilicities of these amines (Figure 1.14) [73].

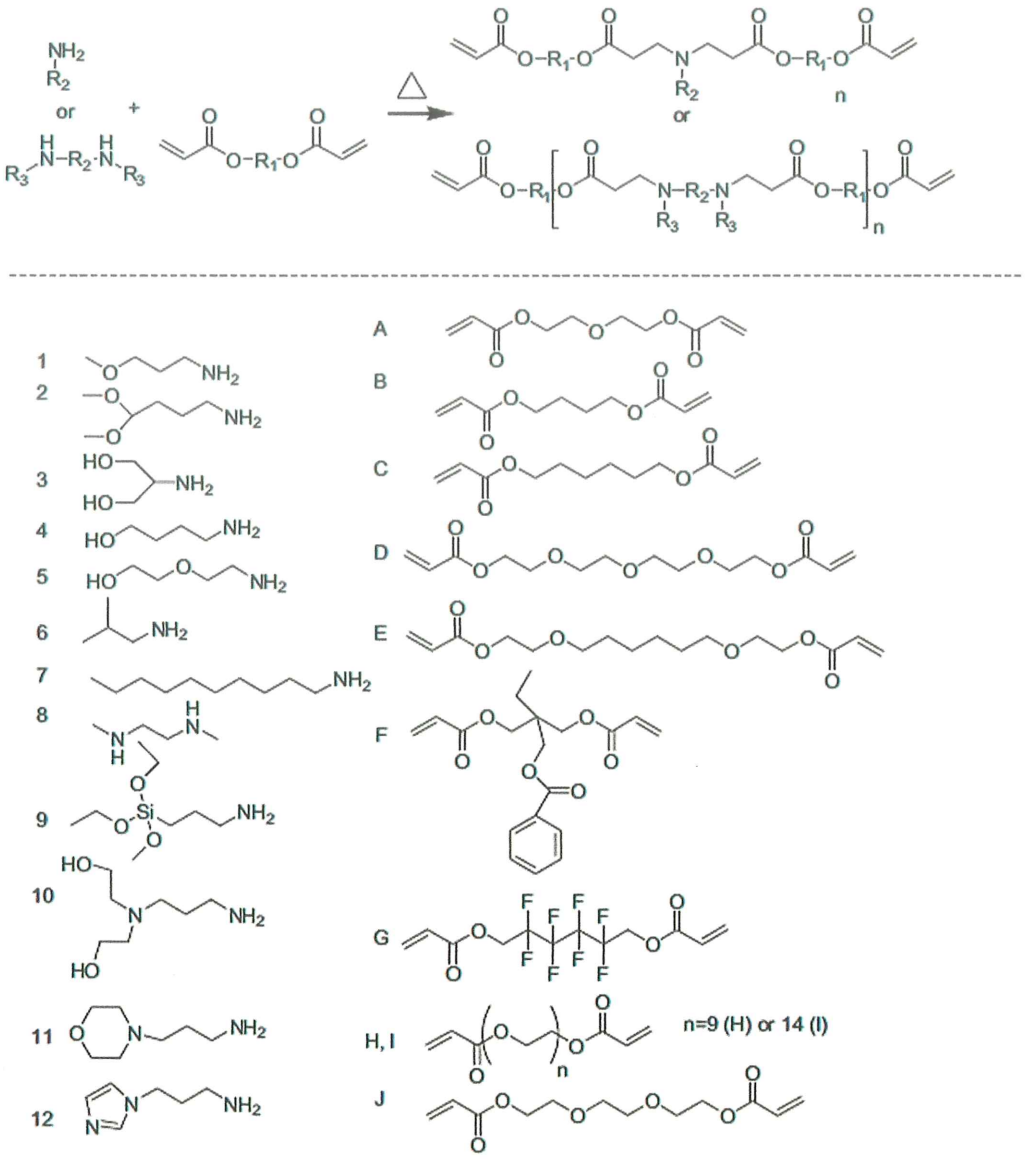

Figure 1.12. General polymerization scheme and the chemical structures of acrylates and amines to produce a library of 120 photopolymerizable macromers [73].

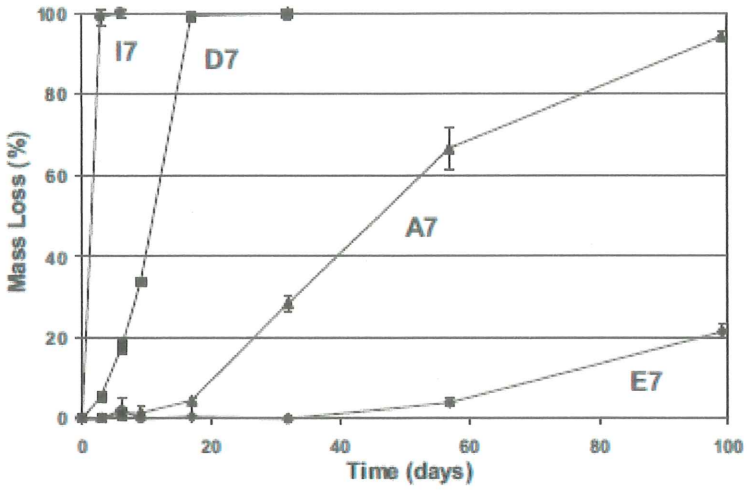

Figure 1.13. Degradation behavior of PBAEs synthesized from one amine and four diacrylates [73].

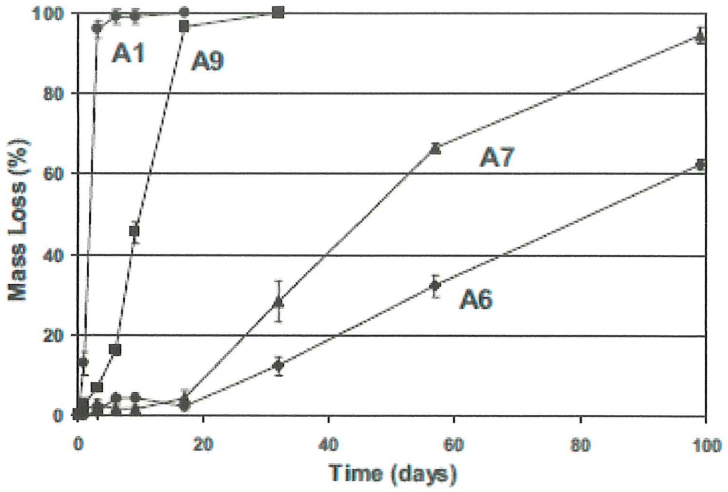

Figure 1.14. Degradation behavior of PBAEs synthesized from one diacrylate and four amines [73].

In this work, we intend to attach bisphosphonate groups to PBAEs to improve their properties, for the first time as far as we know.

2. OBJECTIVES

In this study, the aim is to synthesize novel bisphosphonate- and bisphosphonic acid-containing reactive monomers for biomedical applications. These monomers have potential for use in dental materials as crosslinkers or dental adhesives; also possibly for use in bone targeting delivery systems.

The bisphosphonic acid-containing monomers are expected to have high rate of homo- and copolymerization due to their urea linkage which provides hydrogen bonding, low polymerization shrinkage due to low concentration of double bonds, and will give materials with high mechanical properties due to crosslinking abilities.

Furthermore, hydrogels made from bisphosphonate containing PBAE macromers are expected to be biodegradable, hemocompatible and protein adsorption resistant, therefore be suitable for tissue engineering applications.

3. EXPERIMENTAL

3.1. Materials and Apparatus

3.1.1. Materials

Ethylidene bisphosphonate was prepared from tetraethyl methylene bisphosphonate by the method of Degendardt [74]. 1,4-butanediamine, 1,6-hexanediamine, diethylamine, paraformaldehyde, tetraethyl methylene bisphosphonate, p-toluenesulfonic acid (pTsOH), 1,6-hexane diol diacrylate (HDDA), poly(ethylene glycol) diacrylate (PEGDA, M_n =575), 2-isocyanatoethyl methacrylate (IEM), 2-hydroxyethyl methacrylate (HEMA), hydroxyapatite (HAP), trimethylsilyl bromide (TMSBr), 2,2-bis[4-(2-hydroxy-3-methacryloyloxypropyloxy) phenyl] propane (Bis-GMA), triethylene glycol dimethacrylate (TEGDMA) and photoinitiators 2,2'-dimethoxy-2-phenyl acetophenone (DMPA) were purchased from Aldrich and used as received. 10-methacryloyloxydecyl dihydrogen phosphate (MDP) was a gift from Ivoclar Vivadent. Dichloromethane (CH_2Cl_2), chloroform ($CHCl_3$), dimethyl formamide (DMF) and toluene were dried over molecular sieves. All other solvents were obtained from Aldrich and used as received. Roswell Park Memorial Institute (RPMI) 1640 medium (with l-glutamine and 25 mM HEPES), penicillin-streptomycin and trypsin-EDTA were obtained from Multicell, Wisent Inc. (Canada). Fetal bovine serum was provided by Capricorn Scientific GmbH (Germany). Thiazolyl blue tetrazolium bromide (MTT) and phosphate buffered saline (PBS) tablets were purchased from Biomatik Corp. (Canada). 96-well plates (treated) were provided by Nest Biotechnology Co. Ltd. (China). NIH 3T3 mouse embryonic fibroblast cells were given as a gift from the Kavakli Lab (Koc University, Istanbul, Turkey) for this study.

3.1.2. Apparatus

^{1}H, ^{13}C and ^{31}P NMR spectra were recorded on a Varian Gemini (400 MHz) spectrometer with deuterated chloroform ($CDCl_3$), deuterated methanol (MeOD) and deuterated water (D_2O) as solvent, and tetramethylsilane as an internal standard. A Nicolet

6700 FT-IR spectrophotometer was used for recording IR spectra. Combi Flash Companion Teledyne ISCO Flash Chromatography was used for purification of monomers. The interactions of monomers with HAP were studied by X-ray diffraction (Bruker D8 Advance). The morphology of hydrogels were investigated by using a scanning electron microscope (SEM) (ESEM-FEG) (FEI-Philips XL30). Photopolymerizations were carried out on a Thermo Scientifics Real-Time FT-IR ATR. Gel permeation chromatography (Viscotek) was carried out with THF solvent using polystyrene standards. Gel studies were performed with a photoreactor UV/18. Degradation studies were done with VWR Incubating Mini Shaker. Thermogravimetric analysis was carried out with a TA Instrument Q50.

3.2. Synthesis of Starting Materials

3.2.1. Synthesis of Ethylidene Bisphosphonate

Ethylidene bisphosphonate was prepared from tetraethyl methylene bisphosphonate by the method of Degendardt [74]. In the first step, paraformaldehyde (0.26 g, 8.6 mmol), and diethylamine (0.18 mL, 0.12 g, 1.6 mmol) were combined in 5 mL of methanol and heated at 37 °C until clear solution is obtained. Then heat was removed and tetraethylmethyl bisphosphonate (0.43 mL, 1.7 mmol) was added. The mixture was refluxed for 24 h, then an additional 5 mL of methanol was added, and the solution was concentrated under vacuum. Toluene (2.5 mL) was added and the solution was again concentrated. This step was repeated to ensure complete removal of methanol from the product and a yellow liquid product (tetraethyl (2-methoxyethane-1,1-diyl) bisphosphonate) was obtained.

In the second step, the product of the first step, dry toluene (2.5 mL) and pTsOH (2 mg) were refluxed at 115 °C. Methanol was removed from the reaction mixture by a Dean-Stark trap. After 16 hours, the solution was concentrated. The crude product was diluted with 2.5 mL of chloroform and washed with water (2 × 0.4 mL). The chloroform solution was dried over Na_2SO_4 and concentrated. Yellow liquid product was obtained in 80% yield.

3.2.2. General Procedure for the Synthesis of Amines (BPA1 and BPA2)

Diamine (3.48 mmol) and ethylidene bisphosphonate (8.37 mmol) in dry DMF (25 mL) were mixed at room temperature for two days. After removal of DMF, the residue was washed with petroleum ether and the amines were obtained as light yellow viscous liquids in 80-90% yield.

BPA1

^{1}H-NMR (400 MHz, $CDCl_3$, δ): 1.26 (t, $^{3}J_{HH}$ = 7.2 Hz, 24H, CH_3), 1.39 (m, 4H, CH_2-CH_2-NH), 2.50 (m, 4H, CH_2-NH), 2.61 (m, 2H, CH-P=O), 3.07 (dt, $^{3}J_{HH}$ = 16.4 Hz, J_{HP}= 6.0 Hz, 4H, CH_2-CH-$(P=O)_2$), 4.12 (m, 16H, CH_2-O-P=O) ppm.

^{13}C NMR (101 MHz, $CDCl_3$, δ): 16.33 (CH_3), 27.66 (CH_2-CH_2-NH), 37.44 (CH-$(P=O)_2$), 45.69 (CH_2-CH-$(P=O)_2$), 49.03 (CH_2-NH), 62.54 (CH_2-O-P=O) ppm.

FT-IR (ATR): 3491 (N-H), 2981, 2931 (C-H), 1444 (N-H), 1244 (P=O), 1014, 951 (P-O) cm^{-1}.

BPA2

^{1}H-NMR (400 MHz, $CDCl_3$, δ): 1.29 (m, 4H, CH_2), 1.32 (t, $^{3}J_{HH}$ = 7.2 Hz, 24H, CH_3), 1.45 (m, 4H, CH_2-CH_2-NH), 2.55 (t, 4H, $^{3}J_{HH}$ = 7.2 Hz, CH_2-NH), 2.62 (tt, $^{3}J_{HH}$ = 5.6 Hz, J_{HP}= 23.6 Hz, 2H, CH-P=O), 3.07 (dt, $^{3}J_{HH}$ = 16.4 Hz, J_{HP}= 6.0 Hz, 4H, CH_2-CH-$(P=O)_2$), 4.17 (dq, $^{3}J_{HH}$ = 7.2 Hz, J_{HP}= 24.0 Hz, 16H, CH_2-O-P=O) ppm.

^{13}C NMR (101 MHz, $CDCl_3$, δ): 16.30 (CH_3), 27.24 (CH_2-CH_2-NH), 29.85 (CH_2), 37.38 (CH-$(P=O)_2$), 45.70 (CH_2-CH-$(P=O)_2$), 49.16 (CH_2-NH), 62.54 (CH_2-O-P=O) ppm.

FT-IR (ATR): 3492 (N-H), 2981, 2929 (C-H), 1443 (N-H), 1244 (P=O), 1014, 952 (P-O) cm^{-1}.

3.3. Synthesis of Dental Materials

3.3.1. General Procedure for the Synthesis of Monomers 1a and 1b

To an ice-cold solution of either BPA1 or (1.73 mmol) in 12 mL of dry chloroform under a stream of nitrogen, IEM (3.54 mmol, 0.5 mL) was added dropwise. The solution was stirred at room temperature overnight under nitrogen and then extracted with 1 wt% NaOH (2 x 10 mL), 1 wt% HCl (2 x 10 mL), and brine (2 x 10 mL). The organic layer was dried over anhydrous sodium sulfate, filtered and evaporated under reduced pressure to leave the crude product. The crude product was purified by reversed-phase flash chromatography on C18, eluting with water/methanol (40/60) followed by evaporation of solvents to give the monomers.

1a: The pure product was obtained as a colorless viscous liquid.

^{1}H-NMR (400 MHz, $CDCl_3$, δ): 1.26 (dt, $^{3}J_{HH}$ = 7.2 Hz, J_{HP}= 6 Hz, 24H, *CH*$_3$-CH_2-O), 1.42 (m, 4H, *CH*$_2$-CH_2-N), 1.86 (s,6H, *CH*$_3$-C=CH_2), 2.90 (tt, $^{3}J_{HH}$ = 6 Hz, J_{HP}= 23.6 Hz, 2H, CH-P=O), 3.30 (t, 4H, $^{3}J_{HH}$ = 7.6 Hz, CH_2-N), 3.42 (q, $^{3}J_{HH}$ = 5.6 Hz, 4H, CH_2-NH), 3.68 (dt, $^{3}J_{HH}$ = 14 Hz, J_{HP}= 6.4 Hz, 4H, *CH*$_2$-CH-(P=O)$_2$), 4.06 (m, 16H, CH_2-O-P=O), 4.12 (m, 4H, CH_2-O-C=O), 5.47 (s, 2H, CH_2=C), 6.08 (s, 2H, CH_2=C) ppm.

^{13}C NMR (101 MHz, $CDCl_3$, δ): 15.91 (*CH*$_3$-C=CH_2), 17.88 (*CH*$_3$-CH_2-O), 23.92 (CH_2-CH_2-N), 36.11 (CH-P=O), 39.41 (CH_2-N), 43.87 (*CH*$_2$-CH-(P=O)$_2$), 45.93 (CH_2-NH), 62.56 (CH_2-O-P=O), 63.55 (CH_2-O-C=O), 125.22 (*CH*$_2$=C), 135.82 (CH_2=*C*), 157.84 (O-C=O), 166.95(N-C=O) ppm.

FT-IR (ATR): 3341 (N-H), 2981, 2930 (C-H), 1716, 1636 (C=O), 1636 (C=C), 1536 (N-H), 1245 (P=O), 1016, 955 (P-O-Et) cm^{-1}.

1b: The pure product was obtained as a white solid. Mp: 99 °C

^{1}H-NMR (400 MHz, $CDCl_3$, δ): 1.21 (m, 4H, CH_2), 1.27 (dt, $^{3}J_{HH}$ = 7.2 Hz, J_{HP}= 5.2 Hz, 24H, *CH*$_3$-CH_2-O), 1.44 (m, 4H, *CH*$_2$-CH_2-N), 1.87 (dd, $^{3}J_{HH}$ = 0.8 Hz, 6H, CH_3-C), 2.83

(tt, $^{3}J_{HH}$ = 6 Hz, J_{HP}= 23.6 Hz, 2H, CH-P=O), 3.19 (t, 4H, $^{3}J_{HH}$ = 7.6 Hz, CH_2-N), 3.44 (q, $^{3}J_{HH}$ = 5.6 Hz, 4H, CH_2-NH), 3.69 (dt, $^{3}J_{HH}$ = 14 Hz, J_{HP}= 6.4 Hz, 4H, CH_2-CH-(P=O)$_2$), 4.07 (q, 16H, CH_2-O-P=O), 4.14 (t, 4H, CH_2-O-C=O), 5.49 (s, 2H, CH_2=C), 6.07 (s, 2H, CH_2=C) ppm.

^{13}C NMR (101 MHz, $CDCl_3$, δ): 15.40 (CH_3), 17.30 (CH_3-CH_2-O), 25.78 (CH_2), 26.79 (CH_2-CH_2-N), 34.52-35.81-37.1 (CH-P=O), 39.01 (CH_2-N), 43.65 (CH_2-CH-(P=O)$_2$), 46.78 (CH_2-NH), 61.61-62.10 (CH_2-O-P=O), 63.09 (CH_2-O-C=O), 124.72 (CH_2=C), 135.20 (CH_2=C), 156.83 (O-C=O), 166.49 (N-C=O) ppm.

^{31}P NMR (162 MHz, $CDCl_3$, δ): 22.39 ppm.

FT-IR (ATR): 3358 (N-H), 2981, 2930 (C-H), 1716, 1635 (C=O), 1635 (C=C), 1537 (N-H), 1248 (P=O), 1018, 967 (P-O-Et) cm^{-1}.

3.3.2. General Procedure for the Synthesis of Monomers 2a and 2b

TMSBr (3.6 mmol, 6 eq.) was added to a solution of monomer 1a or 1b (0.6 mmol) in dry DCM (1.2 mL). The mixture was stirred for 5 h at 30 °C. The solvent and the excess of TMSBr were removed under reduced pressure. Methanol (1.2 mL) was added and the mixture was stirred for 15 min. The solution was concentrated under reduced pressure and the product was obtained.

2a: The crude product was obtained as white solid. (pH = 1.73 in 1 w% aqueous solution)

^{1}H-NMR (400 MHz, MeOD, δ): 1.46 (m, 4H, CH_2-CH_2-N), 1.82 (s, 6H, CH_3-C=CH_2), 2.56 (tt, $^{3}J_{HH}$ = 5.6 Hz, J_{HP}= 23.2 Hz, 2H, CH-P=O), 3.26 (m, 4H, CH_2-N), 3.37 (t, ^{3}JHH = 5.6 Hz, 4H, CH_2-NH), 3.73 (dt, $^{3}J_{HH}$ = 14.4 Hz, J_{HP}= 5.6 Hz, 4H, CH_2-CH-(P=O)$_2$), 4.10 (t, $^{3}J_{HH}$ = 5.6, 4H, CH_2-O-C=O), 5.51 (s, 2H, CH_2=C), 6.02 (s, 2H, CH_2=C) ppm.

^{31}P NMR (162 MHz, MeOD, δ): 20.05 ppm.

FTIR (ATR): 3284 (O-H), 2941, 2859 (C-H), 1697, 1676 (C=O), 1626 (C=C), 1557 (N-H), 1159 (P=O), 985, 905 (P-O) cm^{-1}.

2b: The crude product was obtained as white solid. (pH = 1.81 in 1 w% aqueous solution)

^{1}H-NMR (400 MHz, MeOD, δ): 1.25 (m, 4H, CH_2), 1.48 (m, 4H, *CH_2*-CH_2-N), 1.83 (s, 6H, *CH_3*-C=CH_2), 2.59 (tt, $^{3}J_{HH}$ = 5.6 Hz, J_{HP}= 23.6 Hz, 2H, CH-P=O), 3.23 (m, 4H, CH_2-N), 3.38 (t, $^{3}J_{HH}$ = 5.6 Hz, 4H, CH_2-NH), 3.75 (dt, $^{3}J_{HH}$ = 14.4 Hz, J_{HP}= 6 Hz, 4H, *CH_2*-CH-$(P=O)_2$), 4.11 (t, $^{3}J_{HH}$ = 5.2 Hz, 4H, CH_2-O-C=O), 5.53 (s, 2H, CH_2=C), 6.03 (s, 2H, CH_2=C) ppm.

^{31}P NMR (162 MHz, $CDCl_3$, δ): 20.08 ppm.

FTIR (ATR): 3292 (O-H), 2936, 2860 (C-H), 1710, 1698 (C=O), 1628 (C=C), 1556 (N-H), 1160 (P=O), 989, 912 (P-O) cm^{-1}.

3.4. Interactions of Dental Monomers with Hydroxyapatite

HAP particles (0.1 g) were dispersed in 0.5 g of monomer/EtOH/H_2O (15/45/40 wt %) solution under stirring. The monomer-coated HAP particles were isolated by centrifugation after 24 h and washed first with ethanol and then with water and dried at room temperature. The crystal phases on the monomer-coated HAP particles were identified by a powder XRD operated under 40 kV acceleration, 40 mA current, and scanning rate of 2^{o} min^{-1} for 2θ/θ scan [75].

3.5. Hydrolytic Stability

The hydrolytic stability of monomer 2b was investigated by ^{1}H NMR measurement of 5 wt % solution of monomer in methanol-d4/D_2O (1/1, v/v) after storage at 37 °C for 25 days.

3.6. Synthesis of PBAE Macromers and Their Polymers

3.6.1. Synthesis of Poly(β-amino ester) (PBAE) Macromers

The diacrylates (HDDA and PEGDA) and amines (BPA1 and BPA2) were mixed at molar ratios of 1:1 and 1.2:1 in 10 mL scintillation vials at room temperature overnight while stirring. The viscous macromers were washed with petroleum ether or ether to remove unreacted amines and diacrylates, and dried under reduced pressure.

3.6.2. Synthesis of PBAE Network Polymers

The macromers were mixed with the photoinitiator (DMPA, dissolved in 1wt% methylene chloride) and the solvent was removed under reduced pressure. The macromer/initiator mixture was placed into a Teflon mold (5 mm diameter x 0.25 cm thick), covered with a mylar film and polymerized with exposure to UV light (365 nm) for 30 min. The polymer samples were weighed and placed in ethanol for 24 h to remove unreacted macromers and initiators. After drying in a vacuum oven for several days to reach constant weight, gel samples were weighed. The percentage of gelation was calculated according to the following formula:

$$\% \text{ Gelation} = \left(\frac{W_d}{W_i}\right) \times 100 \qquad (3.1)$$

Where W_i is the initial weight of the sample and W_d is the weight of the dried insoluble part of the sample after extraction with ethanol.

3.6.3. Synthesis of HEMA Hydrogels

The PBAE crosslinked HEMA hydrogels were prepared by dissolving HEMA (0.2 g, 0.15 mmol) containing 10 wt% PBAE crosslinkers and 1 wt% Irgacure 2959 in deionized water (1 mL). The mixtures were poured into Teflon molds (5 mm diameter x 0.25 cm thick), covered with a mylar film and polymerized with exposure to UV light (365 nm) for 30 min. The polymer samples were weighed and placed in ethanol for 24 hours to remove

unreacted macromers and initiators. After drying in a vacuum oven for several days to reach constant weight, gel samples were weighed. The percentage of gelation was calculated according to the formula (3.1).

3.7. Photopolymeriation

The photoinitiator (DMPA), as a solution in methylene chloride was added to the dental monomers and macromers at different concentrations and the solvent was removed in a vacuum desiccator. The polymerization behavior was monitored using real-time FTIR-ATR spectroscopy. A drop of the monomer/initiator solution was placed directly on the diamond ATR, covered with a mylar film and exposed to UV-irradiation with an Omnicure 1000 W mercury arc lamp at 320-500 nm. The conversion profiles were calculated from the decay of the absorption bands of the double bond peak at 1635 cm^{-1} with respect to the C=O peak at 1718 cm^{-1}, using peak height according to equation 3.2.

$$DC\ \% = \left(1 - \frac{Abs_{1635}^{sample}/Abs_{1718}^{sample}}{Abs_{1635}^{monomer}/Abs_{1718}^{monomer}}\right) \times 100 \qquad (3.2)$$

3.8. Degradation

Degradation studies were carried out using the polymers as prepared above. The polymer samples were submerged in PBS solution and placed on an orbital shaker at 37 °C. At each time point, samples were removed, dried, and weighed to determine the mass loss. Degradation % calculated according to the following formula:

$$\%\ \text{Degradation} = \left(\frac{W_i - W_f}{W_i}\right) \times 100 \qquad (3.3)$$

where W_i is the initial weight and W_f is the final weight of the sample.

3.9. In Vitro Cytotoxicity Assay

NIH-3T3 cells were cultured in RPMI 1640 complete medium, supplemented with 10 and 1 % FBS and penicillin–streptomycin antibiotic solution, according to ATCC

recommendations. Cells were grown in a 5 % CO2-humidified incubator at 37 °C. Trypsin–EDTA was used for detachment of cells.

To evaluate the cytotoxicity of the polymers on NIH 3T3 cell line, thiazolyl blue tetrazolium bromide (3-(4,5-dimethyl-thiazol-2yl)-2,5-diphenyltetrazolium bromide, MTT) assay was performed. NIH 3T3 cells were seeded at a density of 1x104 cells/well in 96 well plates. The next day, the medium was removed and different concentrations of synthesized polymers (10-100 μM) was added to cells with fresh culture medium. After 24 h incubation, the medium in each well was replaced with 150 μL culture medium and 50 μL of MTT solution (5 mg/mL) which forms purple formazan as a consequence of mitochondrial activity of viable cells. The cells were then further incubated for 4 h. Finally, ethanol:DMSO (1:1 v/v) solution was added to wells to dissolve formed formazan crystals. Following gentle shaking of plates for 15 min, absorbance intensity at 600 nm was measured with a reference wavelength of 630 nm using a microplate reader (BioTek ELx800 Absorbance Microplate Reader). Cells without any treatment were used as controls under the assumption of 100 % viability. Relative cells viability was calculated according to the formula:

$$\%viability = \frac{Asample}{Acontrol} x100 \ \ (n = 5) \tag{3.4}$$

Statistical analysis of the polymers was performed using the non-parametric Kruskal–Wallis test with Dunn's multiple comparisons post-test or Mann-Whitney test of GraphPad Prism 6 software package (GraphPad Software, Inc., USA). Data were reported as mean values ± standard deviation (S.D.). All tests were two-tailed tests and the differences between measurements were considered statistically significant if $p < 0.05$.

4. RESULTS AND DISCUSSION

4.1. Synthesis and Characterization of Starting Materials (BPA1 and BPA2)

Ethylidene bisphosphonate was prepared from tetraethyl methylene bisphosphonate by the method of Degendardt [74] (Figure 4.1). Then two secondary amines (BPA1 and BPA2) for the synthesis of monomers were prepared from the reaction of 1,4-butanediamine and 1,6-hexanediamine with ethylidene bisphosphonate in DMF at room temperature for two days (Figure 4.2). After purification, they were obtained as viscous liquids in high yield (80-90%). When the reaction was conducted at higher temperatures to decrease the reaction time, the retro-Michael's reaction was observed. According to the literature, the length of the carbon chain between the amino and the methylene bisphosphonic groups is of great importance and when a methylene group is present between the amino group and the tetraethyl methylene bisphosphonate, temperatures even a few degrees above 20 °C lead to the rapid formation of the retro-Michael's reaction products [76]. Both amines are readily soluble in polar (e.g. water, alcohols) and weakly polar (e.g. chloroform and diethyl ether) organic solvents but insoluble in very non-polar organic solvents (e.g. petroleum ether and hexanes) (Table 4.1).

Table 4.1. Solubilities of BPA1 and BPA2 in selected solvents

Amines	H_2O	MeOH	Ether	DCM	Petroleum ether	$CHCl_3$
BPA1	+	+	+	+	-	+
BPA2	+	+	+	+	-	+

The structures of the synthesized amines were confirmed by ^{1}H-, ^{13}C-NMR and FT-IR spectroscopy. The ^{1}H NMR spectra of the amines showed complex peaks due to phosphorus-hydrogen coupling and the nonequivalence of atoms within the geminal groups attached to the prochiral phosphorus atom. For example, the single bisphosphonate proton

of BPA1 and BPA2 is observed as a doublet of triplet at 3.0 ppm due to proton and two phosphorus coupling (Figure 4.3, 4.4). The ^{13}C NMR spectra of BPA1 and BPA2 are shown in Figure 4.5. The triplet seen at 37.4 ppm is due to the methine carbon attached to two phosphorus atoms. Other characteristic peaks are methyl protons at 16.3 ppm, methylene protons attached to nitrogen and oxygen at 49.1 and 62.5 ppm. The FTIR spectra of these amines contain absorption peaks of NH, P=O and P-O peaks at 3490, 1244, 1014 and 951 cm^{-1}, respectively (Figure 4.6, 4.7).

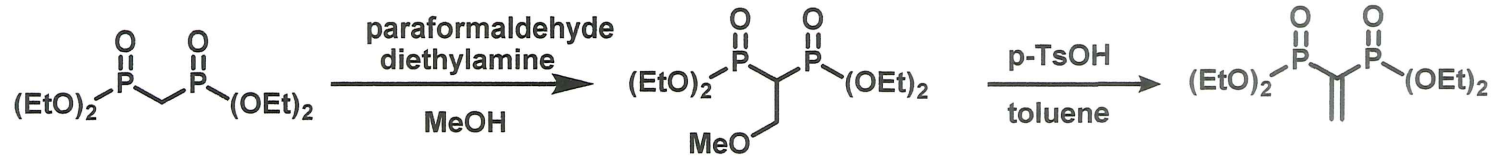

Figure 4.1. Synthesis of ethylidene bisphosphonate.

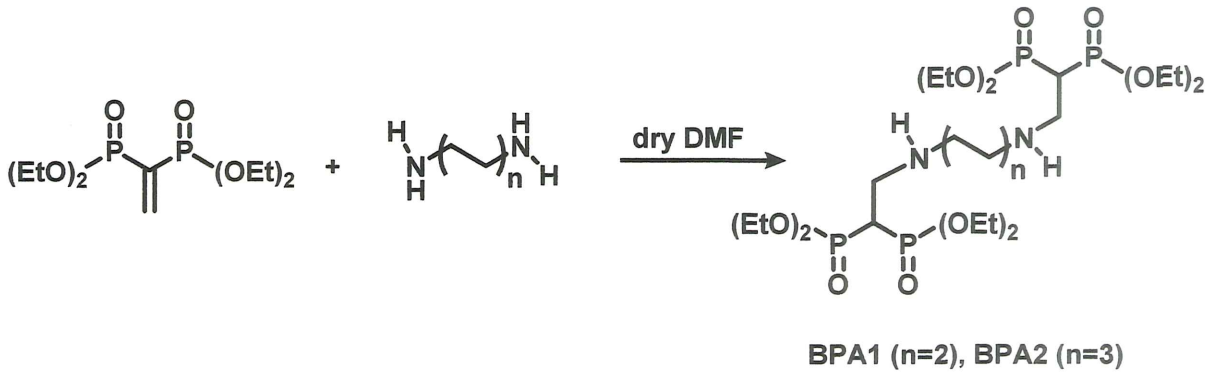

Figure 4.2. Synthesis of BPA1 and BPA2.

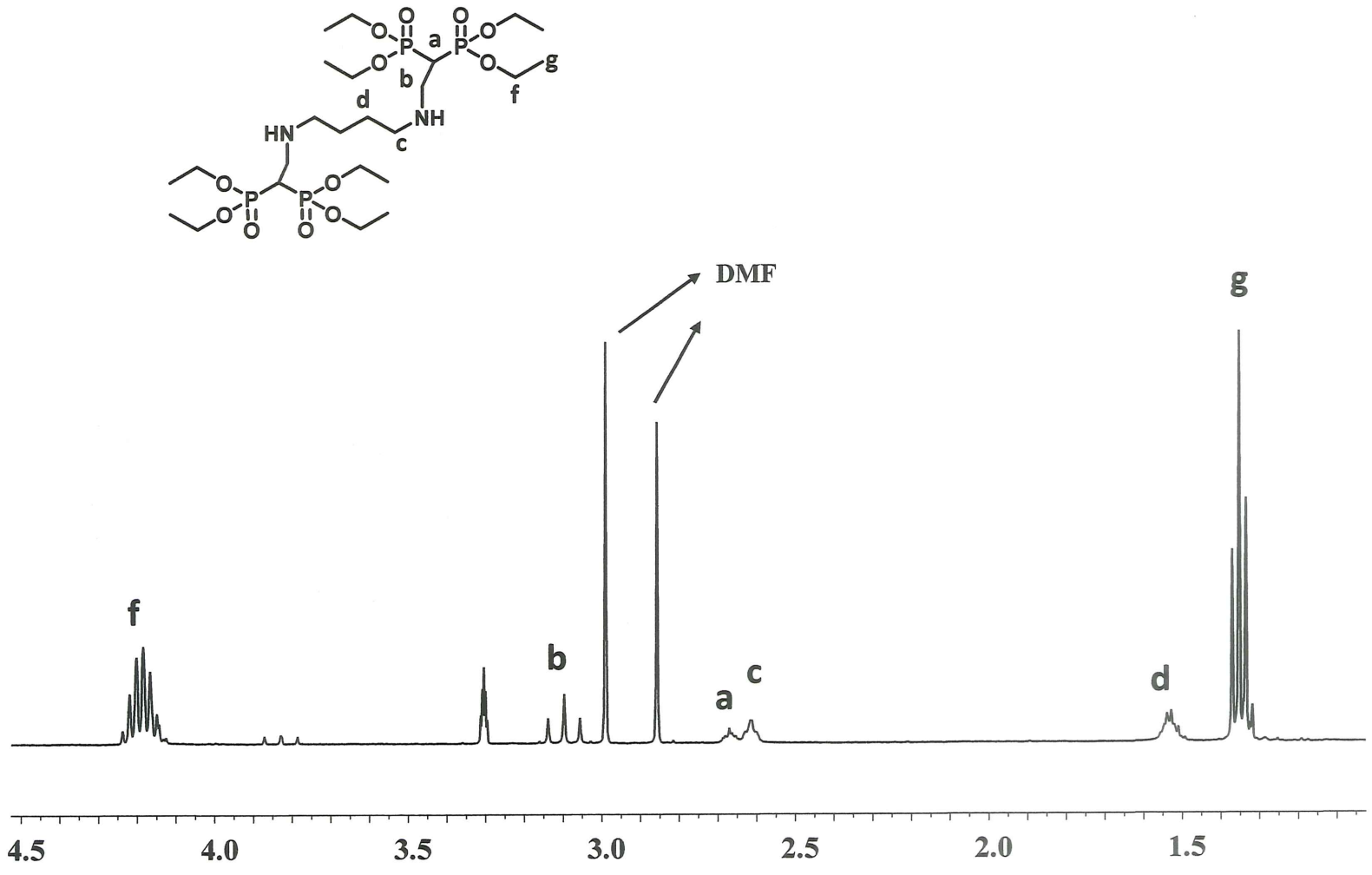

Figure 4.3. ^{1}H NMR spectrum of BPA1.

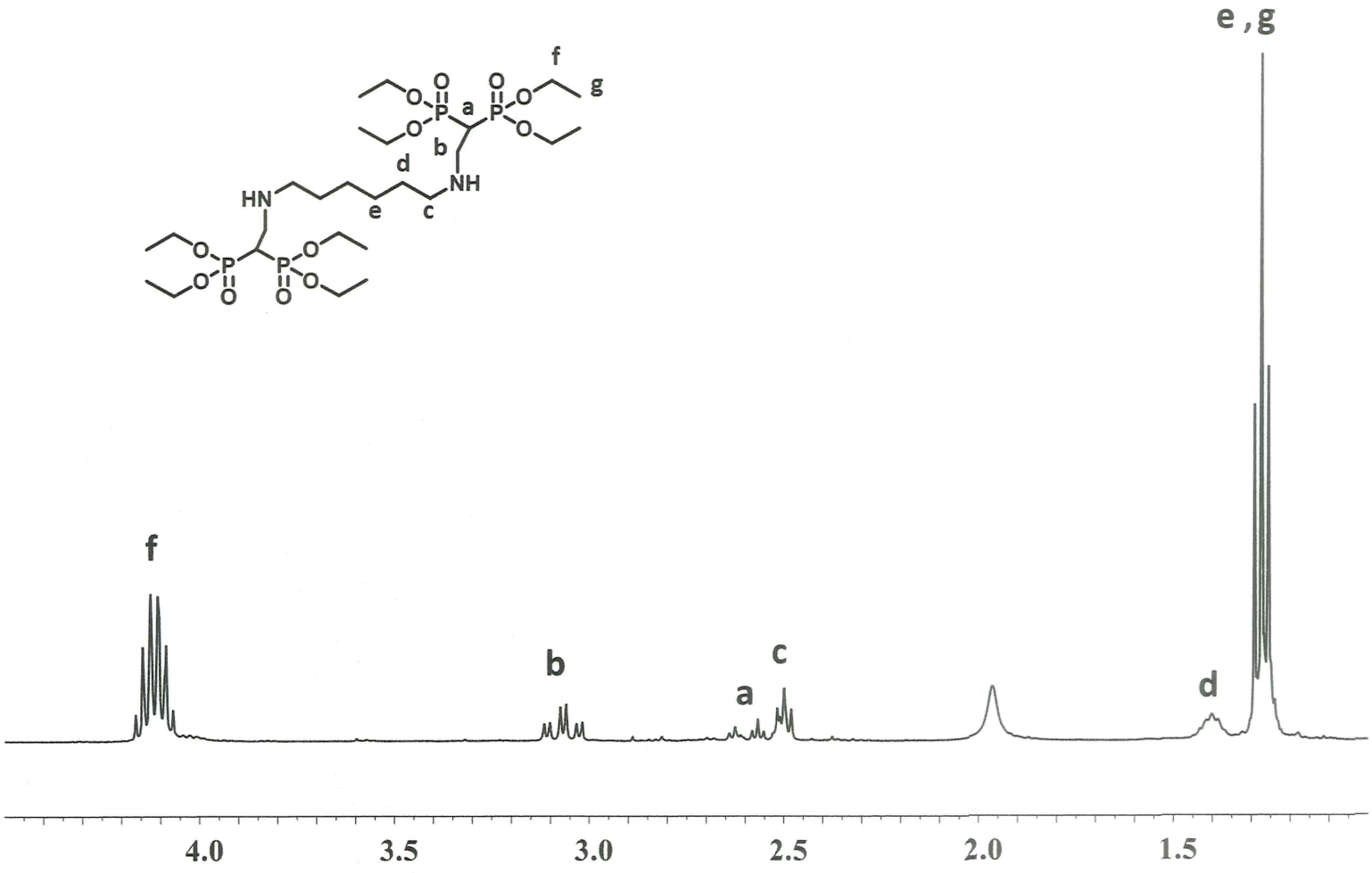

Figure 4.4. ^{1}H NMR spectrum of BPA2.

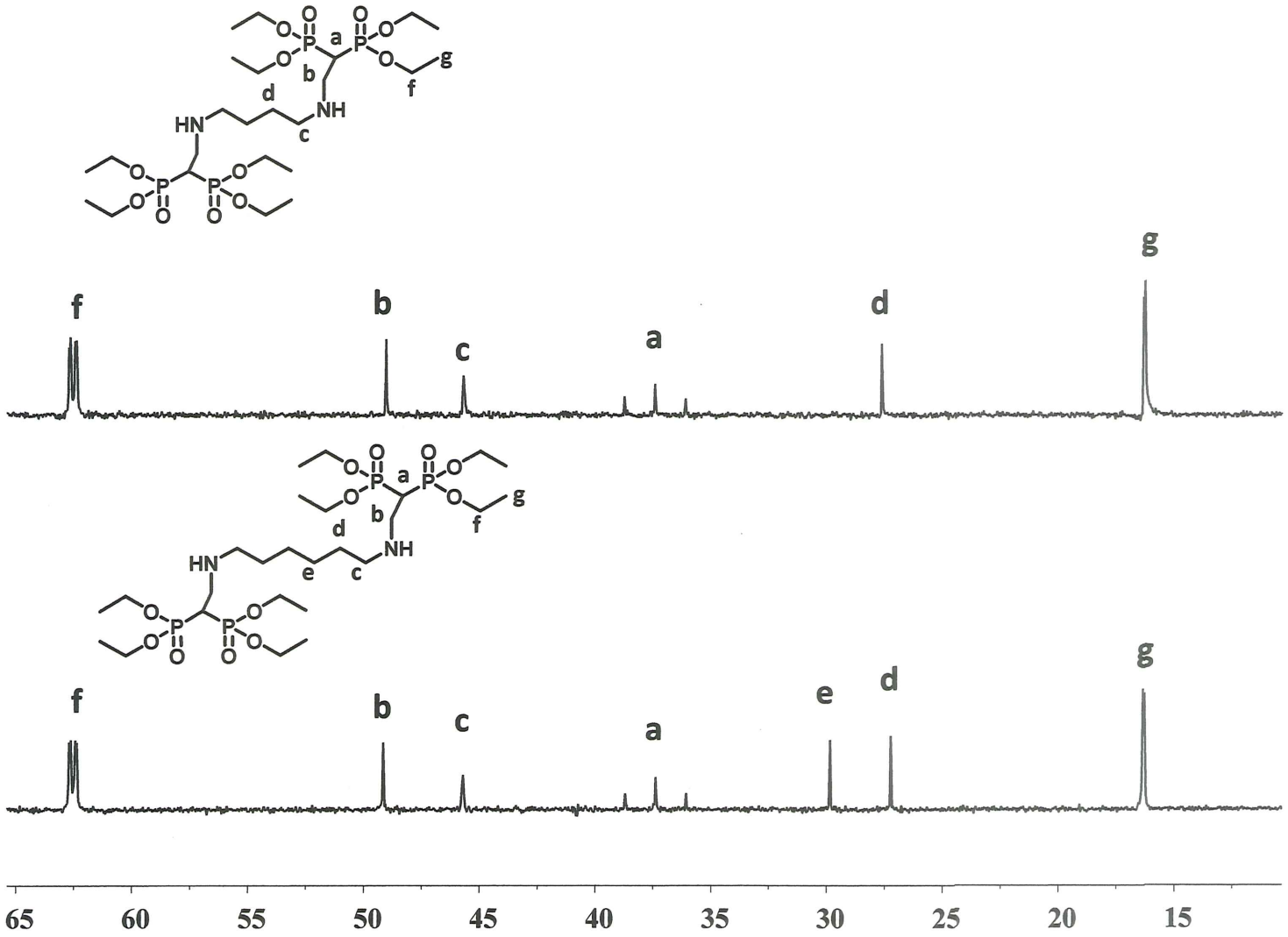

Figure 4.5. ^{13}C NMR spectra of BPA1 and BPA2.

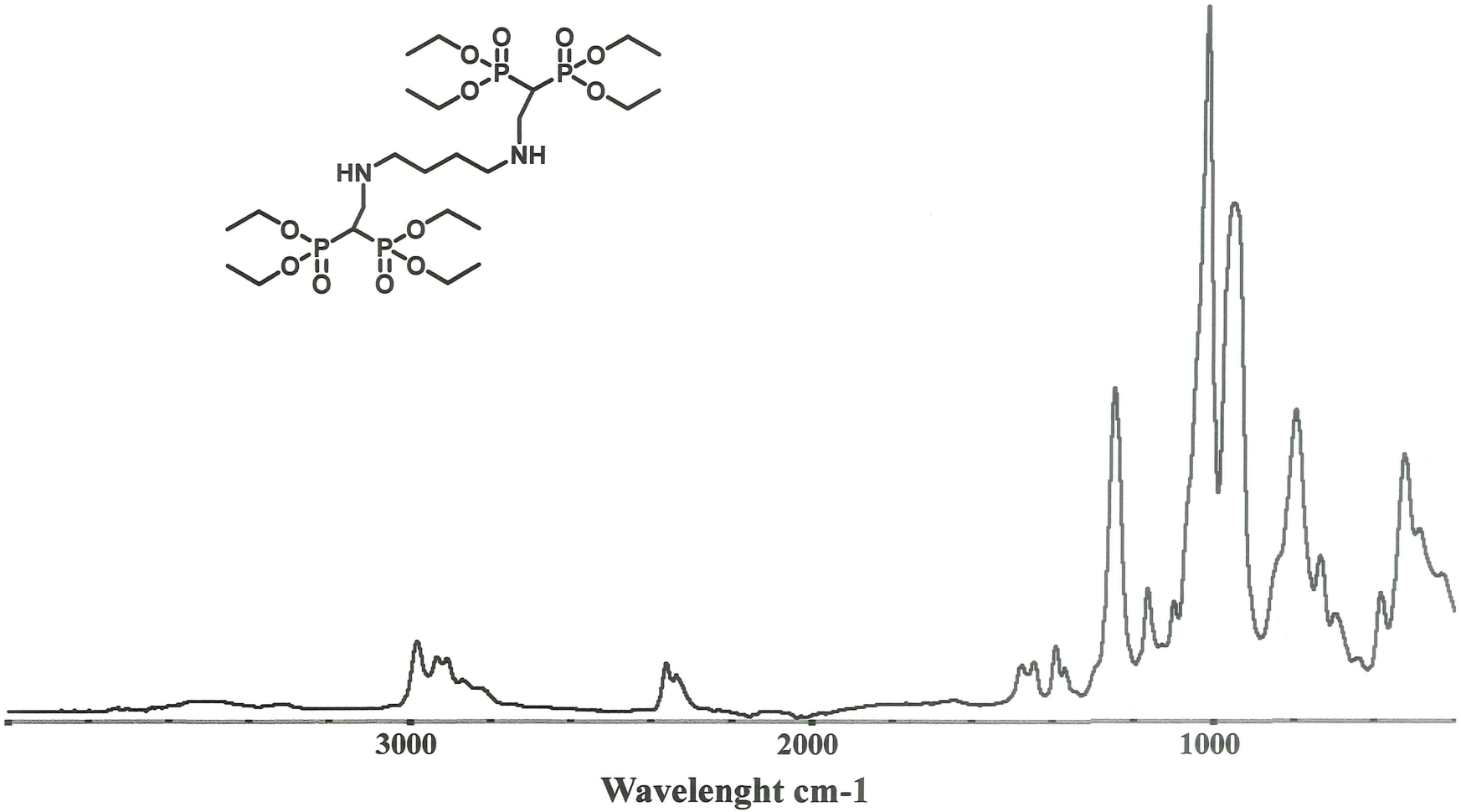

Figure 4.6. FT-IR spectrum of BPA1.

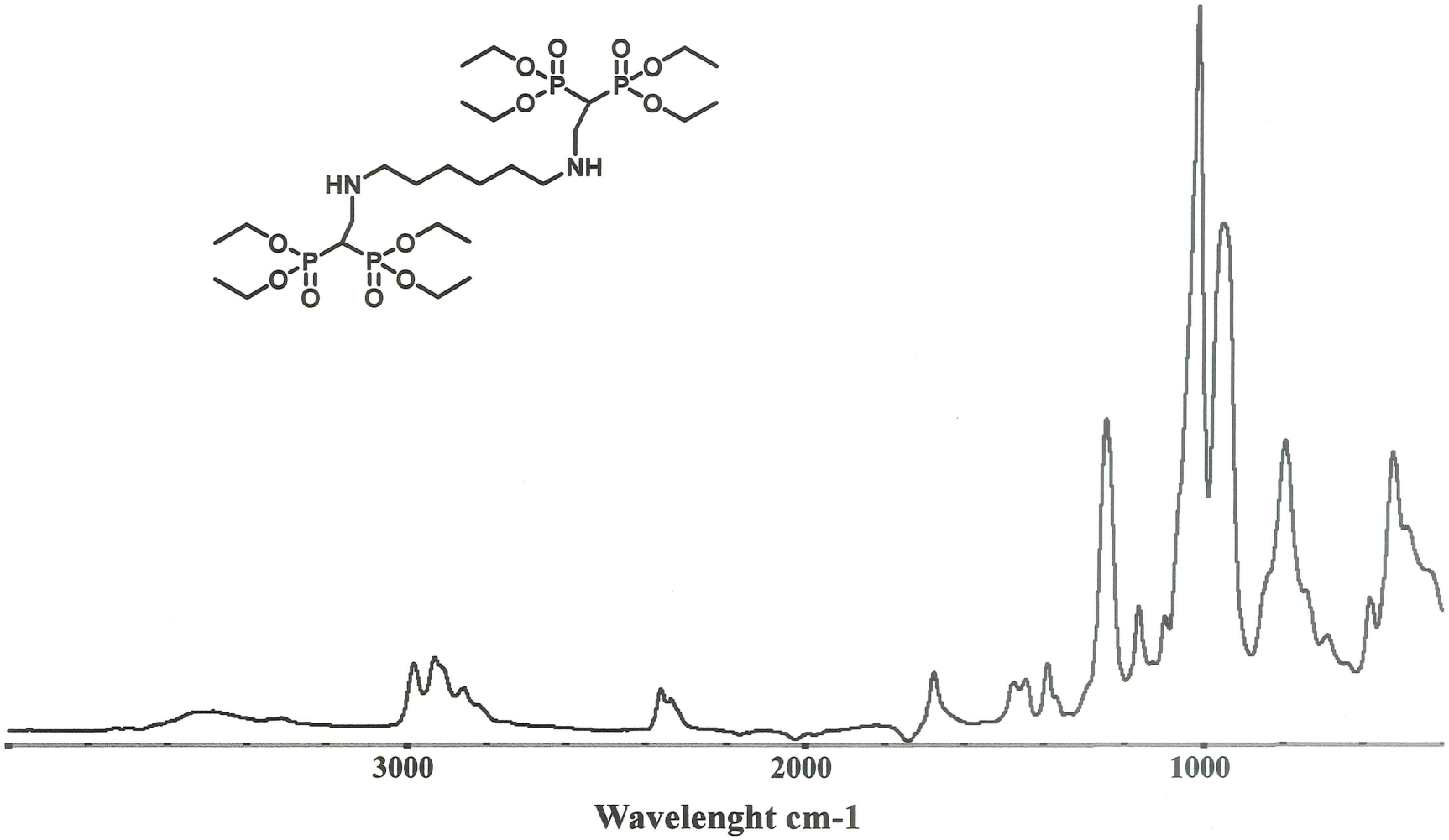

Figure 4.7. FT-IR spectrum of BPA2.

4.2. Dental Materials

4.2.1. Synthesis and Characterization of Dental Monomers

The amines were subsequently treated with IEM at room temperature in dry chloroform to give monomers 1a as a viscous liquid and 1b as a white solid with a melting point of 99 °C (Figure 4.8). Monomers 1a and 1b are well soluble in water, methanol, chloroform and THF but insoluble in diethyl ether (Table 4.2). The spectral data are in agreement with the expected structure of the monomers. For example, the single bisphosphonate proton is supported by the presence of a triplet of triplet at 2.83 (1b) and 2.90 (1a) ppm. The doublet of triplet at 3.63 and 3.69 ppm corresponds to methylene protons attached to methine. The presence NH protons were confirmed by the presence of a broad peak at 5.95 ppm (Figure 4.9, 4.10). In the ^{13}C NMR spectrum of 1b, the triplet seen at 35.81 ppm is due to the methine carbon attached to phosphorus (Figure 4.11). In the ^{31}P NMR spectrum of 1b, the singlet seen at 22.39 ppm is due to phosphorus atoms. (Figure 4.15). The FTIR spectra of each monomer showed NH stretching peaks of the urea groups at approximately 3341 cm^{-1} due to hydrogen bonding, the ester and urea carbonyl stretching peaks at 1716 and 1636 cm^{-1}, the amide II vibration at 1536 cm^{-1} and P=O peak at 1245 cm^{-1} (Figure 4.12).

The silylation of monomers 1a and 1b with TMSBr and methanolysis of the silyl ester groups provided the new bisphosphonic acid-containing urea dimethacrylates (2a and 2b) as white solids (Figure 4.8). Monomer 2b dissolves very well in water, while 2a is slightly soluble in water) (Table 4.2).

Table 4.2. Solubilities of 1a, 1b, 2a and 2b in selected solvents.

Monomers	H_2O	MeOH	Ether	DCM	THF	$CHCl_3$
1a	+	+	-	+	+	+
1b	+	+	-	+	+	+
2a	+	+	-	-	-	-
2b	+	+	-	-	-	-

The ^{1}H NMR spectra of monomers show the complete disappearance of bisphosphonic ester peaks around 1.26 and 4.06–4.21 ppm (Figure 4.13, 4.14). In the ^{31}P NMR spectrum of 1b, the singlet seen at 20.03 ppm is due to phosphorus atoms (Figure 4.15). FTIR spectra of monomers show broad peaks in the region of 3000–2600 cm^{-1} and 2300–2100 cm^{-1} due to OH stretching, 1670–1600 cm^{-1} due to OH bending and strong peaks at 1652, 1610, and 1522 cm^{-1} due to C=O, C=C, and NH stretching, respectively. Also the strong bands at 998 and 915 cm^{-1} correspond to the symmetric and asymmetric vibration of P-O (Figure 4.12).

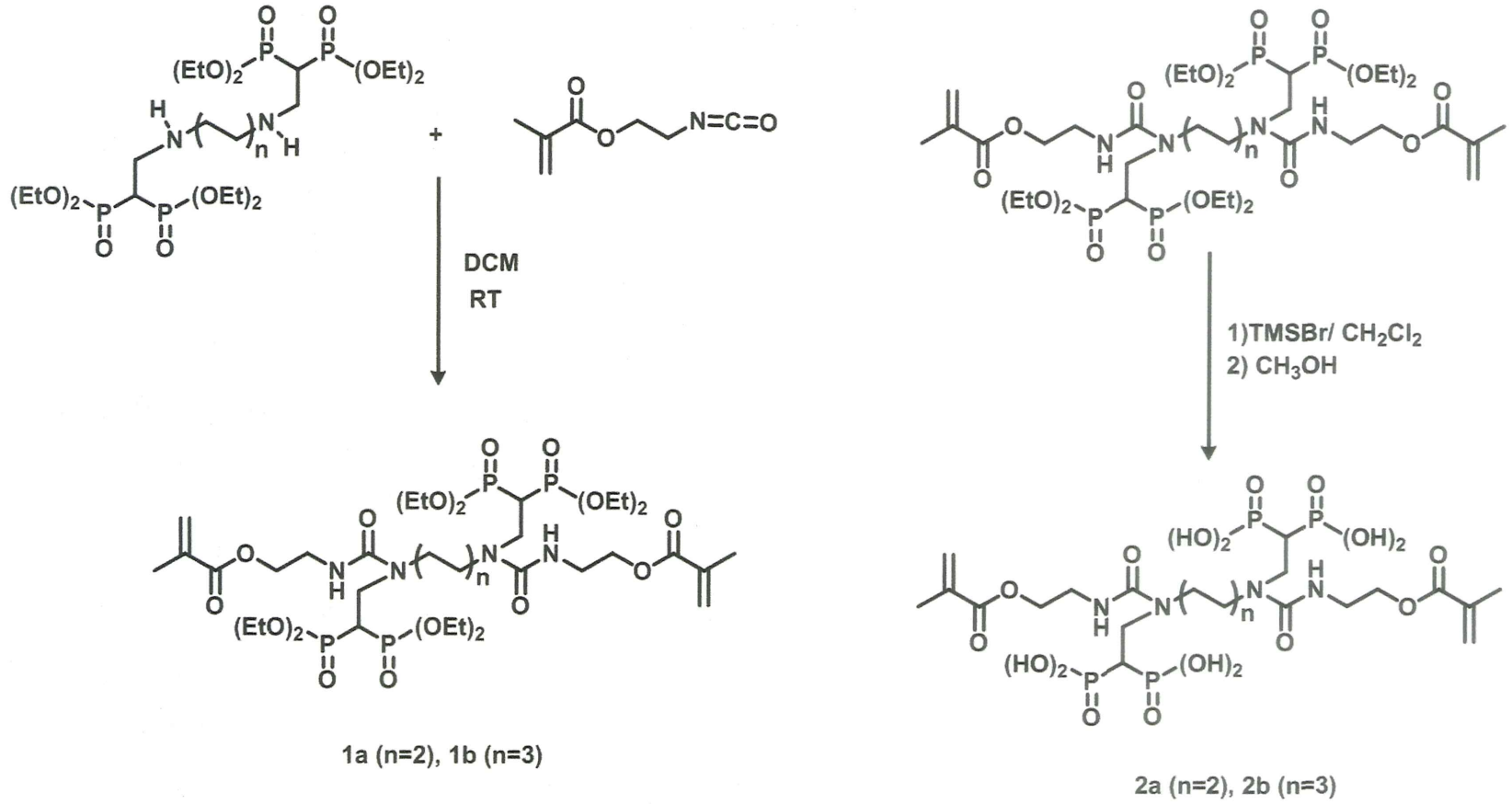

Figure 4.8. Synthesis schemes of 1a, 1b and 2a, 2b.

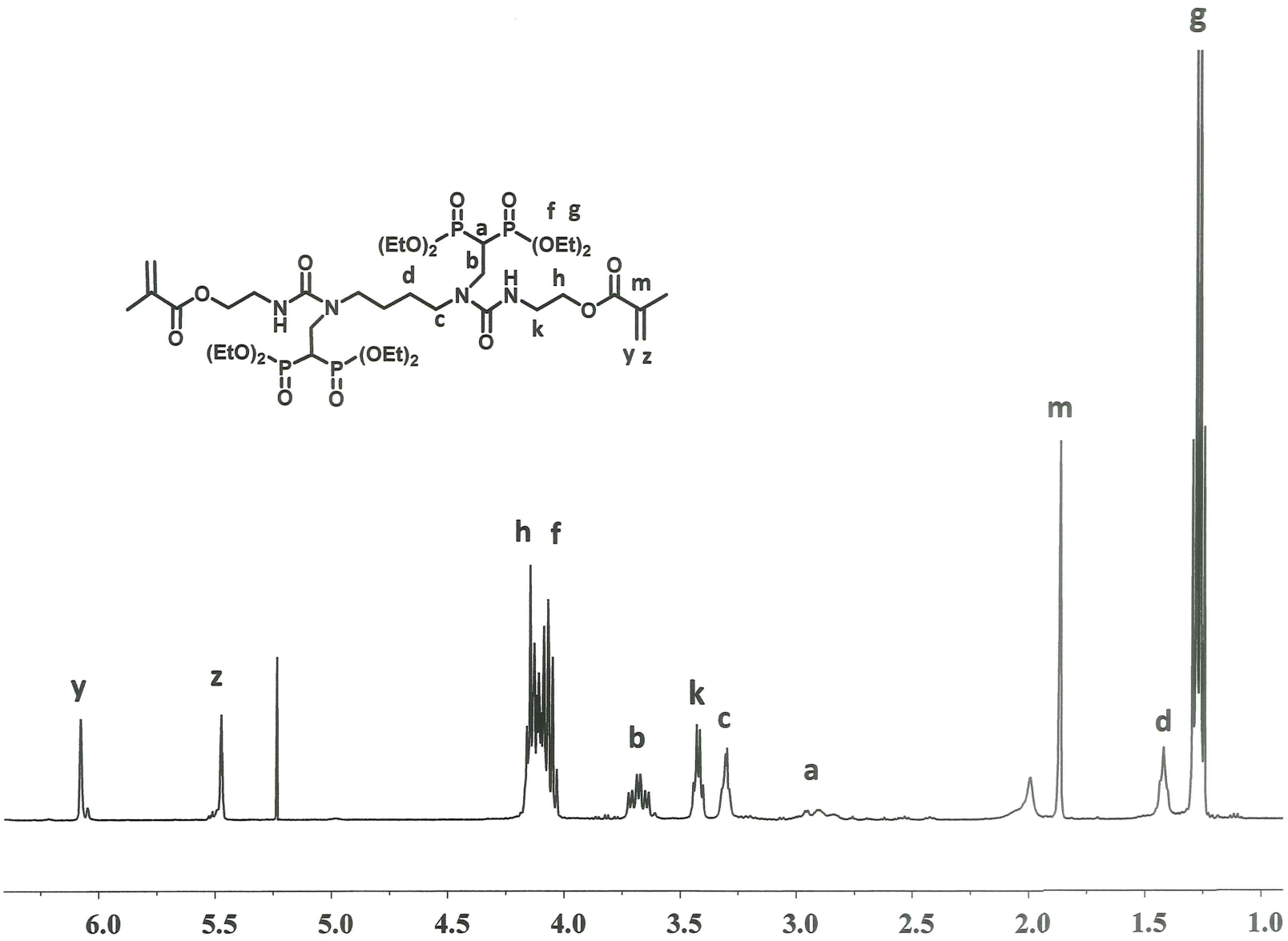

Figure 4.9. ^{1}H NMR spectrum of 1a.

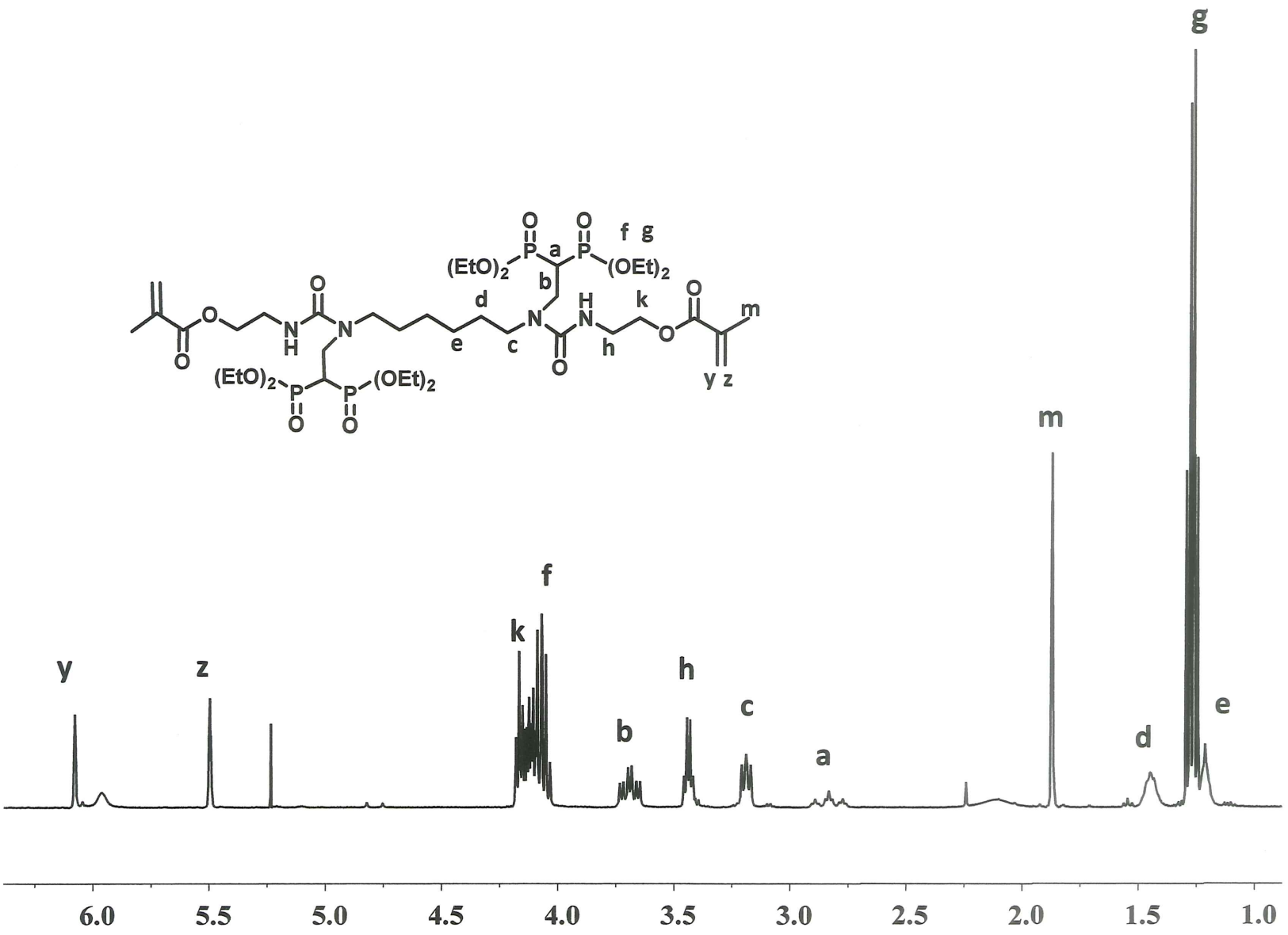

Figure 4.10. ^{1}H NMR spectrum of 1b.

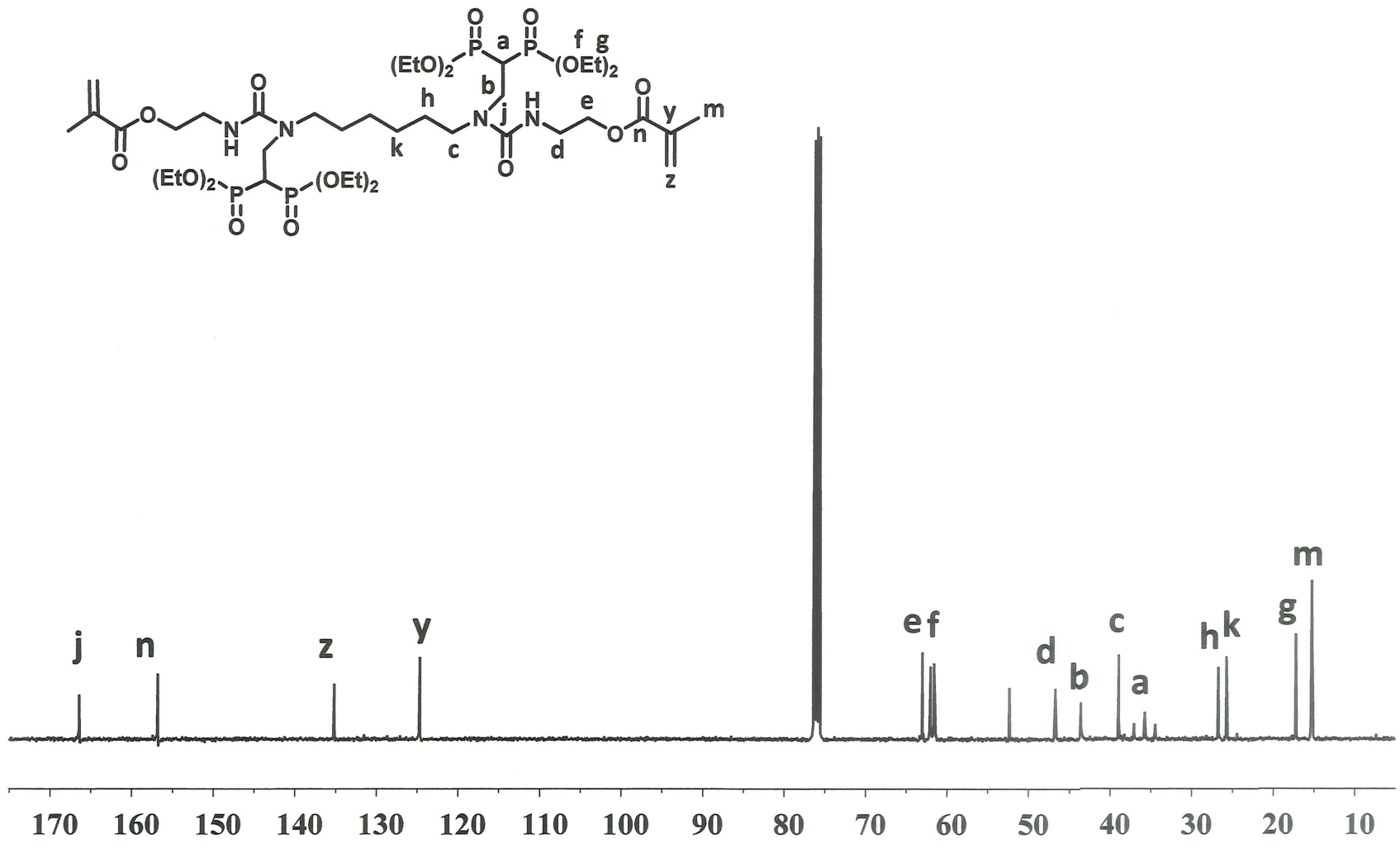

Figure 4.11. ^{13}C NMR spectrum of 1b

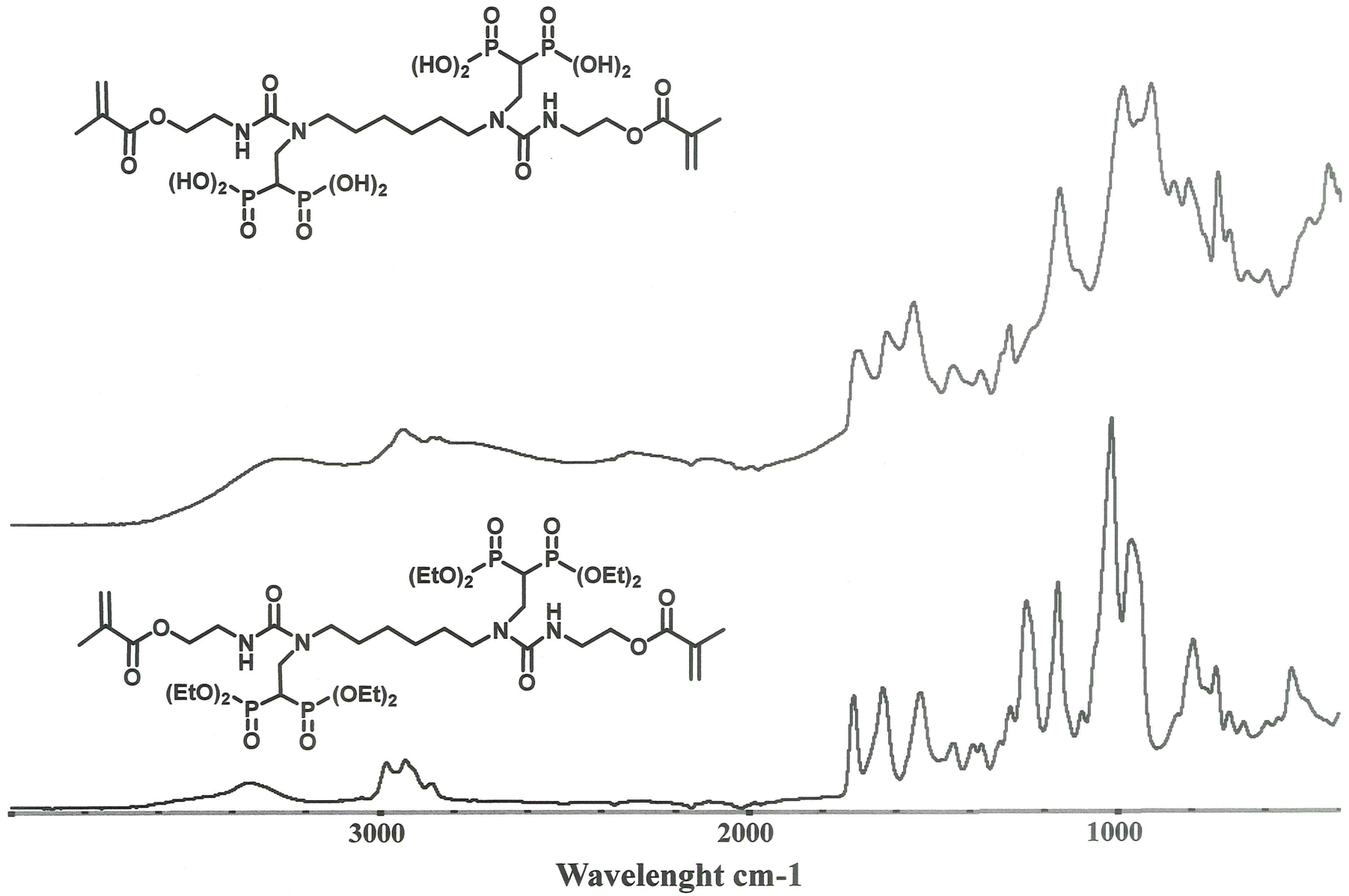

Figure 4.12. FT-IR spectra of 1b and 2b.

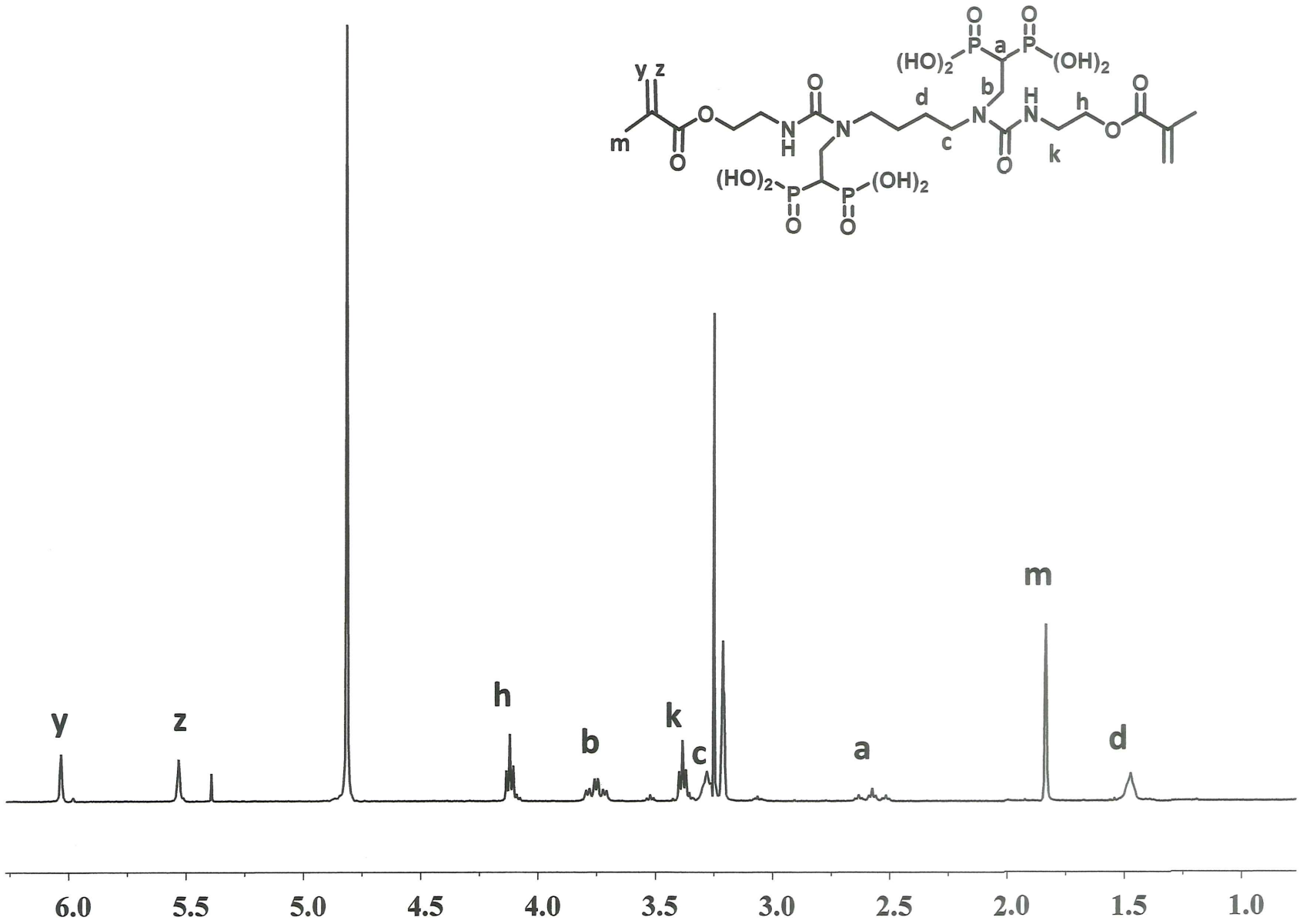

Figure 4.13. ^{1}H NMR spectrum of 2a.

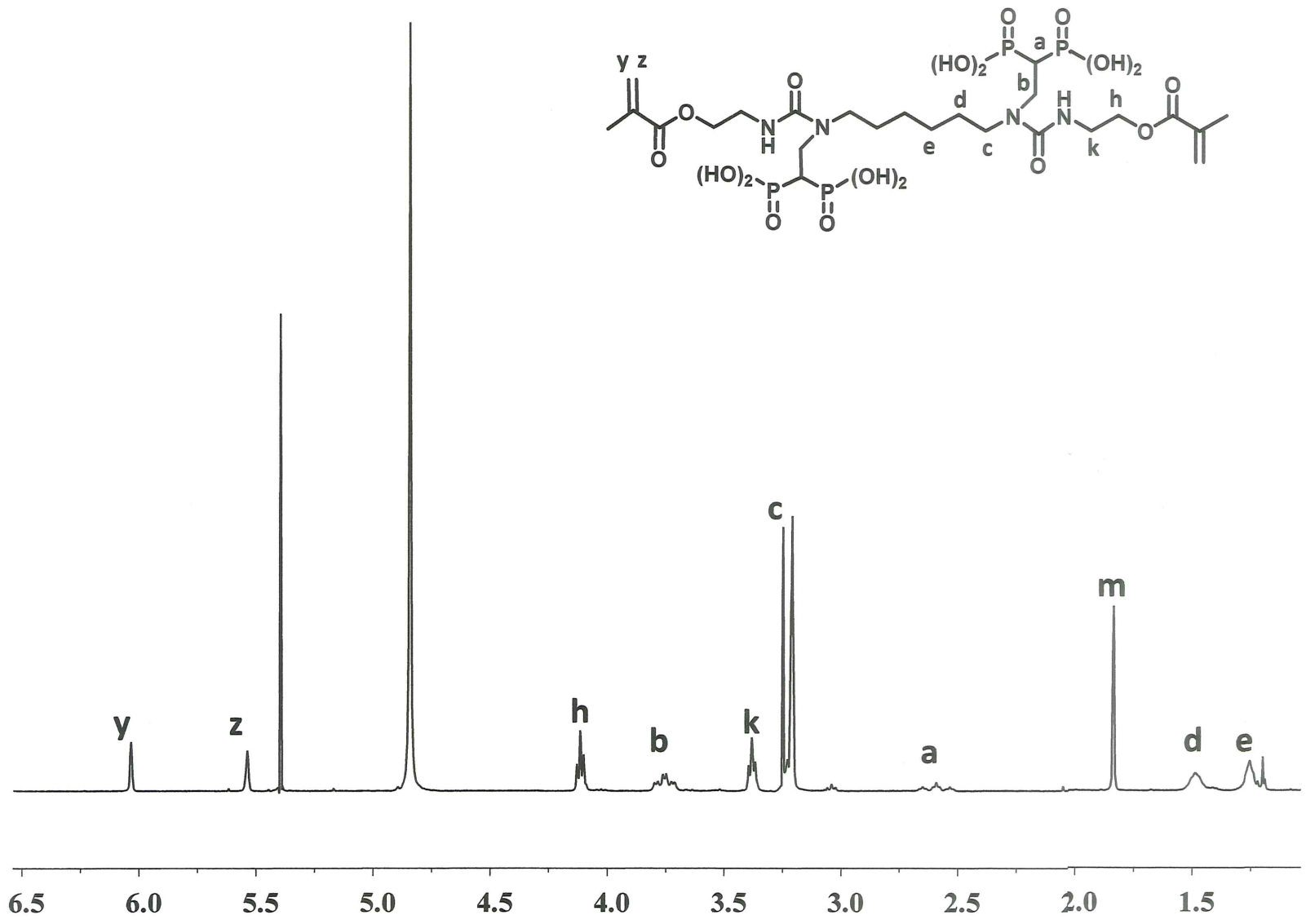

Figure 4.14. ^{1}H NMR spectrum of 2b.

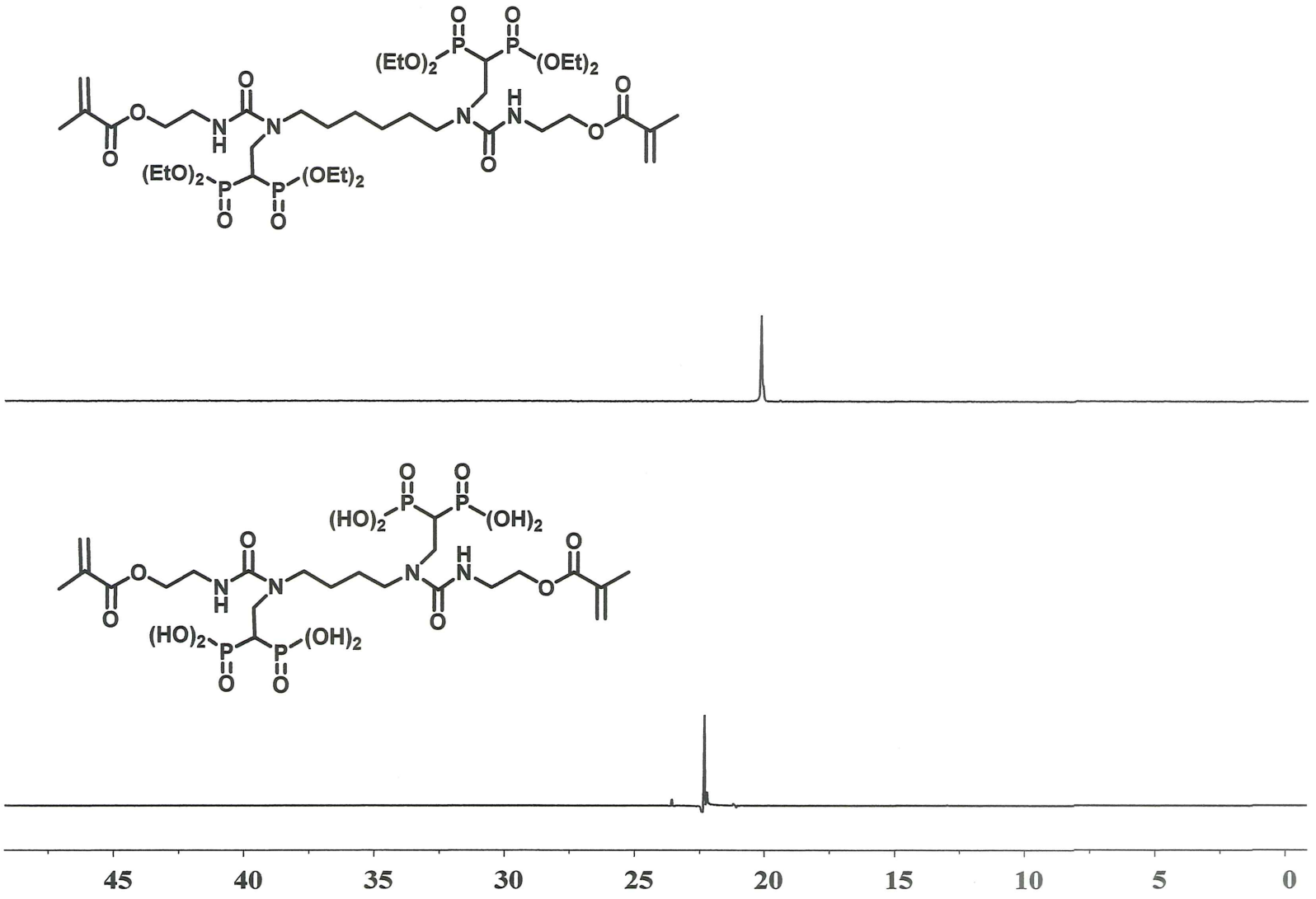

Figure 4.15. ^{31}P NMR spectra of 1b and 2a.

4.2.2. Acidity, Interactions with HAP, and Stability of Acid Monomers

The pH value of aqueous solution of monomer 2a (1 wt %) and 2b (1 wt %) was found to be 1.73 and 1.81, indicating their enamel etching abilities. The higher pH value of 2b solution can be explained partially due to its higher molecular weight.

The interaction of monomers 2a and 2b with dental tissues and bone was demonstrated by investigating their interactions with HAP as a model compound. The monomer-treated HAP solutions were analyzed by XRD to observe the changes in the crystal structure of HAP.

The obtained XRD patterns can be interpreted according to the adhesion–decalcification mechanism proposed by Yoshida and coworkers [75]. According to this mechanism, first, the decalcification of HAP is induced by monomer adsorption from the aqueous solution. Then, calcium salts of monomers ($CaMHP_2$) and $CaHPO_4.2H_2O$ (DCPD) are deposited on HAP depending on their solubilities in water–ethanol solution. XRD spectrum of untreated HAP was used as reference and to compare the performance of the synthesized monomers, MDP, which has been shown to have excellent binding ability, was used as a control monomer.

Upon treatment with monomer 2a/EtOH/H_2O solution, HAP showed a new peak around $2\theta = 5\text{-}8^{\circ}$ which is assigned to Ca salts of monomer. These salts remained attached to HAP even after being washed with ethanol and water, indicating their stabilities and bonding performances. Also, a new peak was detected at $2\theta = 11.6^{\circ}$ which was assigned to deposited DCPD, indicating etching and demineralization (Figure 4. 16).

4.2.3. Photopolymerization Studies of Dental Monomers

The photopolymerization reactivity of the synthesized monomers was investigated with Real-Time FT-IR experiments during their copolymerizations with commercial dental monomers (Bis-GMA, TEGDMA and HEMA) using DMPA (2 mol%) as photoinitiator.

First, formulations consisting of mixtures of Bis-GMA, TEGDMA and 1b at various ratios were prepared. Figure 4.17 shows their photopolymerization results at 25 °C. It was observed that addition of 1b to Bis-GMA:TEGDMA (50:50 mol%) mixture resulted in gradual decreases in the double-bond conversion (DBC) with increasing fraction of 1b. For example, Bis-GMA:TEGDMA mixture containing 20 mol % 1b showed the lowest DBC (29 %). This is expected because the photopolymerization of multifunctional monomers gives polymer networks where the chain mobility decreases and is reduced in DBC.

Conversion also depends on the flexibility of monomers. Polar monomers with high inter- and intramolecular forces decrease the flexibility of the system, increase T_g and decrease DBC. It was observed that addition of 5 % 1b decreased DBC of Bis-GMA:TEGDMA (50:50 mol%) mixture less than that of 1a (Figure 4.17). The reason for higher conversion obtained with monomer 1b is due to its more flexible structure (hexyl versus butyl groups) which increases the mobility of the system.

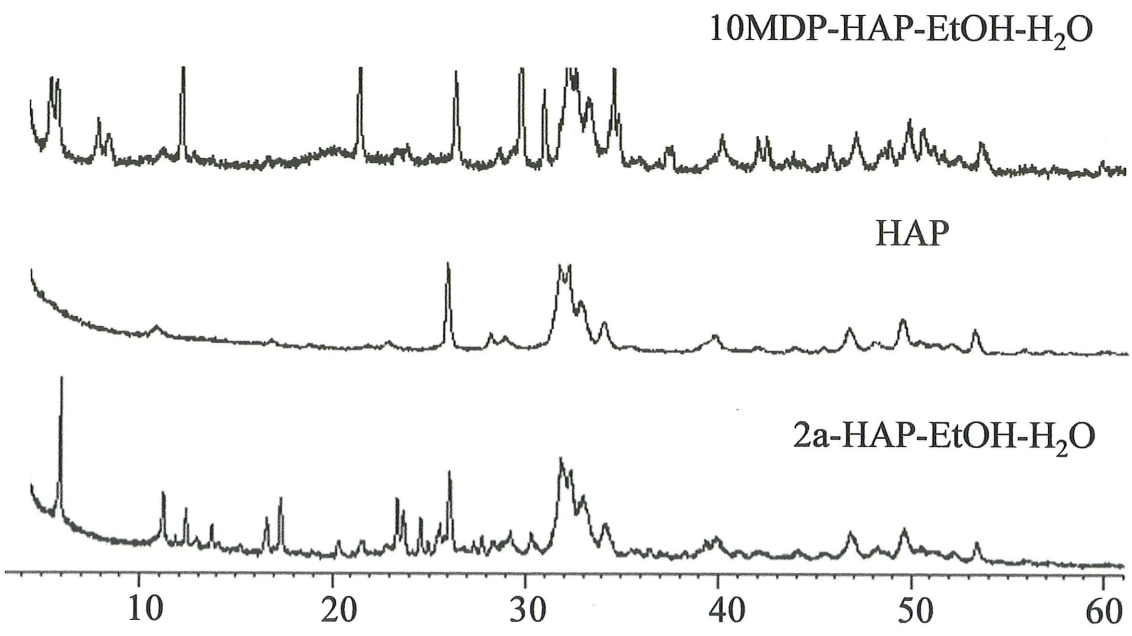

Figure 4.16. XRD patterns of HAP, MDP-HAP and 2a-HAP samples.

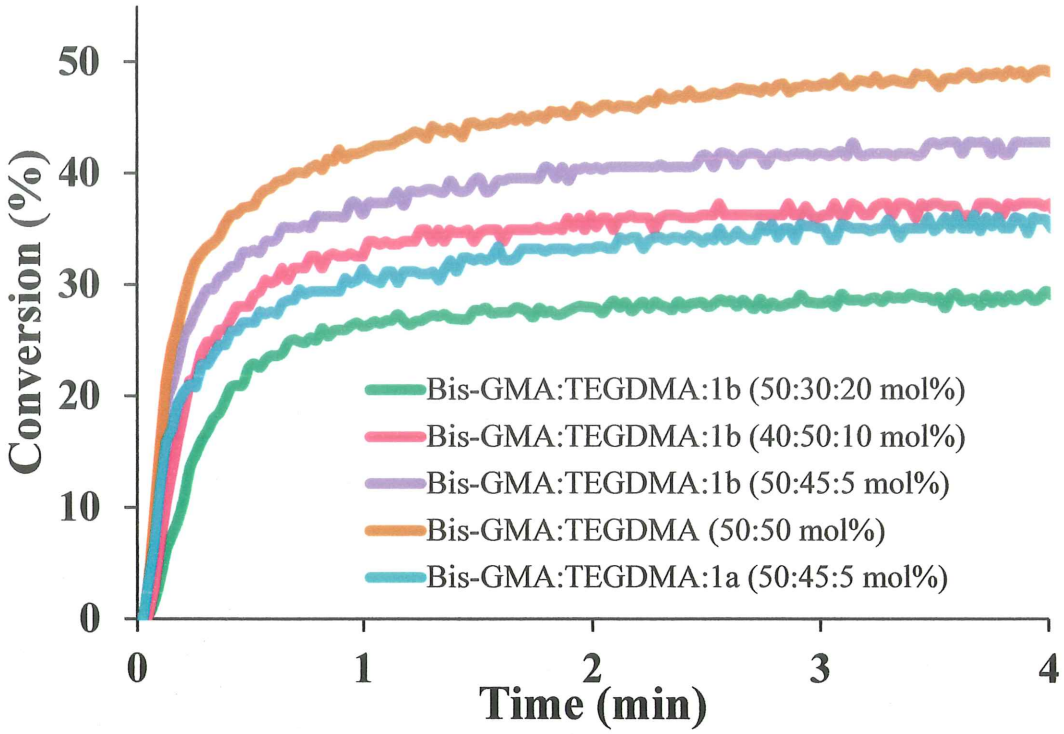

Figure 4.17. Conversion-time plots for the photopolymerization of Bis-GMA, TEGDMA and 1b in different concentrations.

To show the increase of flexibility of the systems with temperature, photopolymerizations of Bis-GMA:TEGDMA (50:50 mol%) and Bis-GMA:TEGDMA:1b (50:45:5 mol%) mixtures were also carried out at 40 °C. The slight improvement in DBC values were observed for both systems, as expected (Figure 4.18).

We also investigated copolymerization of 1b with HEMA at 25 °C. Time-based conversions showed that an increase of 1b leads to a faster reaction but also to a less complete polymerization. For instance, the conversion decreases from 54% to 42% when 1b concentration was increased from 10 to 30 weight% (Figure 4.19).

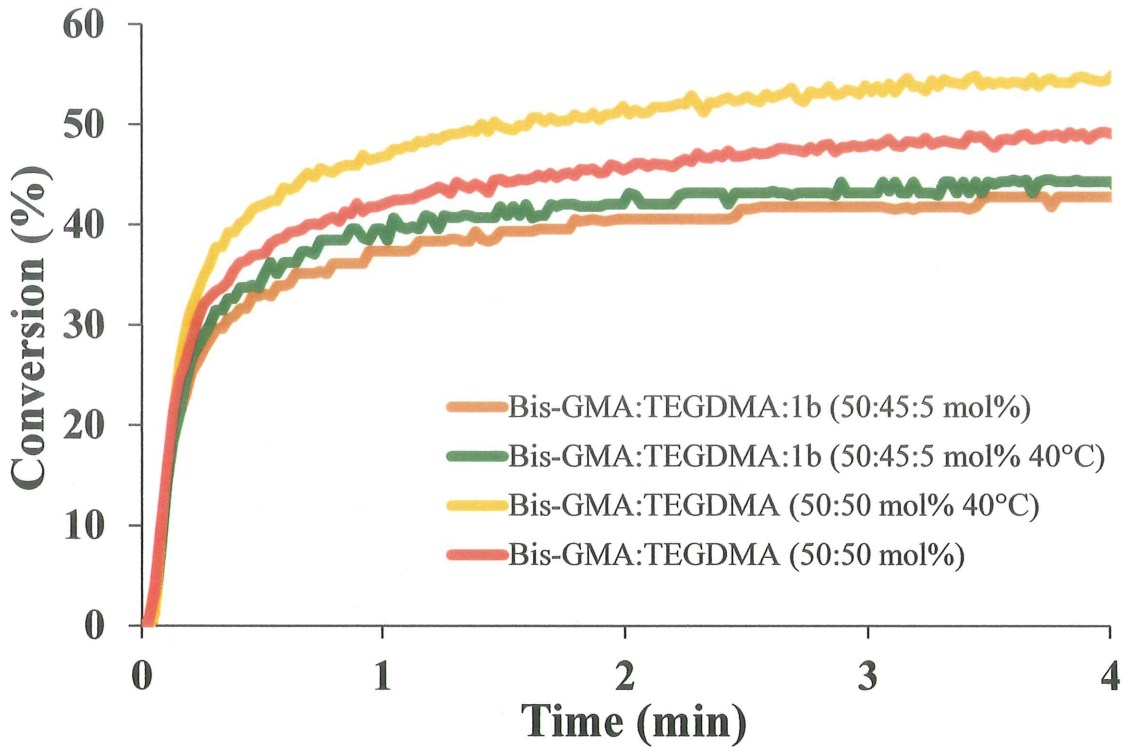

Figure 4.18. Conversion-time plots for the photopolymerization of Bis-GMA, TEGDMA and 1b at different temperatures.

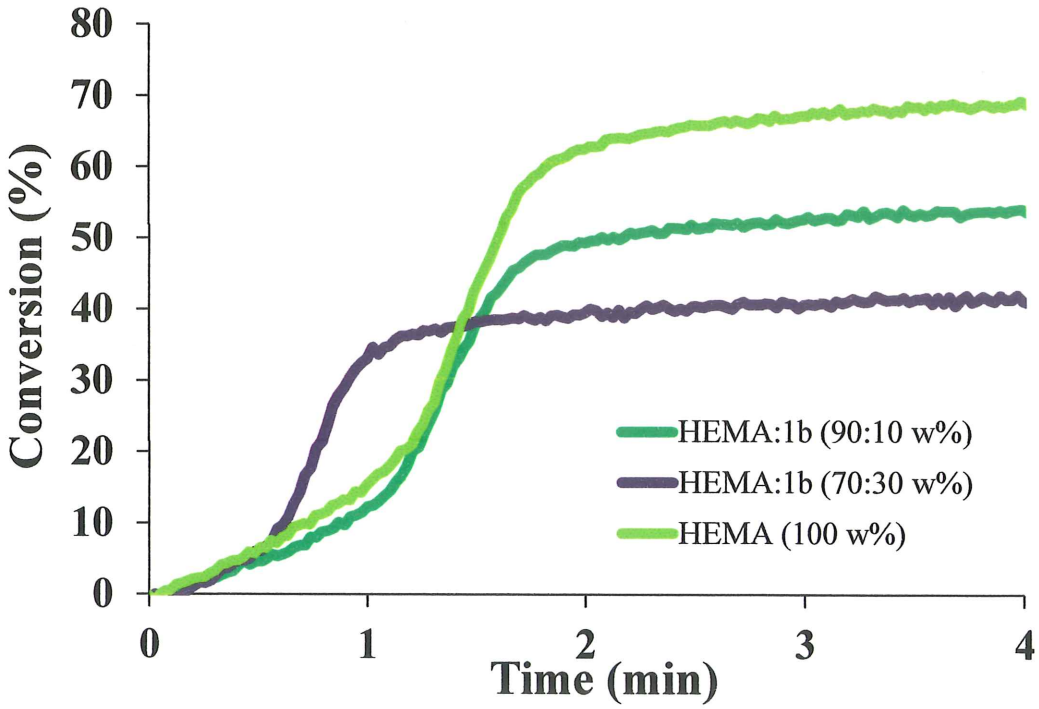

Figure 4.19. Conversion-time plots for HEMA and copolymerization of HEMA and 1b with 90:10 w% and 70:30 w% ratios.

Bulk copolymerization of the synthesized bisphosphonic acid monomers, 2a and 2b, with HEMA was studied to compare their reactivity in adhesive systems. The mixtures of HEMA:2a and HEMA:2b (90:10, 70:30 mol %) were photopolymerized at 25 °C using DMPA (1 w%) as photoinitiator. The following conclusions can be drawn: (i) the time (t_{max}) of the maximum polymerization rate (the slope of conversion-time curves) is reduced compared to HEMA; (ii) incorporation of bisphosphonic acid monomers into HEMA lowered the conversions, proportional with their concentrations in the formulations. DBC values followed the order 57.38 % for HEMA:2a (90:10 mol%), 57.65% for HEMA:2b (90:10 mol%) and 70.15% for HEMA alone, respectively; (iii) conversions obtained for the bisphosphonic acid monomer formulations were about the same as the bisphosphonate formulations, but the polymerizations were about twice as fast (Figure 4.20). The higher rate of polymerizations of the acid containing formulations can be explained by hydrogen bonding due to bisphosphonic acid functionality which generates tri- or tetramethacrylates with an enhanced propagation rate as well as reduction in termination rate.

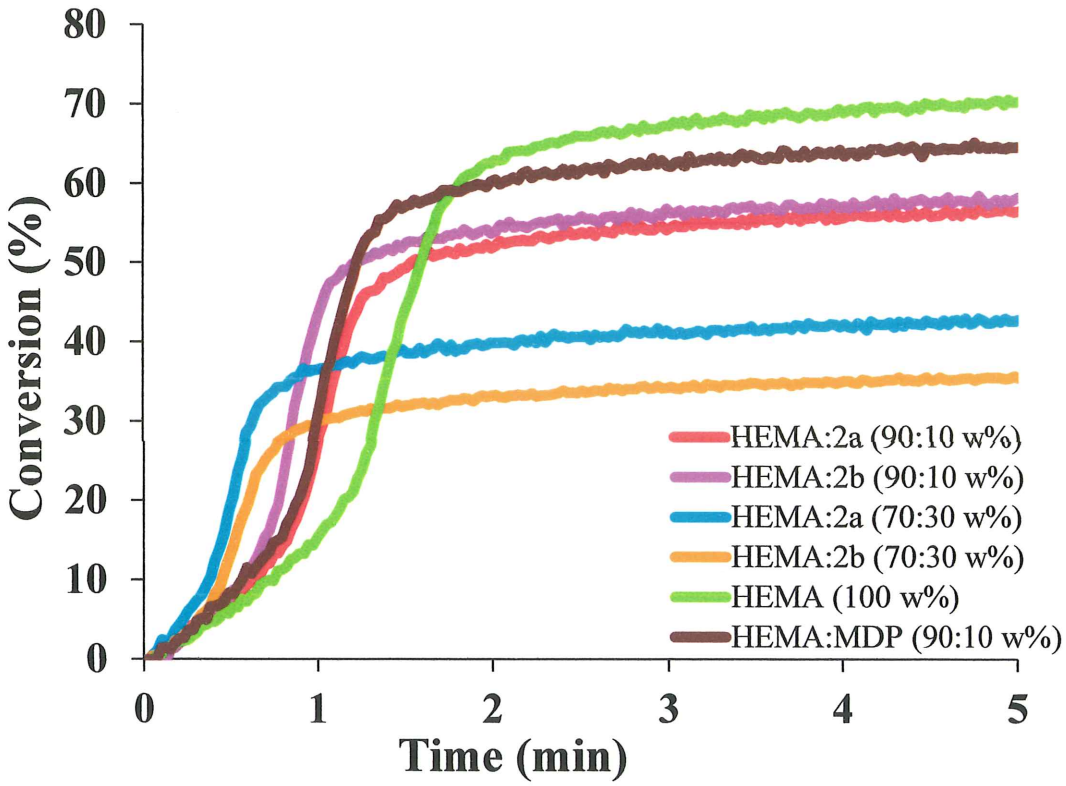

Figure 4.20. Conversion-time plots for copolymerization of HEMA and acid monomers (2a, 2b and commercial MDP).

To investigate the effect of temperature on polymerization of the HEMA:2b formulation, polymerization rates and conversions were measured at various temperatures (25, 40, 80 and 120 °C) (Figure 4.21). The maximum rate of polymerization increases with increasing temperature from 25 to 80 °C. On the other hand, the same formulation shows decrease in the maximum polymerization rate as the temperature is increased from 80 to 120 °C because of the effect of hydrogen bonding on the rate of polymerization. This was explained in the literature as; at high temperatures hydrogen bonded species behave like regular (non-hydrogen bonding) diacrylates or dimethacrylates due to cleavage of hydrogen bonds. Therefore, as temperatures increases the polymerization rate actually decreases or is ameliorated with respect to what is found for regular (meth)acrylates [77].

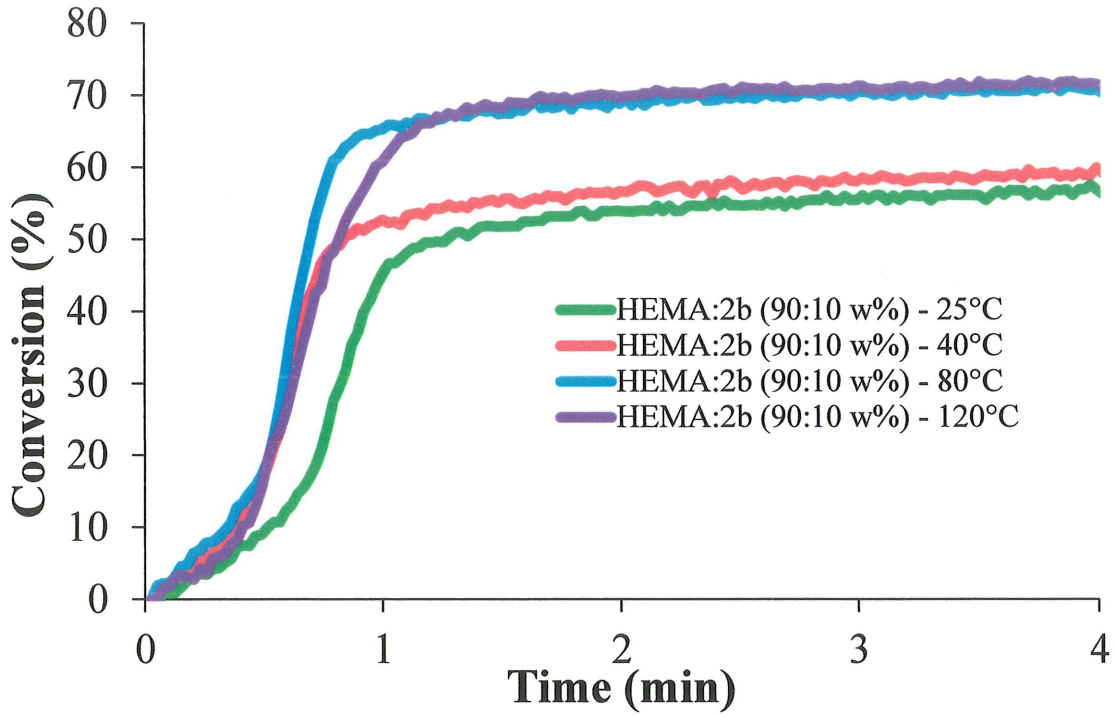

Figure 4.21. Conversion-time plots for copolymerization of HEMA and 2b at different temperatures.

4.2.4. In Vitro Cytotoxicity of Dental Monomers

The cytotoxicity of the two dimethacylate 1b and 2b was tested on NIH 3T3 mouse embryonic fibroblast cells using standart MTT assay and compared with commercial MDP

since it has phosphoric acid functionality. Materials resulting in more than 80% viability are defined as non-cytotoxic according to ISO 10993-5 [78,79]. As seen in Figure 14 no significant cytotoxicity was detected between 10-200 μg/mL in 24 h. Although the standard deviation is a bit large, 2b is slightly more toxic with no dose dependency when compared to MDP or 1b which is the phosphonate analogue of 2b. Overall, the new bisphosphonated dimethcarylates are non-toxic with the tested range (Figure 4.22).

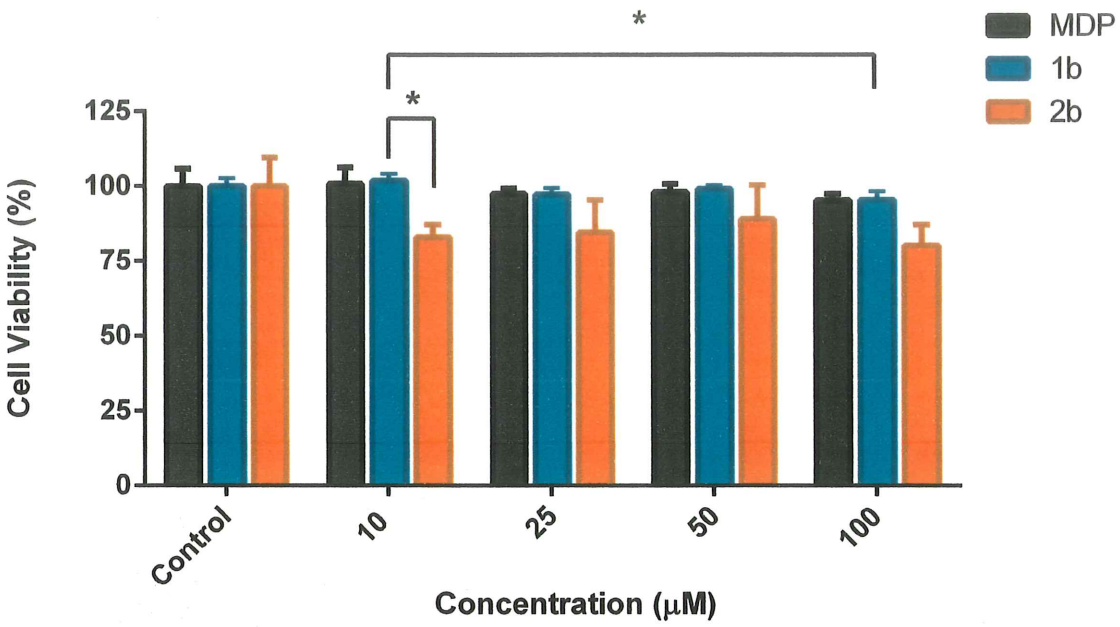

Figure 4.22. Viability of NIH 3T3 cells treated with MDP (10-methacryloyloxydecyl dihydrogen phosphate) as reference and sample 1b and 2b after 24 hours incubation measured with MTT. The data are expressed as mean ± S.D. (n = 5), ($p < 0.05$(*), $p < 0.01$ (**), $p < 0.001$ (***) and $p < 0.0001$(****)).

4.3. PBAE Macromers and Their Polymers

4.3.1. Synthesis and Characterization of PBAE Macromers

Four diacrylate terminated poly(β-amino ester) macromers were prepared using the solvent-free aza-Michael condensation of bisphosphonated amines (BPA1, BPA2) to diacrylates (HDDA, PEGDA) (Figure 4.23). All macromers are well soluble in ethanol and

chloroform, insoluble in hexanes and milky in water. Macromers synthesized from HDDA are soluble in ether but macromers synthesized from PEGDA are not (Table 4.3).

Diacrylates and amines were chosen to provide different hydrophilicities to investigate the effect of chemical structure on degradation properties. Diacrylate to amine molar ratio and the reaction conditions such as catalyst, temperature and solvents were changed to control the extent of polymerization and to try to avoid formation of crosslinked polymers (Table 4.4). Bulk reaction with 1.2:1 ratio at room temperature gave the best result for synthesis of the macromers. The macromers synthesized from HDDA were washed with petroleum ether and the macromers synthesized from PEGDA were washed with ether to remove unreacted diacrylates and amines.

Table 4.3. Solubilities of macromers in selected solvents.

Macromers	Chloroform	Ether	Acetone	Ethanol	Hexane	Water
HDDA-BPA1	+	+	+	+	-	+/-
HDDA-BPA2	+	+	+	+	-	+/-
PEGDA-BPA1	+	-	+	+	-	+/-
PEGDA-BPA2	+	-	+	+	-	+/-

The structures of the synthesized macromers were confirmed using ^{1}H-NMR spectroscopy (Figure 4.24, 4.25, 4.26, 4.27). Their spectra show the maintenance of acrylate peaks, the appearance of complex peaks due to phosphorus-hydrogen coupling and the nonequivalence of atoms within the geminal groups attached to the prochiral phosphorus atom. The average number of repeat units was calculated as n=1.5-3 and the number average molecular weight was calculated as ca. 1500-3000 by using GPC. The FTIR spectra of each macromer showed C=C peak at around 1620 cm^{-1} and C=O peak at around 1725 cm^{-1} (Figure 4.28, 4.29).

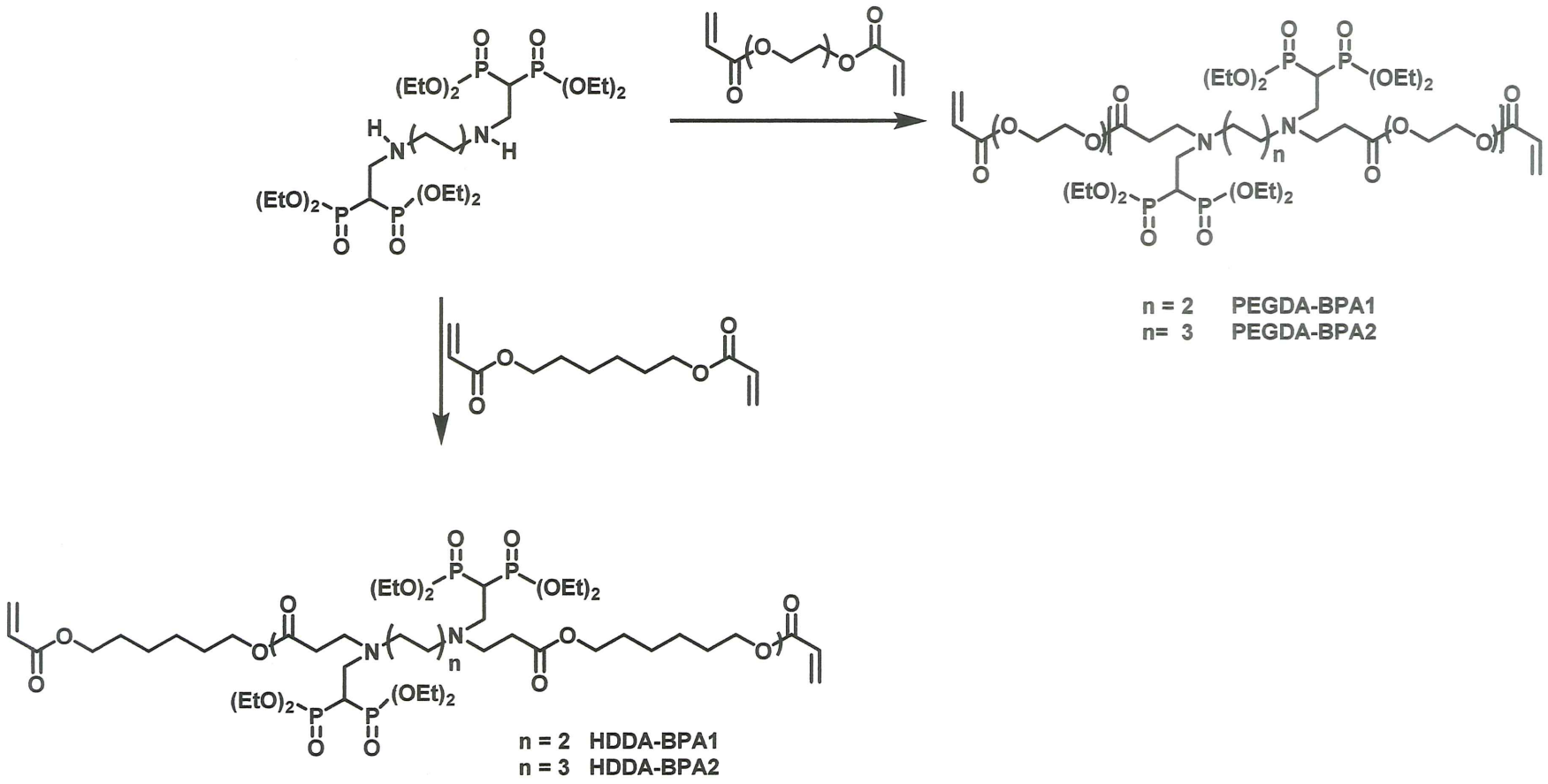

Figure 4.23. Synthesis of PBAE macromers.

Table 4.4. Reaction conditions for the synthesis of macromers.

Amine	Diacrylate	Ratio	Solvent	Catalyst	Temperature (°C)	Time	Polymer
BPA2	PEGDA	1:1	-	-	50	48 h	cross-linked
BPA2	HDDA	1:1	-	-	50	24 h	cross-linked
BPA2	HDDA	1:1	-	-	25	4 d	cross-linked
BPA2	HDDA	1:1	-	-	60	15 h	cross-linked
BPA2	HDDA	1.2:1	-	-	25	8 d	soluble
BPA2	HDDA	1:1	dry THF	CAN[a]	55	24 h	soluble
BPA2	HDDA	1:1	dry THF	-	55	48 h	cross-linked
BPA2	HDDA	1:1	water	borax	25	5 h	soluble
BPA2	PEGDA	1.2:1	-	-	25	8 d	soluble
BPA2	HDDA	1:1	dry acetonitrile	DBU[b]	25	6 h	cross-linked

a: Ceric Ammonium Nitrate

b: 1,8-Diazabicyclo[5.4.0]undec-7-ene

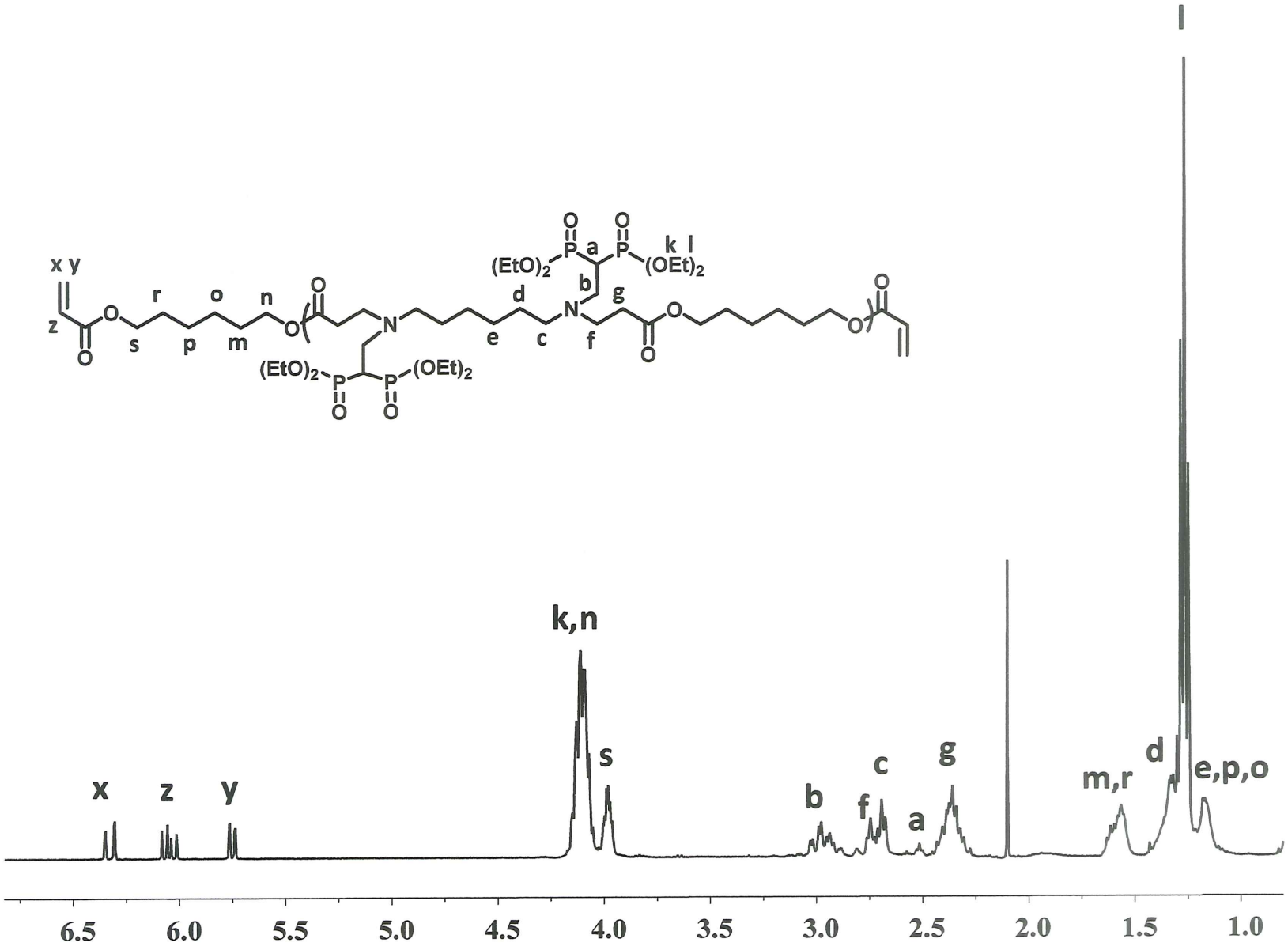

Figure 4.24. ^{1}H NMR spectrum of HDDA-BPA2 macromer.

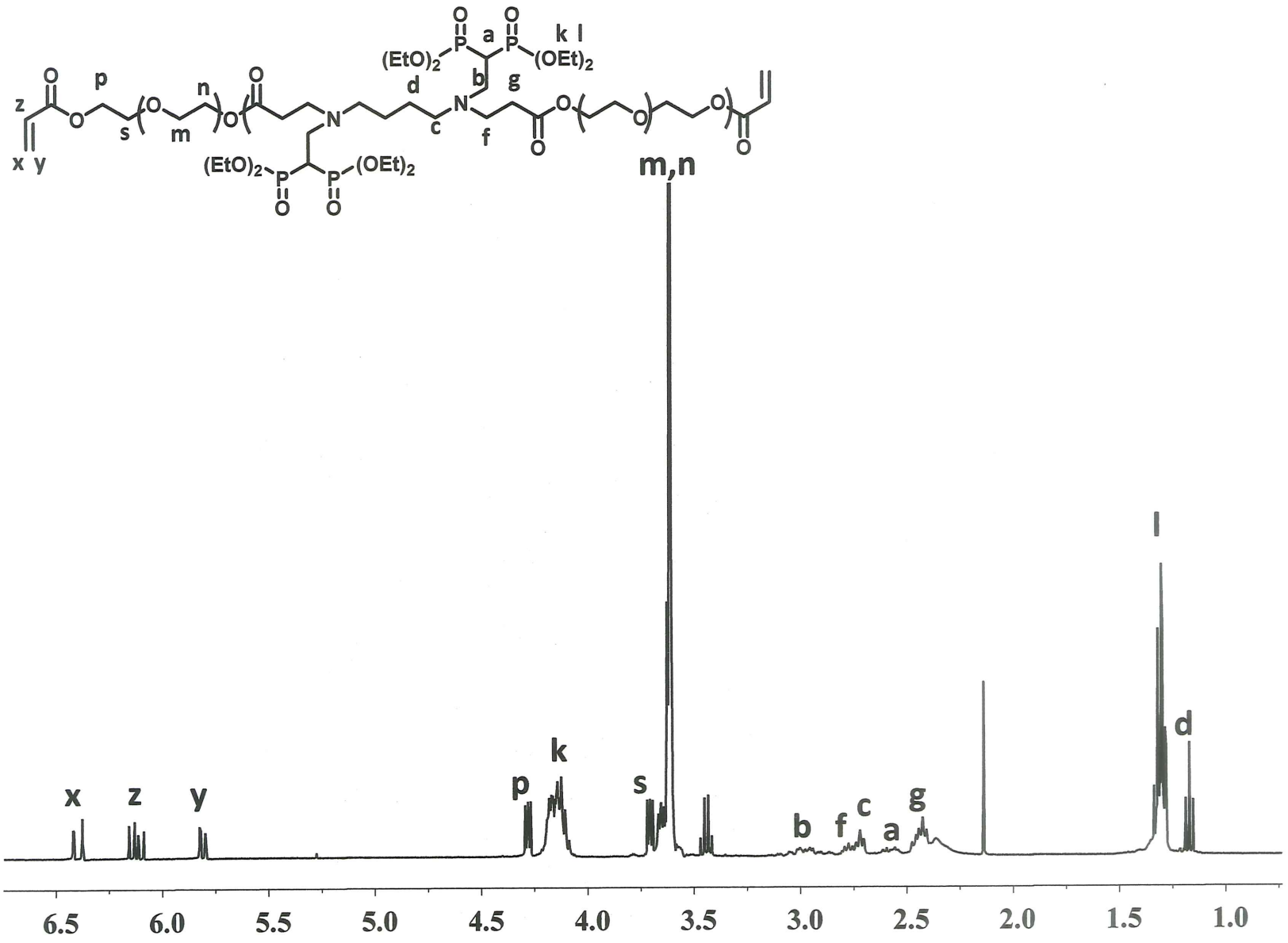

Figure 4.25. ^{1}H NMR spectrum of PEGDA-BPA1 macromer.

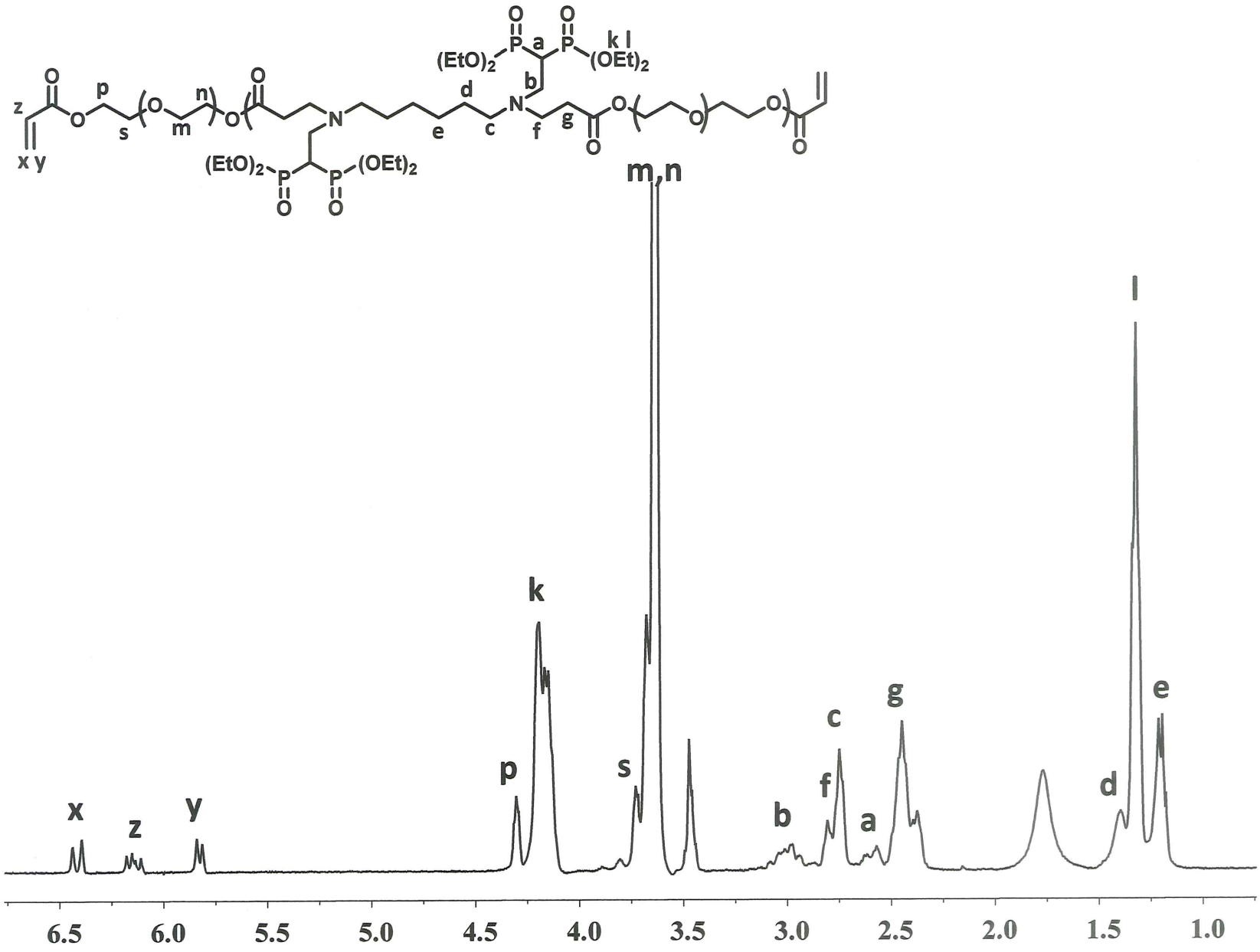

Figure 4.26. ^{1}H NMR spectrum of PEGDA-BPA2 macromer.

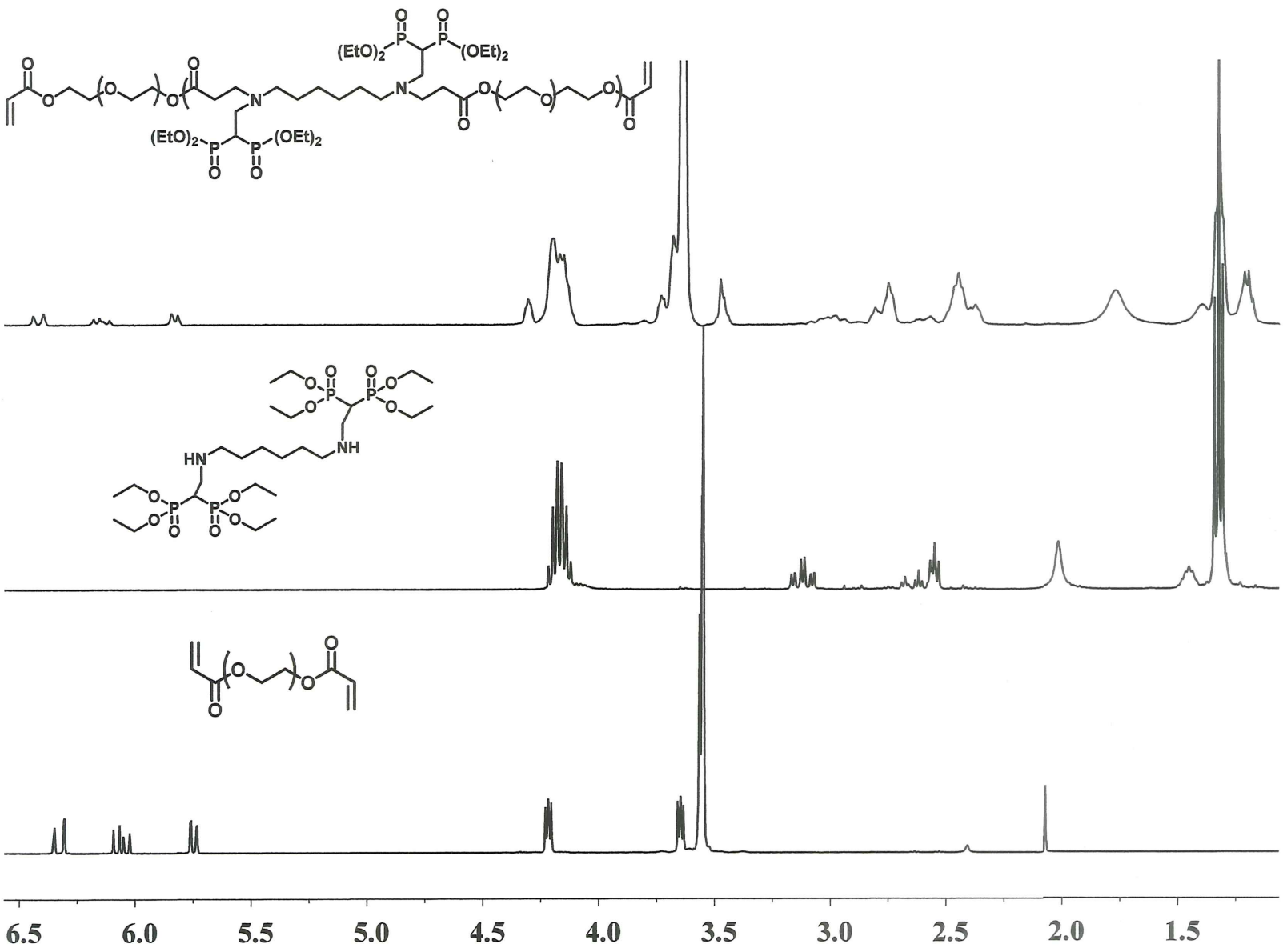

Figure 4.27. ^{1}H NMR spectra of PEGDA, BPA2 and PEGDA-BPA2 macromer.

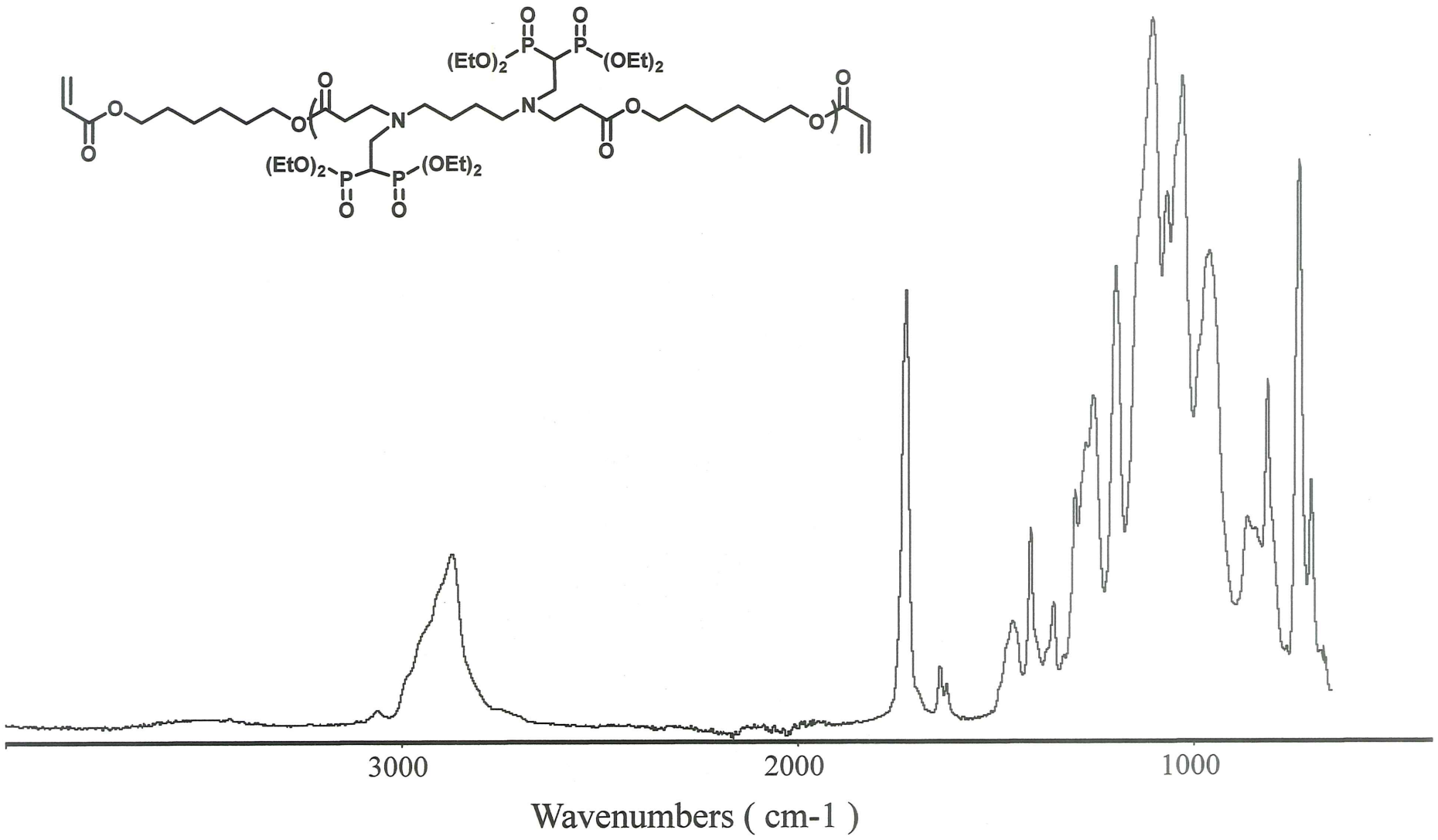

Figure 4.28. FT-IR spectrum of HDDA-BPA1 macromer.

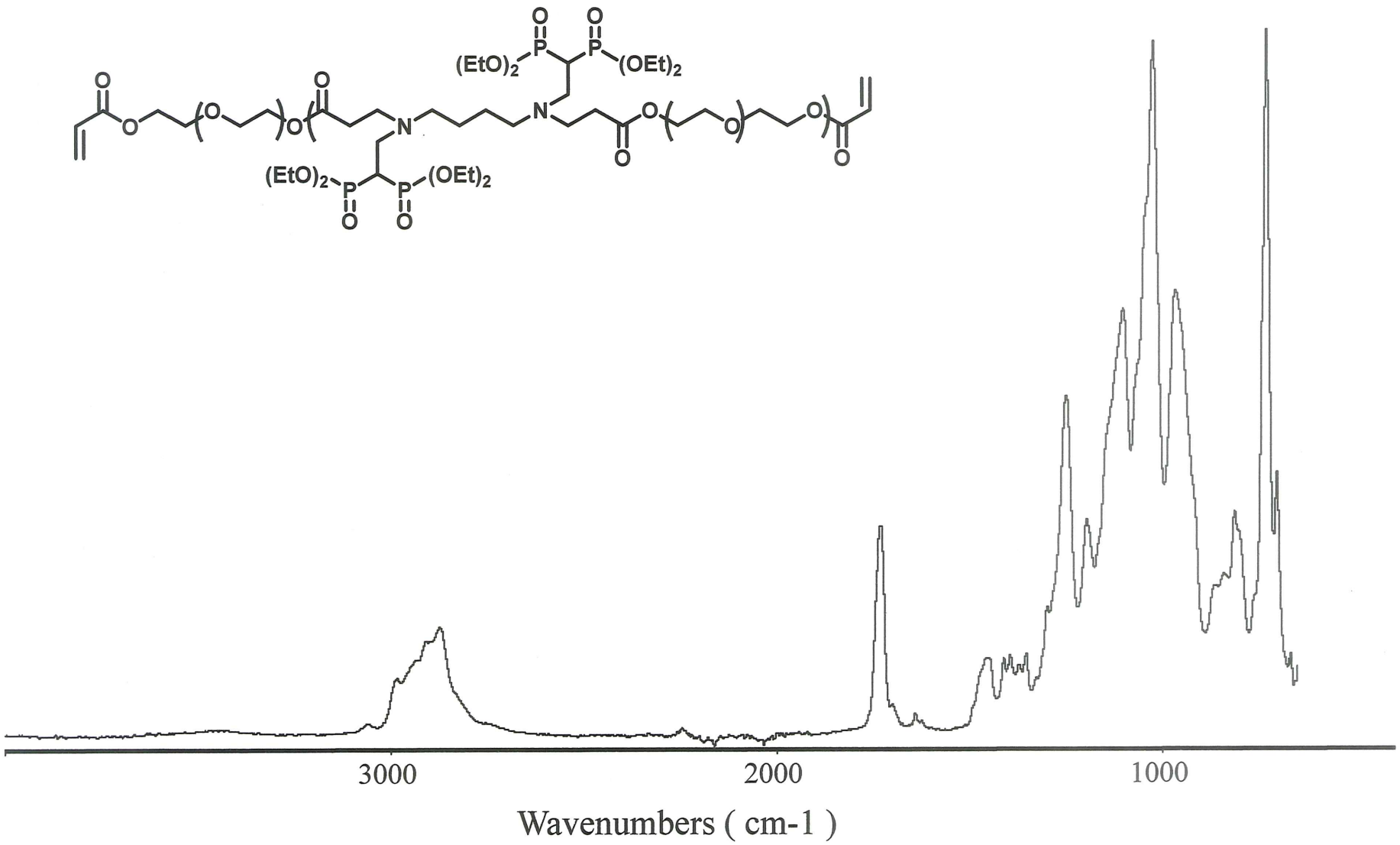

Figure 4.29. FT-IR spectrum of PEGDA-BPA1 macromer.

4.3.2. Photopolymerization Studies of PBAE macromers

The photoinitiator (DMPA) was added to the macromers at a concentration of 1% (w/w) by the addition of a 10% (w/v) solution of DMPA in methylene chloride and solvent was removed in a vacuum desiccator. The polymerization behavior was monitored using real-time FTIR-ATR spectroscopy at 25 °C. The decrease in the C=C peak (1635 cm^{-1}) with respect to C=O peak (1718 cm^{-1}) was monitored during free radical photopolymerization of macromers and the double bond conversion values were calculated from equation (3.2).

It is seen that the macromers synthesized from PEGDA have higher double bond conversion than the HDDA containing ones. This is expected because PEGDA's oxygen atoms in its backbone makes it more flexible than HDDA. It is also observed that BPA2 containing macromers showed higher DBC % as expected, because BPA2 has a longer aliphatic chain, BPA2 containing macromers have higher molecular weight and higher chain mobility which increases DBC % (Figure 4.30).

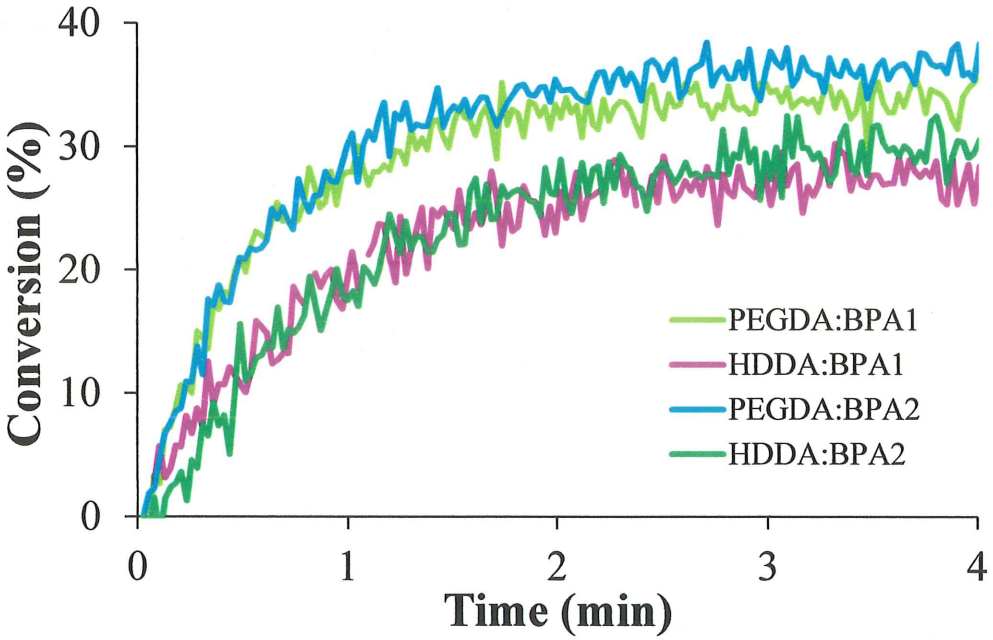

Figure 4.30. Conversion-time plots for four macromers.

The macromers were bulk photopolymerized into networks using ultraviolet light exposure in the presence of DMPA (1 %) as photoinitiator at room temperature for 30 min. The polymer samples were weighed and placed in ethanol for removing unreacted macromers and initiators. After drying in a vacuum oven until constant weight has reached, gel samples were weighed. The percentage of gelation was calculated according to the formula (3.2) (Figure 4.31). The values were found to be similar, ranged from 54-70%, and higher for PEGDA-based macromers.

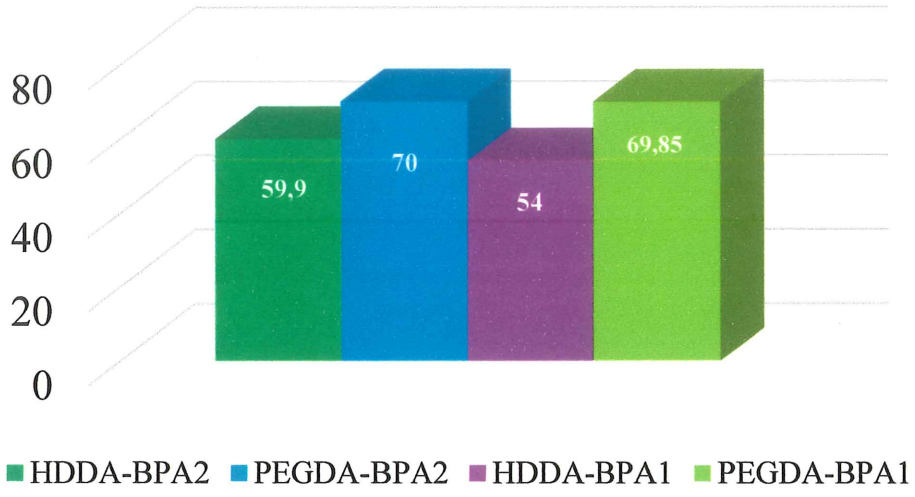

Figure 4.31. Gelation (%) values of four PBAE hydrogels.

4.3.4. Synthesis of HEMA Hydrogels

The PBAE crosslinked HEMA hydrogels were prepared using HEMA, 10 wt% PBAE crosslinkers, 1 wt% Irgacure 2959 and deionized water. PEGDA (M_n = 575) crosslinked hydrogels were also prepared for comparison under the same conditions. The mixtures were poured into Teflon molds, covered with a mylar film polymerized with exposure to UV light (365 nm) for 30 min. The polymer samples were weighed and placed in ethanol for 24 h to remove unreacted macromers and initiators. After drying in a vacuum oven for several days to reach constant weight, gel samples were weighed. The percentage of gelation was calculated according to the formula 3.2 (Figure 4.32).

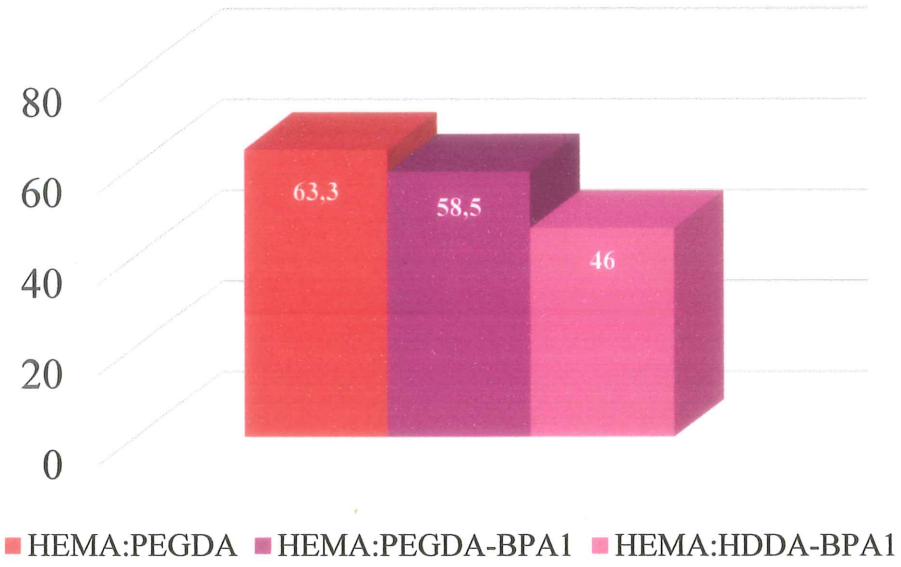

Figure 4.31. Gelation (%) values of PHEMA hydrogels.

4.3.5. Degradation Studies

The degradation of the synthesized networks was investigated in PBS at 37 °C for 24 h. Since the soluble fractions due to unreacted macromers are removed before the tests, there is no rapid mass loss initially. The rate of degradation depends on the chemical structure of the macromers.

We observed that polymers formed from PEGDA-BPA2 showed the highest mass loss (67% after 24 h), indicating highest degradation rate and the polymers formed from HDDA-BPA1 showed the lowest mass loss (52% after 24 h). We expected that PEGDA containing hydrogels should have higher mass loss than the HDDA containing ones due to their hydrophilic backbone structure. Also hydrogels with BPA2 should have higher degradation (%) than BPA1 because of their longer backbone chains that increase the flexibility and molecular mass. Overall, these four macromers have very high degradation % due to their bisphosphonate groups that make them very hydrophilic. Even after 24 hours they all show more than 50% degradation (Figure 4.33).

Furthermore, degradation values of HEMA hydrogels synthesized from HEMA:PEGDA, HEMA:PEGDA-ABP1 and HEMA:HDDA-ABP1 were calculated.

Increasing degradations were observed when HEMA incorporated with BPA1 containing macromers (Figure 4.34).

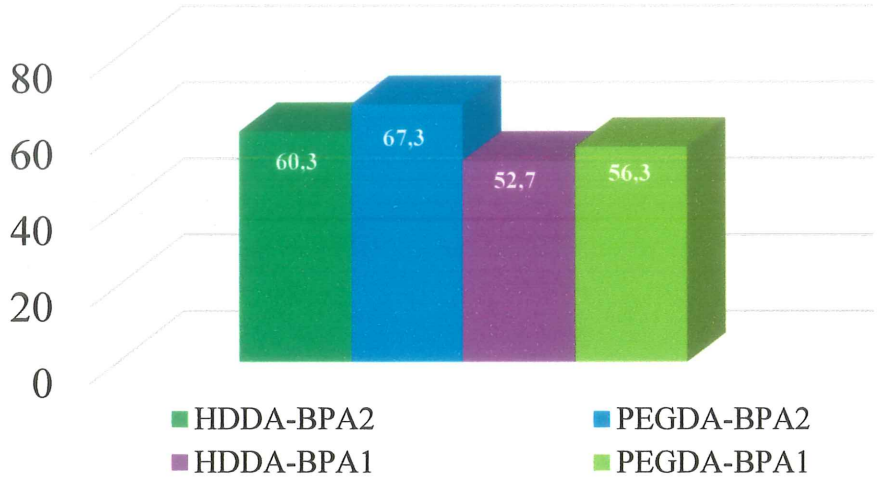

Figure 4.33. The mass losses of four hydrogels in PBS at 37 °C after 24 h.

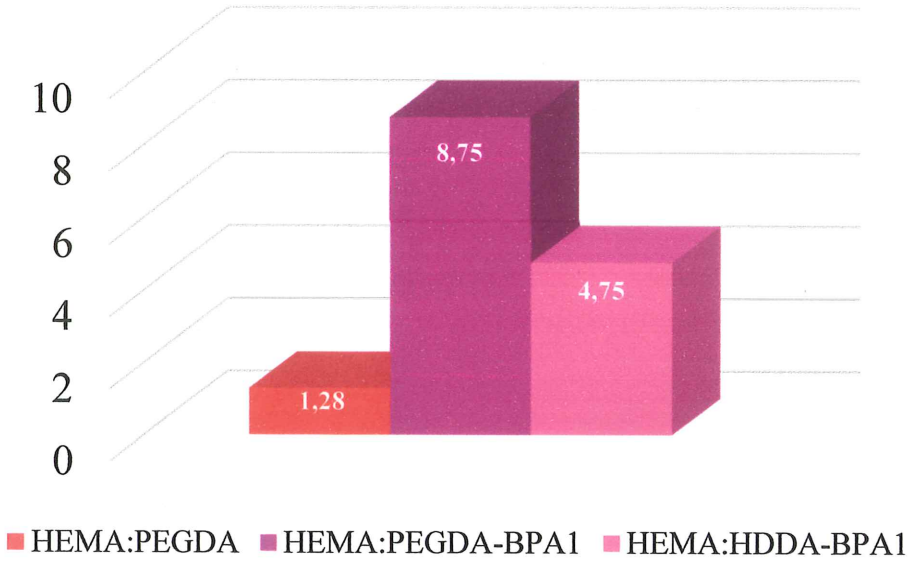

Figure 4.34. The mass losses of PHEMA hydrogels.

4.3.6. Scanning Electron Microscope (SEM) Images of Network Polymers

Morphological evaluations of hydrogels were performed by using a scanning electron microscope (SEM) (ESEM-FEG) (FEI-Philips XL30). The hydrogels were lyophilized and then the fractured surface was sputter-coated with gold before observation. Figure 4.35 shows that the SEM images of two of the hydrogel samples before and after degradation in PBS at 37 °C after 24 h. The images show that the hydrogels have more porous structure after degradation. Also, it is observed that the hydrogel synthesized from more hydrophilic macromer (PEGDA- BPA2) has bigger pores than that of synthesized from HDDA-BPA1 macromer.

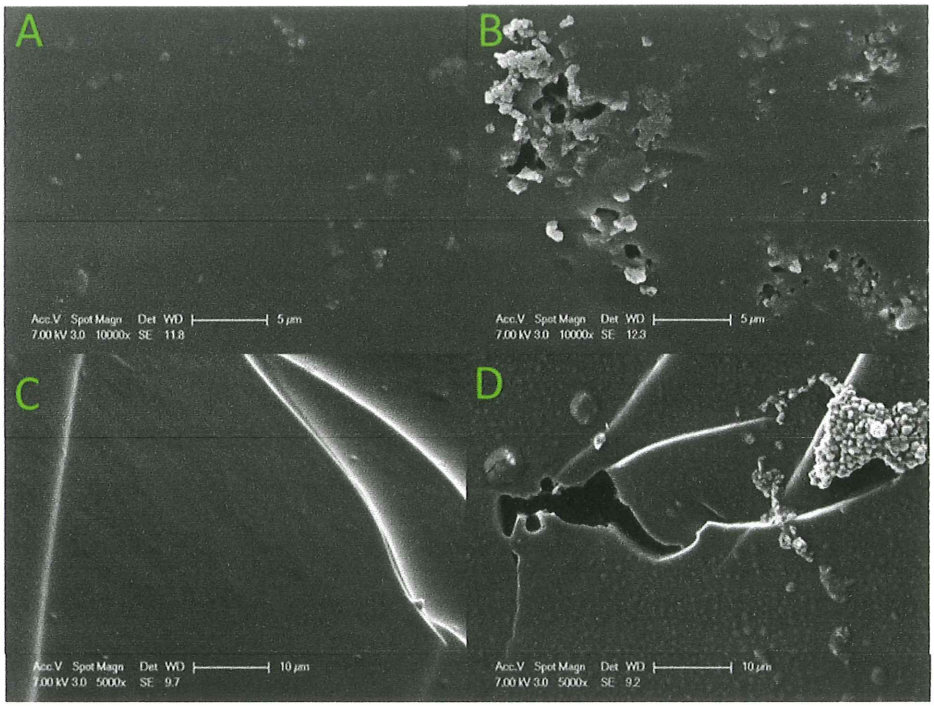

Figure 4.35. SEM images of hydrogels from HDDA-BPA1 macromer A) before, B) after degradation and PEGDA-BPA2 macromer C) before, D) after degradation.

4.3.7. Thermogravimetric Analysis (TGA) of PBAE Polymers

Thermal stabilities of the polymers prepared from PEGDA-BPA2 and HDDA-BPA2 macromers were inverstigated using TGA under nitrogen at 10 ^{o}C/minute (Figure 4.36).

Polymers started to lose weight around 200 °C due to decomposition of ester groups and then degraded gradually to give char yields of 9.7 and 14.6 % for polymer from PEGDA-BPA2 and HDDA-BPA2 macromers, respectively.

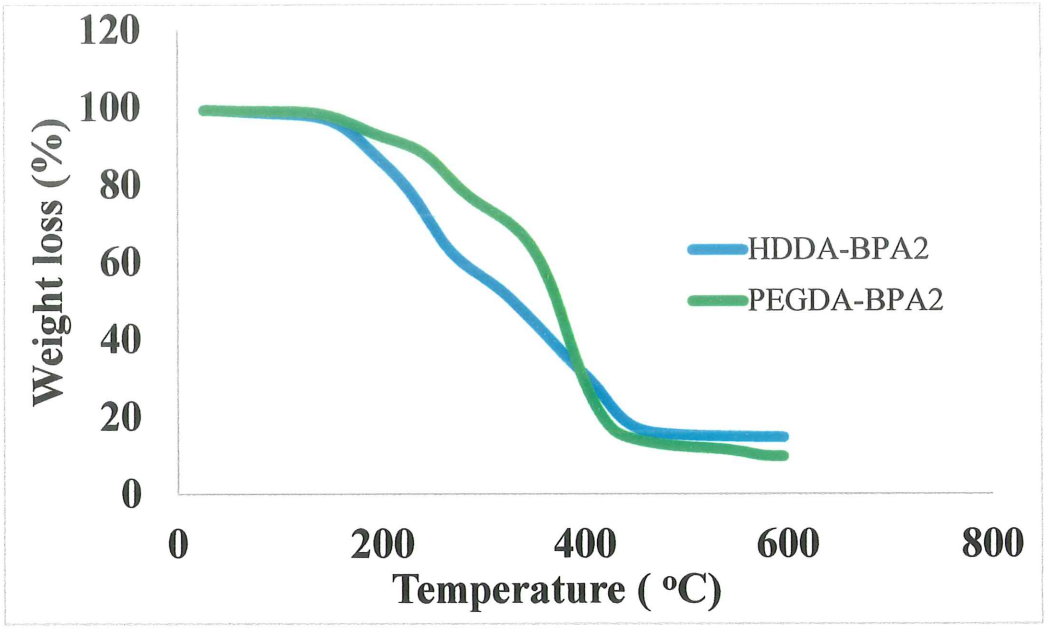

Figure 4.36. TGA curves of the polymers formed from HDDA-BPA2 and PEGDA-BPA2 macromers

5. CONCLUSIONS

In the first part of this work, the reactions of IEM with secondary bisphosphonated diamines were used to prepare new bisphosphonated-urea-methacrylates and their bisphosphonic acid derivatives. The pH values of the bisphosphonic acid monomers were found to be in the range of mild self-etching adhesives. Although these monomers contain ester linkages, they were found to be hydrolytically stable, which is an important property for good shelf life and bonding reliability. Photopolymerization results indicated that all monomers were able to homo and copolymerizable efficiently with Bis-GMA:TEGDMA mixtures and HEMA. The bisphosphonic acid containing monomers showed higher rates of polymerizations than bisphosphonate containing ones due to hydrogen bonding. Incorporation of the synthesized monomers to Bis-GMA:TEGDMA mixtures or HEMA lowered the conversions, proportional with their concentrations in the formulations due to their crosslinking abilities. X-ray diffraction result of one of the bisphosphonic acid monomers showed both dicalcium phosphate dehydrate formation due to decalcification and monomer-Ca salt upon interaction with hydroxyapatite. Overall, the synthesized bisphosphonated-urea-methacrylate monomers have potential in dental composites and their bisphosphonic acid derivatives are good candidates in self-etching dental adhesives.

In the second part of this work, new bisphosphonate-functionalized PBAE macromers were successfully synthesized and photopolymerized to give network polymers. Although degradation of PBAE networks were found to be very fast (53 - 69% over 24 hours), HEMA networks obtained by incorporation of PBAE as crosslinkers show smaller degradation rates controllable by the amount of PBAE macromers used. The ability to tailor the degradation rate makes such networks suitable for wide range of tissue engineering applications.

REFERENCES

1. Petroianu, G.A., "Pharmacist Theodor Salzer (1833-1900) And The Discovery Of Bisphosphonates.", *Pharmazie*, Vol. 66, pp. 804–807, 2011.

2. Nancollas, G.H., R. Tang, R.J. Phipps, Z. Henneman, S. Gulde, W. Wu, A. Mangood, R.G.G. Russell, and F.H. Ebetino, "Novel Insights Into Actions Of Bisphosphonates On Bone: Differences In Interactions With Hydroxyapatite.", *Bone*, Vol. 38, pp. 617–627, 2006.

3. Paolino, D., M. Licciardi, C. Celia, G. Giammona, M. Fresta, and G. Cavallaro, "Bone Targeted Drug Delivery Systems.", *Journal of Materials Chemistry B: Materials for biology and medicine*, Vol. 3, pp. 250–259, 2014.

4. Palmerini, C.A., F. Tartacca, M. Mazzoni, L. Granieri, L. Goracci, A. Scrascia, and S. Lepri, "Synthesis Of New Indole-based Bisphosphonates And Evaluation Of Their Chelating Ability In PE / CA-PJ15 Cells.", *European Journal of Medicinal Chemistry*, Vol. 102, pp. 403–412, 2015.

5. Hochdörffer, K., K. Abu Ajaj, C. Schäfer-Obodozie, and F. Kratz, "Development Of Novel Bisphosphonate Prodrugs Of Doxorubicin For Targeting Bone Metastases That Are Cleaved pH Dependently Or By Cathepsin B: Synthesis, Cleavage Properties, And Binding Properties To Hydroxyapatite As Well As Bone Matrix.", *Journal of Medicinal Chemistry*, Vol. 55, pp. 7502–7515, 2012.

6. Russell, R.G.G., N.B. Watts, F.H. Ebetino, and M.J. Rogers, "Mechanisms Of Action Of Bisphosphonates: Similarities And Differences And Their Potential Influence On Clinical Efficacy.", *Osteoporosis International*, Vol. 19, pp. 733–759, 2008.

7. Sunberg, R.J., F.H. Ebetino, C.T. Mosher, and C.F. Roof, "Designing Drugs For Stronger Bones .", *Chemtech*, Vol. 21, pp. 304–309, 2016.

8. Rodan, G. A, and T.J. Martin, "Therapeutic Approaches To Bone Diseases.", *Science (New York, N.Y.)*, Vol. 289, pp. 1508–1514, 2000.

9. Francis, M.D., R.G.G. Russell, and H. Fleisch, "Diphosphonates Inhibit Formation Of Calcium Phosphate Crystals In Vitro And Pathological Calcification In Vivo.", *Science*, Vol. 165, pp. 1264–1266, 1969.

10. Reid, I.R., and D.J. Hosking, "Bisphosphonates In Paget's Disease.", *Bone*, Vol. 49, pp. 89–94, 2011.

11. Tamerler, C., and M. Sarikaya, "Molecular Biomimetics: Genetic Synthesis, Assembly, And Formation Of Materials Using Peptides.", *MRS Bulletin*, Vol. 33, pp. 504–512, 2008.

12. Gil, L., Y. Han, E.E. Opas, G.A. Rodan, R. Ruel, J.G. Seedor, P.C. Tyler, and R.N. Young, "Prostaglandin E2-bisphosphonate Conjugates: Potential Agents For Treatment Of Osteoporosis.", *Bioorganic and Medicinal Chemistry*, Vol. 7, pp. 901–919, 1999.

13. Hirabayashi, H., T. Takahashi, J. Fujisaki, T. Masunaga, S. Sato, J. Hiroi, Y. Tokunaga, S. Kimura, and T. Hata, "Bone-specific Delivery And Sustained Release Of Diclofenac, A Non-steroidal Anti-inflammatory Drug, Via Bisphosphonic Prodrug Based On The Osteotropic Drug Delivery System (ODDS).", *Journal of Controlled Release*, Vol. 70, pp. 183–191, 2001.

14. Houghton, T.J., K.S.E. Tanaka, T. Kang, E. Dietrich, Y. Lafontaine, D. Delorme, S.S. Ferreira, F. Viens, F.F. Arhin, I. Sarmiento, D. Lehoux, I. Fadhil, K. Laquerre, J. Liu, V. Ostiguy, H. Poirier, G. Moeck, T.R. Parr, and A.R. Far, "Linking Bisphosphonates To The Free Amino Groups In Fluoroquinolones: Preparation Of Osteotropic Prodrugs For The Prevention Of Osteomyelitis.", *Journal of Medicinal Chemistry*, Vol. 51, pp. 6955–6969, 2008.

15. Page, P.C.B., M.J. McKenzie, and J.A. Gallagher, "Novel Synthesis Of Bis(phosphonic

Acid)-steroid Conjugates.", *Journal of Organic Chemistry*, Vol. 66, pp. 3704–3708, 2001.

16. Kubíček, V., J. Rudovsky, J. Kotek, P. Hermann, L. Vander Elst, R.N. Muller, Z.I. Kolar, H.T. Wolterbeek, J.A. Peters, and I. Lukeš, "A Bisphosphonate Monoamide Analogue Of DOTA: A Potential Agent For Bone Targeting.", *Journal of the American Chemical Society*, Vol. 127, pp. 16477–16485, 2005.

17. Ogawa, K., T. Mukai, Y. Arano, M. Ono, H. Hanaoka, S. Ishino, K. Hashimoto, H. Nishimura, and H. Saji, "Development Of A Rhenium-186-labeled MAG3-conjugated Bisphosphonate For The Palliation Of Metastatic Bone Pain Based On The Concept Of Bifunctional Radiopharmaceuticals.", *Bioconjugate Chemistry*, Vol. 16, pp. 751–757, 2005.

18. Wright, J.E.I., S.A. Gittens, G. Bansal, P.I. Kitov, D. Sindrey, C. Kucharski, and H. Uludağ, "A Comparison Of Mineral Affinity Of Bisphosphonate-protein Conjugates Constructed With Disulfide And Thioether Linkages.", *Biomaterials*, Vol. 27, pp. 769–784, 2006.

19. Wang, L., M. Zhang, Z. Yang, and B. Xu, "The First Pamidronate Containing Polymer And Copolymer.", *Chemical communications*, pp. 2795–2797, 2006.

20. Zhang, S., J.E.I. Wright, N. Özber, and H. Uludağ, "The Interaction Of Cationic Polymers And Their Bisphosphonate Derivatives With Hydroxyapatite.", *Macromolecular Bioscience*, Vol. 7, pp. 656–670, 2007.

21. Yewle, J.N., D.A. Puleo, and L.G. Bachas, "Enhanced Affinity Bifunctional Bisphosphonates For Targeted Delivery Of Therapeutic Agents To Bone.", *Bioconjugate Chemistry*, Vol. 22, pp. 2496–2506, 2011.

22. Giger, E. V., B. Castagner, J. Räikkönen, J. Mönkkönen, and J.C. Leroux, "SiRNA Transfection With Calcium Phosphate Nanoparticles Stabilized With PEGylated Chelators.", *Advanced Healthcare Materials*, Vol. 2, pp. 134–144, 2013.

23. Greiner, S.H., B. Wildemann, D.A. Back, M. Alidoust, P. Schwabe, N.P. Haas, and G. Schmidmaier, "Local Application Of Zoledronic Acid Incorporated In A Poly(D,L-lactide)-coated Implant Accelerates Fracture Healing In Rats.", *Acta Orthopaedica*, Vol. 79, pp. 717–725, 2008.

24. Portet, D., B. Denizot, E. Rump, J.J. Lejeune, and P. Jallet, "Nonpolymeric Coatings Of Iron Oxide Colloids For Biological Use As Magnetic Resonance Imaging Contrast Agents.", *Journal of Colloid and Interface Science*, Vol. 238, pp. 37–42–, 2001.

25. Stadelmann, V.A., A. Terrier, O. Gauthier, J.M. Bouler, and D.P. Pioletti, "Prediction Of Bone Density Around Orthopedic Implants Delivering Bisphosphonate.", *Journal of Biomechanics*, Vol. 42, pp. 1206–1211, 2009.

26. Giger, E. V., B. Castagner, and J.C. Leroux, "Biomedical Applications Of Bisphosphonates.", *Journal of Controlled Release*, Vol. 167, pp. 175–188, 2013.

27. Cramer, N.B., J.W. Stansbury, and C.N. Bowman, "Recent Advances And Developments In Composite Dental Restorative Materials.", *Journal of Dental Research*, Vol. 90, pp. 402–16, 2011.

28. Moszner, N., and U. Salz, "New Developments Of Polymeric Dental Composites.", *Progress in Polymer Science (Oxford)*, Vol. 26, pp. 535–576, 2001.

29. Altin, A., B. Akgun, Z. Sarayli Bilgici, S. Begum Turker, and D. Avci, "Synthesis, Photopolymerization, And Adhesive Properties Of Hydrolytically Stable Phosphonic Acid-containing (Meth)acrylamides.", *Journal of Polymer Science, Part A: Polymer Chemistry*, Vol. 52, pp. 511–522, 2014.

30. López-Suevos, F., and S.H. Dickens, "Degree Of Cure And Fracture Properties Of Experimental Acid-resin Modified Composites Under Wet And Dry Conditions.", *Dental Materials*, Vol. 24, pp. 778–785, 2008.

31. Moszner, N., U. Salz, and J. Zimmermann, "Chemical Aspects Of Self-etching Enamel-dentin Adhesives: A Systematic Review.", *Dental Materials*, Vol. 21, pp. 895–910, 2005.

32. Mou, L., G. Singh, and J.W. Nicholson, "Synthesis Of A Hydrophilic Phosphonic Acid Monomer For Dental Materials.", *Chemical Communications*, pp. 345–346, 2000.

33. Ikemura, K., K. Ichizawa, and T. Endo, "Design Of A New Self-etching HEMA-free Adhesive.", *Dental Materials Journal*, Vol. 28, pp. 558–64, 2009.

34. Fu, B., X. Sun, W. Qian, Y. Shen, R. Chen, and M. Hannig, "Evidence Of Chemical Bonding To Hydroxyapatite By Phosphoric Acid Esters.", *Biomaterials*, Vol. 26, pp. 5104–5110, 2005.

35. Altin, A., B. Akgun, O. Buyukgumus, Z. Sarayli Bilgici, S. Agopcan, D. Asik, H. Yagci Acar, and D. Avci, "Synthesis And Photopolymerization Of Novel, Highly Reactive Phosphonated-urea-methacrylates For Dental Materials.", *Reactive and Functional Polymers*, Vol. 73, pp. 1319–1326, 2013.

36. Zeuner, F., N. Moszner, and T. Völkel, "Silicon And The Related Elements Synthesis And Dental Aspects Of Acrylic Phosphoric And Phosphonic Acids.", *Phosphorus, Sulfur and Silicon*, Vol. 144-146, pp. 133–136, 1999.

37. Catel, Y., L. Le Pluart, P.J. Madec, and T.N. Pham, "Synthesis And Photopolymerization Of Phosphonic Acid Monomers For Applications In Compomer Materials.", *Journal of Applied Polymer Science*, Vol. 117, pp. 2676–2687, 2010.

38. Catel, Y., M. Degrange, L.L.E. Pluart, P.J. Madec, T.N. Pham, F.E.I. Chen, and W.D. Cook, "Synthesis, Photopolymerization, And Adhesive Properties Of New Bisphosphonic Acid Monomers For Dental Application.", *Journal of Polymer Science, Part A: Polymer Chemistry*, Vol. 47, pp. 5258–5271, 2009.

39. Avci, D., and A. Ziylan Albayrak, "Synthesis And Copolymerization Of New

Phosphorus-containig Acrylates.", *Journal of Polymer Science, Part A: Polymer Chemistry*, Vol. 41, pp. 2207–2217, 2003.

40. Avci, D., and L.J. Mathias, "Synthesis And Polymerization Of Phosphorus-containing Acrylates.", *Journal of Polymer Science, Part A: Polymer Chemistry*, Vol. 40, pp. 3221–3231, 2002.

41. Edizer, S., G. Sahin, and D. Avci, "Development Of Reactive Phosphonated Methacrylates.", *Journal of Polymer Science, Part A: Polymer Chemistry*, Vol. 47, pp. 5737–5746, 2009.

42. Torii, Y., K. Itou, Y. Nishitani, M. Yoshiyama, K. Ishikawa, and K. Suzuki, "Effect Of Self-etching Primer Containing N-acryloyl Aspartic Acid On Enamel Adhesion.", *Dental Materials*, Vol. 19, pp. 253–258, 2003.

43. Bala, J.L.F., B. A. Kashemirov, and C.E. McKenna, "Synthesis Of A Novel Bisphosphonic Acid Alkene Monomer.", *Synthetic Communications*, Vol. 40, pp. 3577–3584, 2010.

44. Catel, Y., V. Besse, A. Zulauf, D. Marchat, E. Pfund, T.N. Pham, D. Bernache-Assolant, M. Degrange, T. Lequeux, P.J. Madec, and L. Le Pluart, "Synthesis And Evaluation Of New Phosphonic, Bisphosphonic And Difluoromethylphosphonic Acid Monomers For Dental Applications.", *European Polymer Journal*, Vol. 48, pp. 318–330, 2012.

45. Senaratne, S.G., and K.W. Colston, "Direct Effects Of Bisphosphonates On Breast Cancer Cells.", *Breast Cancer Res*, Vol. 4, pp. 18–23, 2002.

46. Berchtold, K.A., J. Nie, J.W. Stansbury, B. Hacioğlu, E.R. Beckel, and C.N. Bowman, "Novel Monovinyl Methacrylic Monomers Containing Secondary Functionality For Ultrarapid Polymerization: Steady-state Evaluation.", *Macromolecules*, Vol. 37, pp. 3165–3179, 2004.

47. Jansen, J.F.G.A., A.A. Dias, M. Dorschu, and B. Coussens, "Fast Monomers: Factors Affecting The Inherent Reactivity Of Acrylate Monomers In Photoinitiated Acrylate Polymerization.", *Macromolecules*, Vol. 36, pp. 3861–3873, 2003.

48. Tauscher, S., Y. Catel, and N. Moszner, "Monomers For Adhesive Polymers, 17. Synthesis, Photopolymerization And Adhesive Properties Of Polymerizable Phosphonic Acids Bearing Urea Groups.", *Designed Monomers and Polymers*, Vol. 19, pp. 77–88, 2016.

49. Piantino, J., J.A. Burdick, D. Goldberg, R. Langer, and L.I. Benowitz, "An Injectable, Biodegradable Hydrogel For Trophic Factor Delivery Enhances Axonal Rewiring And Improves Performance After Spinal Cord Injury.", *Experimental Neurology*, Vol. 201, pp. 359–367, 2006.

50. Anseth, K.S., A.T. Metters, S.J. Bryant, P.J. Martens, J.H. Elisseeff, and C.N. Bowman, "In Situ Forming Degradable Networks And Their Application In Tissue Engineering And Drug Delivery.", *Journal of Controlled Release*, Vol. 78, pp. 199–209, 2002.

51. Hill-West, J.L., S.M. Chowdhury, M.J. Slepian, and J.A. Hubbell, "Inhibition Of Thrombosis And Intimal Thickening By In Situ Photopolymerization Of Thin Hydrogel Barriers.", *Proceedings of the National Academy of Sciences of the United States of America*, Vol. 91, pp. 5967–71, 1994.

52. Chung, C., J. Mesa, M.A. Randolph, M. Yaremchuk, and J.A. Burdick, "Influence Of Gel Properties On Neocartilage Formation By Auricular Chondrocytes Photoencapsulated In Hyaluronic Acid Networks.", *Journal of Biomedical Materials Research - Part A*, Vol. 77, pp. 518–525, 2006.

53. Burkoth, A.K., and K.S. Anseth, "A Review Of Photocrosslinked Polyanhydrides: In Situ Forming Degradable Networks.", *Biomaterials*, Vol. 21, pp. 2395–2404, 2000.

54. Nguyen, K.T., and J.L. West, "Photopolymerizable Hydrogels For Tissue Engineering

Applications.", *Biomaterials*, Vol. 23, pp. 4307–4314, 2002.

55. Hatefi, A., and B. Amsden, "Biodegradable Injectable In Situ Forming Drug Delivery Systems.", *Journal of Controlled Release*, Vol. 80, pp. 9–28, 2002.

56. McBath, R.A., and D.A. Shipp, "Swelling And Degradation Of Hydrogels Synthesized With Degradable Poly(β-amino Ester) Crosslinkers.", *Polymer Chemistry*, Vol. 1, pp. 860, 2010.

57. Geever, L.M., D.M. Devine, M.J.D. Nugent, J.E. Kennedy, J.G. Lyons, A. Hanley, and C.L. Higginbotham, "Lower Critical Solution Temperature Control And Swelling Behaviour Of Physically Crosslinked Thermosensitive Copolymers Based On N-isopropylacrylamide.", *European Polymer Journal*, Vol. 42, pp. 2540–2548, 2006.

58. Iza, M., G. Stoianovici, L. Viora, J.L. Grossiord, and G. Couarraze, "Hydrogels Of Poly(ethylene Glycol): Mechanical Characterization And Release Of A Model Drug.", *Journal of Controlled Release*, Vol. 52, pp. 41–51, 1998.

59. Wang, D., S. Miller, M. Sima, P. Kopeckova, and J. Kopecek, "Synthesis And Evaluation Of Water-soluble Polymeric Bone-targeted Drug Delivery Systems.", *Bioconjugate Chemistry*, Vol. 14, pp. 853–859, 2003.

60. Hulsart-Billström, G., P.K. Yuen, R. Marsell, J. Hilborn, S. Larsson, and D. Ossipov, "Bisphosphonate-linked Hyaluronic Acid Hydrogel Sequesters And Enzymatically Releases Active Bone Morphogenetic Protein-2 For Induction Of Osteogenic Differentiation.", *Biomacromolecules*, Vol. 14, pp. 3055–3063, 2013.

61. Sandiford, L., A. Phinikaridou, A. Protti, L.K. Meszaros, X. Cui, Y. Yan, G. Frodsham, P.A. Williamson, N. Gaddum, R.M. Botnar, P.J. Blower, M.A. Green, and R.T.M. De Rosales, "Bisphosphonate-anchored Pegylation And Radiolabeling Of Superparamagnetic Iron Oxide: Long-circulating Nanoparticles For In Vivo Multimodal (T1 MRI-SPECT) Imaging.", *ACS Nano*, Vol. 7, pp. 500–512, 2013.

62. Lynn, D.M., D.G. Anderson, D. Putnam, and R. Langer, "Accelerated Discovery Of Synthetic Transfection Vectors: Parallel Synthesis And Screening Of A Degradable Polymer Library.", *Journal of the American Chemical Society*, Vol. 123, pp. 8155–8156, 2001.

63. Song, W., Z. Tang, M. Li, S. Lv, H. Yu, L. Ma, X. Zhuang, Y. Huang, and X. Chen, "Tunable pH-Sensitive Poly(β-amino Ester)s Synthesized From Primary Amines And Diacrylates For Intracellular Drug Delivery.", *Macromolecular Bioscience*, Vol. 12, pp. 1375–1383, 2012.

64. Chen, J., X. Qiu, J. Ouyang, J. Kong, W. Zhong, and M.M.Q. Xing, "pH And Reduction Dual-sensitive Copolymeric Micelles For Intracellular Doxorubicin Delivery.", *Biomacromolecules*, Vol. 12, pp. 3601–3611, 2011.

65. Lynn, D.M., M.M. Amiji, and R. Langer, "pH-responsive Polymer Microspheres: Rapid Release Of Encapsulated Material Within The Range Of Intracellular pH.", *Angewandte Chemie - International Edition*, Vol. 40, pp. 1707–1710, 2001.

66. Shen, Y., H. Tang, Y. Zhan, E.A. Van Kirk, and W.J. Murdoch, "Degradable Poly(β-amino Ester) Nanoparticles For Cancer Cytoplasmic Drug Delivery.", *Nanomedicine: Nanotechnology, Biology, and Medicine*, Vol. 5, pp. 192–201, 2009.

67. Metter, R.B., J.L. Ifkovits, K. Hou, L. Vincent, B. Hsu, L. Wang, R.L. Mauck, and J.A. Burdick, "Biodegradable Fibrous Scaffolds With Diverse Properties By Electrospinning Candidates From A Combinatorial Macromer Library.", *Acta Biomaterialia*, Vol. 6, pp. 1219–1226, 2010.

68. Tan, A.R., J.L. Ifkovits, B.M. Baker, D.M. Brey, R.L. Mauck, and J.A. Burdick, "Electrospinning Of Photocrosslinked And Degradable Fibrous Scaffolds.", *Journal of Biomedical Materials Research - Part A*, Vol. 87, pp. 1034–1043, 2008.

69. Brey, D.M., J.L. Ifkovits, R.I. Mozia, J.S. Katz, and J.A. Burdick, "Controlling Poly(β-amino Ester) Network Properties Through Macromer Branching.", *Acta Biomaterialia*,

Vol. 4, pp. 207–217, 2008.

70. Brey, D.M., I. Erickson, and J.A. Burdick, "Influence Of Macromer Molecular Weight And Chemistry On Poly(β-amino Ester) Network Properties And Initial Cell Interactions.", *Journal of Biomedical Materials Research - Part A*, Vol. 85, pp. 731–741, 2008.

71. Zugates, G.T., D.G. Anderson, S.R. Little, I.E.B. Lawhorn, and R. Langer, "Synthesis Of Poly(β-amino Ester)s With Thiol-reactive Side Chains For DNA Delivery.", *Journal of the American Chemical Society*, Vol. 128, pp. 12726–12734, 2006.

72. Akinc, A., D.G. Anderson, D.M. Lynn, and R. Langer, "Synthesis Of Poly(β-amino Ester)s Optimized For Highly Effective Gene Delivery.", *Bioconjugate chemistry*, Vol. 14, pp. 979–988, 2003.

73. Anderson, D.G., C.A. Tweedie, N. Hossain, S.M. Navarro, D.M. Brey, K.J. Van Vliet, R. Langer, and J.A. Burdick, "A Combinatorial Library Of Photocrosslinkable And Degradable Materials.", *Advanced Materials*, Vol. 18, pp. 2614–2618, 2006.

74. Degenhardt, C.R., and D.C. Burdsall, "Synthesis Of Ethenylidenebis(phosphonic Acid) And Its Tetraalkyl Esters.", *The Journal of Organic Chemistry*, Vol. 51, pp. 3488–3490, 1986.

75. Yoshihara, K., Y. Yoshida, S. Hayakawa, N. Nagaoka, Y. Torii, A. Osaka, K. Suzuki, S. Minagi, B. Van Meerbeek, and K.L. Van Landuyt, "Self-etch Monomer-calcium Salt Deposition On Dentin.", *Journal of dental research*, Vol. 90, pp. 602–606, 2011.

76. Bailly, T., R. Burgada, T. Prangé, and M. Lecouvey, "Synthesis Of Tetradentate Mixed Bisphosphonates - New Hydroxypyridinonate Ligands For Metal Chelation Therapy.", *Tetrahedron Letters*, Vol. 44, pp. 189–192, 2003.

77. Zhou, H., Q. Li, T.Y. Lee, C.A. Guymon, E.S. Jönsson, and C.E. Hoyle, "Photopolymerization Of Acid Containing Monomers: Real-time Monitoring Of

Polymerization Rates.", *Macromolecules*, Vol. 39, pp. 8269–8273, 2006.

78. López-García, J., M. Lehocký, P. Humpolíček, and P. Sáha, "HaCaT Keratinocytes Response On Antimicrobial Atelocollagen Substrates: Extent Of Cytotoxicity, Cell Viability And Proliferation.", *Journal of functional biomaterials*, Vol. 5, pp. 43–57, 2014.

79. I.O.F. Standardization, Geneva, Switzerland, 2009.